ABSTRACT

LOWRIE, JAMES BALLANFONTE. Development of a Micro-Tube Hydroforming System. (Under the direction of Dr. Gracious Ngaile).

The rising demand for small parts with complex shapes for micro-electrical mechanical systems (MEMS) and medical applications has caused researchers to focus on metal forming as a possible way to mass produce miniature components. Studies into the miniaturization of macro-scale metal forming processes have mainly been focused in the sheet metal and extrusion fields and only a few researchers have attempted to take on the problem of miniaturizing the tube hydroforming process. The research that has been done into micro-tube hydroforming has been limited to simple expansion studies and no researchers have yet been able to combine axial feeding of the ends of the micro-tubular blank with simultaneous expansion of the tube. This has significantly reduced the complexity of the micro-parts which can be created using the tube hydroforming system. Combining material feed and expansion must be accomplished in order to create a micro-tube hydroforming process which is capable of producing metallic components with complex tubular geometries.

The major objective of the research presented in this thesis is the development of a micro-tube hydroforming system which is capable supplying both axial feed and expansion to the tube simultaneously. This was accomplished by first breaking down the concepts of the conventional hydroforming tooling so that they could be analyzed for problems when being scaled down. Once the problems with the conventional tooling and the basic needs of the hydroforming system were established, the information was used to develop a new form a hydroforming tooling, called floating die tooling, which could apply both material feed and expansion to tubular blanks. The finite element method was then used to establish the process forces which must be produced by the new hydroforming tooling and to vet the design concepts developed during the conceptualization of the tooling. This information was then used to design, develop, and fabricate a floating die micro-tube hydroforming system. Experiments were then carried out on the new tooling in order to prove the concept of the tooling. The experiments were carried out on 1mm and 2mm diameter stainless steel (SS304) with wall thicknesses of 100μm and 150μm, respectively. It was found that the tube

hydroforming equipment developed in this thesis could create simultaneous expansion and axial feeding of the 1mm and 2mm tubular blanks used in the study. The parts which were created were not fully formed, due to a lack of a pressure supply capable of producing sufficiently high pressure, but served as a proof of concept for the floating die tooling. In order to obtain more complete parts in the future and automation system was developed with the goals of increasing the repeatability and accuracy of the applied axial feeding.

Development of a Micro-Tube Hydroforming System

by

James Ballanfonte Lowrie

A thesis submitted to the Graduate Faculty of
North Carolina State University
in partial fulfillment of the
requirements for the degree of
Master of Science

Mechanical Engineering

Raleigh, North Carolina

2014

APPROVED BY:

Dr. Gracious Ngaile
Chair of Advisory Committee

Dr. Kara Peters

Dr. Tiegang Fang

BIOGRAPHY

James Lowrie was born on February 4th, 1991 to Bruce Lowrie and Sara Devine in Winston-Salem, North Carolina. He spent his childhood in Pfafftown, North Carolina and graduated from high school at Mount Tabor High School in 2009. In December 2012, he received his Bachelors of Science Degree in Mechanical Engineering from North Carolina State University, where he developed his skills in design and numerical analysis. In January 2013, James began his master's carrier at NC State University under the advisement of Dr. Gracious Ngaile. Here he conducted research in the metal forming field with the majority of his focus in micro-tube hydroforming. He received his Masters of Science degree in Mechanical Engineering in December 2014.

ACKNOWLEDGMENTS

Firstly, I would like to acknowledge the National Science Foundation, through which this work was funded under Project No. CM # 0900148. Any opinions, findings, and conclusions or recommendations expressed in this thesis are those of the author and do not necessarily reflect the views of the National Science Foundation.

Thank you to my parents, Bruce and Sara, for always being there for me and for supporting me unconditionally.

I would like to extend thanks to Dr. Chen Yang, whom I never had the pleasure of meeting in person, but was key to the research presented in this thesis. Dr. Yang was responsible for the first leg of this research in 2008 and without his initial designs this research would not have been possible.

Thank you Steve Cameron for your machining advice and guidance in the design process. Also, thank you for fabricating the tools and dies that were used in the research presented in this thesis. Gary Lofton, thanks for always agreeing to help me on such short notice.

I would also like to acknowledge my colleagues at the Advanced Metal forming and Tribology Laboratory. Specifically, thanks to Kyle Pender for teaching me what you know about machining and providing design advice to me. I feel glad that we were able to help each other in our master's careers. Also, thanks to Bandar Alzahrani for your constant support and guidance, you are a great role model to myself and all the other members of the lab. Lin Li, thank you for feeding me and providing fresh view points on my research, it was invaluable. My time spent in the lab with you all will not be forgotten and I would like to say that could not have gone as far as I have without all your support.

Finally, I would like to thank my advisor Dr. Gracious Ngaile, who has been the embodiment of everything an advisor should be for their students. Thank you for your constant support and guidance, which were immensely important to this research and my development as a researcher.

TABLE OF CONTENTS

LIST OF FIGURES

CHAPTER 1: INTRODUCTION AND RESEARCH OBJECTIVES

1.1 Introduction

Metal forming is a versatile and large field which encompasses many commonly used manufacturing techniques, including extrusion, forging, stamping, and hydroforming. In general, it is a process in which hard tools, or dies, are used to plastically deform a metallic workpiece in order to obtain desired shape, though in some cases a hard tool is replaced with a soft die, or pressurized fluid. As compared to other popular manufacturing techniques, like machining or casting, metal forming offers the advantages or low waste, improved mechanical properties, quick cycle times, and typically low cost per part. However, due to the expense of the equipment which is used in the metal forming process it is typically only used when the number of parts to be created is very high. As the demand for micro-scale parts increases in the electronics and medical fields, the application of this versatile manufacturing process to the micro-scale is becoming more and more attractive. This is causing extensive research to be carried out in the field of microforming, which is defined as a branch of metal forming in which the formed part has at least two dimensions in the sub-millimeter range.

Although many metal forming techniques have already been successfully scaled down to the micro-level, the tube hydroforming process has yet to be fully realized on the micro-scale. The tube hydroforming process is capable of creating complex tubular shapes by using high pressure fluid in the place of a hard tool to plastically deform a tubular blank into a desired shape. In order for shapes of increased complexity to be created, axial feed must be provided to the tube as the deformation process takes place. The research that will be presented in this thesis will propose a system which is capable of creating complex micro-tubular components using the tube hydroforming process.

1.2 Research Objectives

In order to develop micro-tube hydroforming tooling, which is capable of providing both high pressure fluid to the inside of the tube and axial feeding, the careful application of fundamental knowledge about the tube hydroforming process, the finite element method, and the use of extensive experiments must be applied. Therefore, the following objectives were set for this study:

i. Establish the specific functions of each tool-workpiece interface in the conventional tube hydroforming (THF) process
ii. Conceptualize a new class of tube hydroforming equipment which can overcome the limitations of conventional tooling when it comes to hydroforming on the micro-scale
iii. Through use of the finite element method determine the forces, pressures, and other process variables that are likely to arise during the micro-tube hydroforming process
iv. Using the information gained from the micro-THF simulations, design, develop, and fabricate a micro-THF system
v. Conduct micro-THF experiments in which both expansion and axial feed are provided to the workpiece

Provide a method for the micro-THF system to be automated so that the entire process is computer controlled

1.3 Thesis Organization

The main objective of this study is to develop a set of tooling which is capable of performing a micro-tube hydroforming process which utilizes both expansion and axial feed. It is therefore necessary to establish a basic set of background information from which potential challenges and opportunities can be established. This is accomplished in the second chapter of the thesis. The third chapter builds upon the information established in the second chapter to develop the basic concept of a new class of hydroforming equipment which can be used to accomplish the objectives of this study. In the fourth chapter, the finite element method is employed to study the material flow and determine the forming forces which could be encountered during the process and to vet various tooling designs for their usefulness in the micro-THF process. Next, the fifth chapter dives into the fabrication of the micro-THF tooling, as well as, covering the experimental set up and going over the results and discussion of the experiments in the study. Chapter six describes design consideration for system automation. Finally, the conclusions of the study as well as suggestions for future work are presented in chapter seven of the thesis.

CHAPTER 2: LITERATURE REVIEW ON MICROFORMING

2.1 Introduction

Microforming is the application of near net shape manufacturing techniques to create parts that have at least two dimensions in the sub-millimeter range. These micro-scale parts have a wide array of applications, from computer and mobile technology to cutting edge medical applications. Specifically, micro-parts are used as electrical connectors, micro-switches, micro-gears and shafts for MEMS devices, and even micro knives for precise surgical applications. Figure 1 shows some examples of micro parts which can be used in some of these applications.

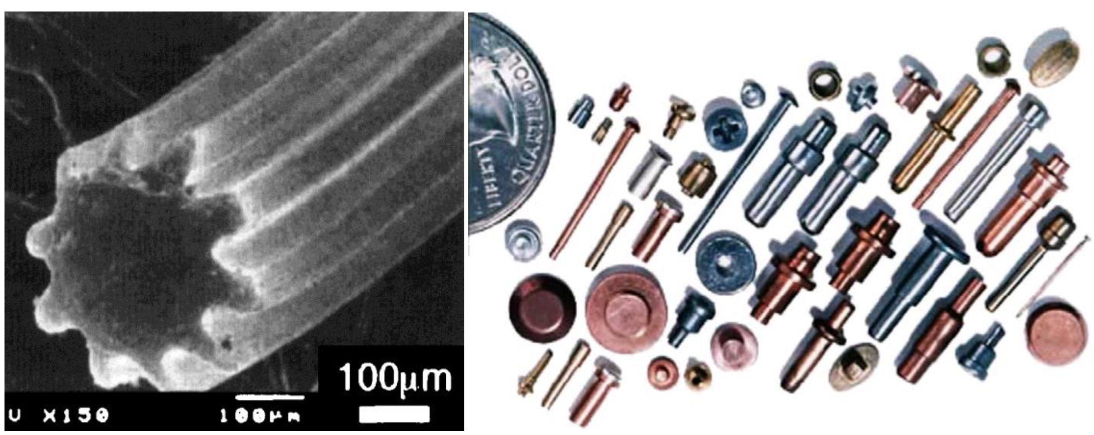

(a) (b)

Figure 1: Micro-Parts created by Microforming Techniques (a) Micro Gear Created by Micro Extrusion [1] (b) Parts Created with Micro Heading [2]

As consumer and high tech devices become smaller and more complex the demand for smaller and smaller parts is rising rapidly. Though many of these parts can be produced with methods such as micro-machining, laser machining and electric discharge machining, these processes are slow and energy intensive and, thus, difficult to scale up to the large production rates that are necessary for mass production of micro-components. As is the case in traditional manufacturing, these methods of producing small features are best suited for creating tools and dies, filling low part volume manufacturing needs, and performing finishing operations near net shape parts. The best way to meet the new demand for the large scale production of micro-parts is through a near net shape process like metal forming due to its accuracy, cost effectiveness, and ability to produce a large number of parts rapidly. However, the material behaves much differently on the micro-scale, affecting the flow stress of the material, the interface friction, and the repeatability of the process. It has also been found that processes that are feasible on the macro-scale may be nearly impossible to apply to micro-scale applications because they behave so drastically different when the features being produced are very small. It is for these reasons that there has been a considerable effort in the past decade and a half to conduct research into the microforming process to better understand the so called 'size effect'.

2.2 Microforming Challenges

There are numerous problems associated with decreasing the dimensions of the part that is to be formed. Size effects change the way that a work piece behaves when it deforms. These are generally caused by the change in the size of surface topography and grains relative to overall part dimensions. As part size decreases material handling and machine tolerances become big issues. Increased tool wear becomes a problem on the micro scale as well, as tool life is integral in the cost effectiveness of microforming [3]. Finally, the simulation of the microforming process is difficult because traditional models do not account for size effects [4].

2.2.1 Size Effects

Size effects in micro forming are caused by a change in the surface topography and grain size relative to part dimensions. For example, consider the grains of a macro scale part. The grains have a size on the order of micrometers and therefore there are so many grains that the part's properties can be considered an average of all the grains in the part. Now consider the grains in a micro scale part. The part dimensions are on the order of micrometers and the grain size is also on the order of micrometers. This means that the material which composes the part can no longer be considered the average of many grains, but rather takes on properties depending of the orientation and tendencies of each of its grains. Size effects can cause changes in the frictional response of the work-piece and can even change the flow stresses and formability of the part. Lastly, size effects are responsible for large scatter in part shape and material properties.

2.2.1.1 Size effects in Friction

Friction is of great concern in microforming. This is because the ratio of frictional energy increases in comparison to the energy consumed by the deformation of the material, one must ensure that the part is well lubricated. Traditional methods of lubrication, like zinc phosphate conversion coating, may add a significant thickness to the part because the thickness of the conversion coating may be on the order of the thickness of the part [5].

In general it can be assumed that as part size decreases friction will increase, however, this is not the whole story. The increase in friction is only seen when the part is lubricated with a liquid lubricant [6]. The open and closed lubrication pocket model, illustrated in Figure 2, can explain this phenomenon. This model assumes that parts are characterized by small ridges and valleys on their surfaces and when a part is deformed the tool tends to flatten the ridges, decreasing their height and applying pressure to the lubricant in the valleys of the piece. If there is no opportunity for the lubricant to escape the valleys, the pressure on the fluid increases and the lubricant assists in deforming the part. On the other hand, if the lubricant has the opportunity to flow to the edges of the part and escape, then it will escape and fail to assist in deforming the part. This increases the normal force on the metal of the actual part and causes the friction effect to be higher in areas where open pockets are abundant [7]. This effect can cause the friction coefficient to increase to 20 times its normal level (its macro scale level) [8].

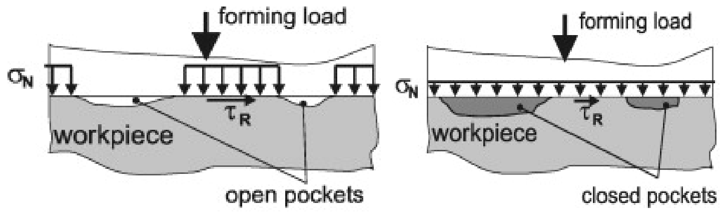

Figure 2: Left- Open Lubrication Pockets, Right- Closed Lubrication Pockets [8]

Due to the fact the closed pockets must be isolated from the front and back edges of the part in order to prevent lubricant loss, open pockets are far more numerous at the edges of the part. The extent of the zone where open pockets dominate is largely controlled by the surface topography of the part, which is not influenced by part size. So for a part with a fixed surface topography, the open pocket zone will exist in all areas which are within a certain distance of the edge of the part. Consequently, as the part size decreases, all areas become closer to the edges of the part and the relative number of open pockets to closed pockets increases, as shown in Figure 3. This creates an apparent increase in friction [8].

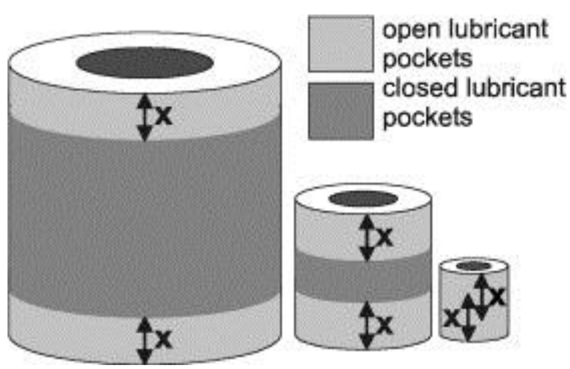

Figure 3: Example of the Reduction in Closed Lubrication Pockets with Reduction in Part Dimensions [8]

This model can be confirmed by experiment. It can be observed that when liquid lubricants are used the friction effect increase as part size decreases. When no lubricant is used, or when a solid spray lubricant is used, there is no observable size effect. Additionally SEM photographs of macro size parts show a distinct flattening of the ridges in the open pocket area as compared to the center of the part [7].

The double cup and forward-backwards cup extrusion test are both experiments that allow the friction size effect to be examined. The double cup extrusion test is performed by positioning the blank (a cylinder) between two punches, one punch moves and the other is stationary. The relative motion of the punches and the presence of friction cause the metal to move towards the direction of the moving punch primarily. If punch speed is held constant, the ratio of the height of the large cup to the small cup will change based on the amount of friction present between the work-piece and tool (see Figure 4). Higher friction will cause the ratio to increase and lower friction will make the ratio tend towards 1:1. The forward backward extrusion test works in a similar way, with the amount of friction being represented by the ratio of rod length to cup height [7].

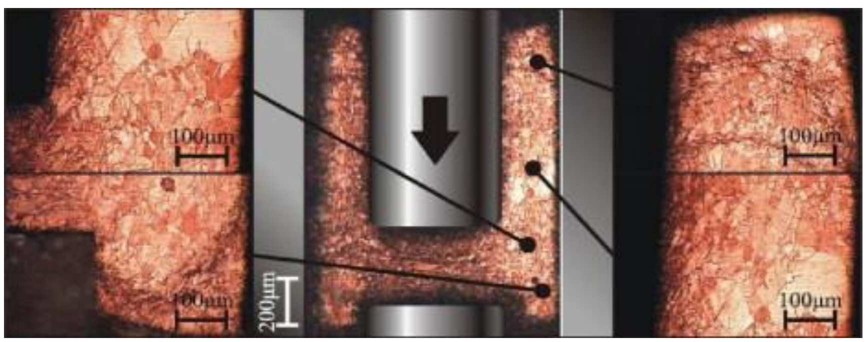

Figure 4: Friction Causes More Material to Flow towards the Moving Punch in the Double Cup Extrusion Test [9]

The upsetting test is also useful for determining the effect of friction of the forming process because the amount of barreling seen in the deformed specimen can be traced back to the amount of friction present in the system. This technique can be used to separate the effects of friction from the material's flow curve [10].

2.2.1.2 Size effects in Formability

Due to the low number of grains in the deformation zone of micro-parts, the formability of micro-parts is decreased. Because on the micro scale a part can no longer be considered a homogeneous, isotropic substance, the behavior of the part is significantly different than its macro scale counterpart. On the micro level each individual grain's size, properties, orientation, and position in the part can come into play. The ability of the part to be shaped can be adversely affected by just one grain being in an unfavorable position, whereas on the macro level other grains would be present to make up for the lack of formability in one grain. Furthermore it has been found that the formability of parts when there is only one grain in the deformation zone is significantly decreased. Essentially, the flow of the material is dictated by the random properties this single grain, resulting in inhomogeneous flow of the material [9]. Moreover, because the work-piece now behaves more similarly to a material made up of only a few crystals, the number of slip systems that are active in the part are significantly decreased. This has the result of reducing the fracture strain and overall formability of parts which have feature sizes on the order of the grain size in the material [11] [12] [13]. It should be noted that when a micro tube is put through the flaring test that this size effect was not observed [14].

Another factor which affects the formability of the material on the micro-scale is the relative size of surface defects created during billet preparation. For example, the size of the surface flaws created via rolling and EDM do not very with the size of the part. This has the result of creating defects in the part which become large relative to the part size when characteristic dimension of the part is on the order of 100μm. This 'large' defect is likely to cause the premature necking of the work-piece leading to a significant drop in the formability of the material [11].

Super plastic materials have been used to overcome this decrease in formability. For example, super plastic materials have been used to make gears modules of as small as 10 micrometers and micro-tubes [1][15]. By utilizing the already high formability of these materials, the negative effects of the formability size effect can be compensated for.

Increasing the temperature of the work piece can also increase formability, much as it would in a normal forming process [16][17][18].

2.2.1.3 Size effects in Flow Stress

It has been shown that as part size decreases the flow stress curve of the parts tends to decrease. This can partially be explained by the change in the number of surface grains as compared to volume grains (as seen in Figure 5). As the relative number of surface grains increase so does their influence on the system response as a whole. Surface grains are less restricted than their analogous volume grains, due to them being at least partially free from contact with other grains [2][6][12]. It therefore stands to reason that a micro part which is much more composed of surface grains is freer to deform under load.

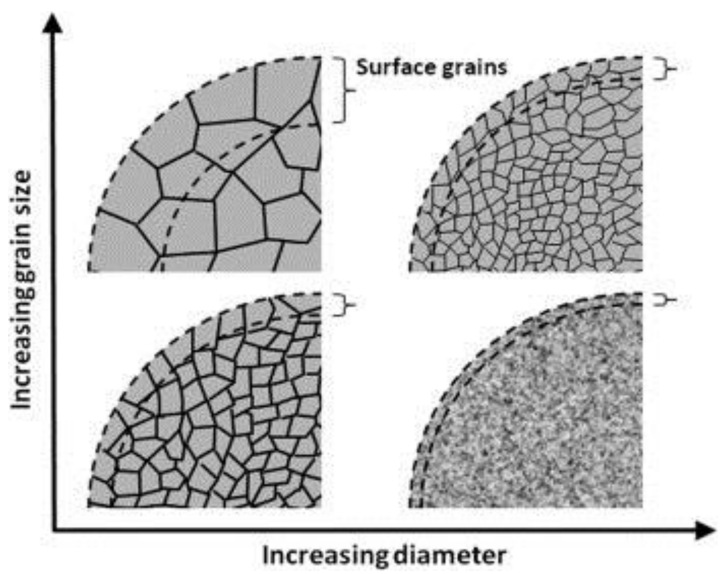

Figure 5: Relative Number of Surface Grains Increase with Decreasing Part Size [3]

Chan et al. proposed that another explanation of this effect was a decrease in the volume fraction of the material which was composed of grain boundaries [9]. The reduction in the amount of grain boundaries allowed the dislocations to flow more freely through the material because the grain boundary is typically responsible for causing the pileup of defects in the material which result in strain hardening. This is essentially a Hall-Petch relationship.

In order to better estimate the flow stress as it relates to part size and feature size Mahabunphachai and Koc ran hydraulic bulge tests on thin sheets of SS304 [19]. They realized that as the thickness of the sheets decreased the flow stress of the material decreases. This has been readily explained with the surface layer model, which states that grains on the surface of a part experience less strain (work hardening) than their counterparts inside the material. Also, as part size decreases the proportion of grains which are on the surface of the part increases, ultimately leading to a reduction in the flow stress of the material. The researchers also observed a tendency for the flow stress of the material to decrease as the size of the bulging die was decreased, until a critical size was reached and the effect began to reverse. The surface layer model fails to predict this outcome and so a new material model must be constructed to account for this phenomenon. To this effect, a material model was created which utilized the Hall Petch relation, Hill's theory of plastic deformation, and the material power law to predict the flow stress of the material with varying feature size and part size, relative to the grain size. The equation took the form of:

$$\sigma = \left(a + b\sqrt{N} + c\left(\frac{M^2}{e^{\varepsilon}}\right)\right)\varepsilon^n$$

Where a, b, and c are material constants that must be obtained through experimentation and n is the strain hardening exponent. Additionally, the constant M is the ratio of the bulge diameter to original thickness of the sheet and the constant N is the ratio of the original thickness of the sheet to the size of the grains in the sheet. It can be seen that the relationship developed takes the form of that traditional flow stress curve predicted by the power law, but that there is a correction factor which is added to account for size effects (M and N). It was shown that this material model showed good agreement with the experimental data collected by the authors, as well as, with data collected in an independent hydraulic bulging test. [19]

2.2.1.4 Size effects in Reproducibility

Microforming studies typically have some problems in reproducibility which increases as the part size decreases. The increased scatter seen in microforming operations is a result of the low number of grains in the deformation zone of the part. The random orientations of each grain come into play in the final shape and properties of the final part [2]. The increase in scatter can also be considered the result of an increase in the relative size of grains as compared to part dimensions. This can be examined without the interference of the friction size effect if the part size is held constant and the grain size is increased [20]. This scatter effect causes an inconsistent and unpredictable final shape and is very inconvenient for those attempting to achieve low tolerances [21].

The effect of scatter can be mitigated through by heating up the work piece to a temperature between the room temperature and the recrystallization temperature [16]. Increasing the process temperature has the effect of activating new slip systems allowing grains in unfavorable positions to be plastically deformed. It has been shown that even increasing the temperature moderately has a marked effect on reducing the scatter in the hardness distribution of upset and backward extruded micro-parts, while at the same time maintaining the same average hardness value as a cold formed part. Egerer and Engle have also shown that the scatter in the flow stress curves and the final part dimensions can be significantly reduced via the use of warm forming techniques. Overall, it has been shown that the scatter can be reduced in the microforming process without losing the benefits of work hardening by increasing the process temperature to the warm forming range [17].

2.2.2 Material Handling

In macro-sized applications the use of conventional grippers is highly effective because the weight of the parts is much higher than the adhesive forces on the part. This is not the case when part size is decreased to a significantly low level. Because of the relatively high adhesion forces in the microforming process, special consideration must be made when handling the work piece. Vacuum operated or noncontact grippers would be ideal for this process due to their ability to avoid the adhesion problem that conventional friction based grippers have. There are numerous ideas to accomplish this feat, such as the use of the Bernoulli Effect, ultrasonic levitation, or small tubes that maintain a vacuum [22].

Another problem in the material handling field that must be accounted for on the micro level is that precise control over the force applied to the part is needed. Small parts are much easier to deform or break due to their small cross-sectional areas or tiny features. Therefore the tolerance in applied force is very small and must be closely monitored and regulated during the handling steps of the forming process [22].

In some cases grippers can be avoided all together. If the parts are being stamped or formed out of pieces of wire, the parts can simply be formed without cutting them from the base material. This reduces the handling of the material to the handling of the wire or sheet, but raises new problems because the dimensions of the base material change significantly during the forming process. In the case of parts connected by a wire, it has been shown that cameras and sophisticated control systems could be used to accurately measure and compensate for the change in the position of the parts, relative to each other. [23]

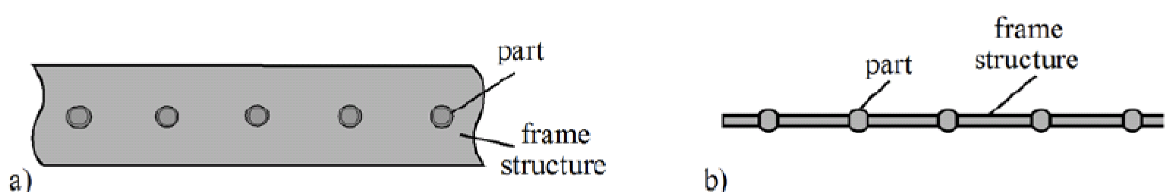

Figure 6: Illustration of Parts Held together with a Frame Structure (a) Parts are Connected via a Sheet (b) Parts are Connected Via a wire [23]

2.2.3 Microforming Tooling

Metal forming becomes advantageous only when the number of parts produced by each punch or die is high due to the high cost of fabricating this tooling. Tooling therefore poses a large problem to the usefulness of microforming because of the increased rate of wear associated with scaling down to the micro-level. An additional problem is that the manufacture of dies must be performed with special, high precision techniques that are relatively expensive [2]. This problem is compounded by the need to use very hard materials to lengthen tool life. The combination of these restraints generally requires that the tools be fabricated at their desired hardness. Fabricating tools in this way is, in most cases, more costly, but hardening after shaping the tool can remove much needed precision from a microforming system.

Due to the large surface area of micro-parts warm and hot forming of parts creates special problems. Namely, heating of the part outside of the die set and then moving it into position becomes impossible because of the rapid dissipation of heat that occurs as a result of the high surface to volume ratios in micro-parts. Thus, it is necessary to do all heating of micro-work-pieces via the die surfaces, which requires special heaters to be included in the dies. This may also present challenges to the life of dies, especially in the case of hot forming, as elevated temperatures in the die generally result in increased wear [17].

There are several options for the creation of micro-dies used in the forming process. The die can be created out of a photo-chemically machinable glass, which is created by chemically removing pieces of the material that have been treated with UV radiation [1]. (This technique was used to make micro-gear dies). Micro-dies may also be machined with micro milling and lathing tools, although it is difficult to ensure that tool wear does not become an issue in this case. Variations on the EDM process can be used to make accurate parts, as well as laser erosion (ablation) [2]. It should be noted that laser erosion can be time consuming and is a two to three step process that generally is marked by a rough pass, a smoothing pass, and sometimes a polishing pass. In some cases the surface quality of the micro-tool can be improved through the use of ion sputtering in which the tool is covered in a thin film of ions that are showered over it [24].

2.2.4 Micromanufacturing Machines

There may be several benefits to the reduction of size in micro-manufacturing. The reduction in the mass of the moving components means that the machines may move much quicker without creating high stresses associated with inertial forces. The small size of the machines also lends itself to 'desk' or 'bench' top manufacturing, in which the machine can create a high number of parts without taking up a large amount of floor space or affecting other machines and process in the plant [25]. However, there are several costs in the miniaturization of conventional machines.

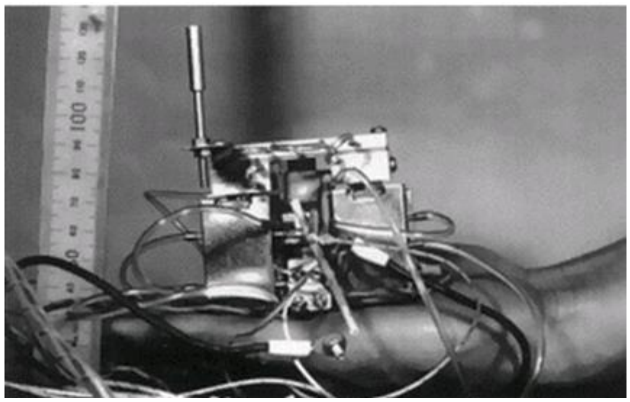

Figure 7: A Micro-Extrusion Machine for the Super Plastic Extrusion of Gear Shafts [1]

Human labor is commonly used to make sure that everything is in the correct position, which drives up the cost of manufacturing micro-parts [22]. Decreasing the cycle time and increasing the cost effectiveness of micro-manufacturing will require the development of control systems which can automatically position blanks, carry out the forming process, and remove the part rapidly and without human intervention. This will require the use of complex sensors which have resolutions in the sub-micron range. The size of the sensor will need to be very small, as bulky sensors will not be able to fit into micro-manufacturing machines. [25]

Precise positioning of the blank and the tools used to create the part are needed in order to ensure the close tolerances needed in microforming. This means that the backlash and subtle vibrations associated with large scale machines must be eliminated. The machines that carry out the microforming process must have a resolution on the scale of micrometers and have high repeatability in order to be of use. This is especially important in the micro-stamping process in which progressive forming needs to place features within a few microns of each other. Errors in the positioning and motion of the tools can damage the part, creating high scrap rates or preventing the stamping operation entirely. Thus, extremely accurate feeding of the sheet and action of the tools must be achieved to create a cost effective stamping operation [25]. Machines like these have been used to create small 3D shapes in very thin foils with the help of a SEM [26]. Currently, there are numerous machines capable of meeting the requirements of microforming, but they tend to be bulky and expensive.

2.2.5 Simulation of size effects in Microforming

Because of the size effects present in microforming, traditional simulation techniques cannot be applied if very accurate results are needed. Traditional techniques fail to predict the size effect and thus are subject to large errors when tasked with predicting the behavior of small work pieces [9][20]. There are several methods to work around this problem, including experimentally determining physical properties and then modifying conventional FE methods to reflect the new process. However, this method is of limited use, as it is typically only applicable to one or two scenarios for which it was designed. It also fails to predict the scatter that is associated with the microforming process.

Additionally, there have been some efforts to model the grains in the material that cause many of the differences between micro and macro scales. This has been done either through the use of new element types that represent individual grains and grain boundaries [27] or by creating crystal-plasticity finite element model, which places a mesh over a predetermined, randomized grain structure [21]. The former method is good at accounting for the decreased flow stress and formability, but is unable to predict scatter. The latter method is good at predicting the decreased flow stress and scatter, but does not take into account the role that the inter-grain boundaries play in the part deformation. Figure 8 shows how a finite element model which uses multiple grains can simulate the localized necking observed in a micro tube hydroforming process. In many cases, the models which have been developed to simulate the action of grains in the material can only predict qualitative results and cannot be used to simulate actual process. This is especially true when the simulation results depend on knowing the exact orientation, position, and properties of each grain in the workpiece. However, there are some useful applications of these grain models. Namely, they can be used to predict the size of the grains in the material which will cause the scatter in the process to decrease [28].

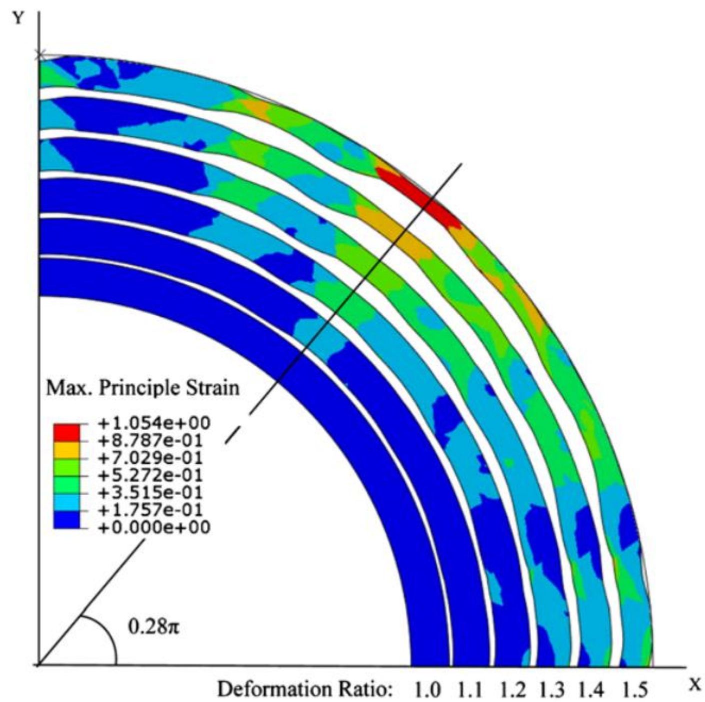

Figure 8: Localized Necking Predicted by a Finite Element Model which used a Mesh Placed over a Predetermined Grain Structure

In some simulations new constitutive models have been developed which account for the size effects observed in micro-forming. In a study conducted by J Liu et al., a model of the flow stress curve was derived via the combination of the grain size effect and the surface layer model [29]. The material in the model was considered a mixture of grain interiors and grain boundaries. The higher the fraction of grain boundaries in a body the higher the flow stress in the material. The fraction of grain boundaries in the material decreases with increasing grain size, which has the overall effect of decreasing the flow stress on the material.

Furthermore, because the material is much freer to move on the surface of the part, the grains in this area were considered to have no grain boundaries. This serves the purpose of decreasing the flow stress when the size of the part decreases and the grain size increases. Validation of the model showed good results for the simple process of cylindrical upsetting and uniaxial tension of a thin strip. However, the simulation of a more complex micro-forward extrusion predicts a different load stroke curve than was observed in experiments of the extrusion process. Specifically, the load predicted in the simulations is too high at low strokes, but at the end of the stroke the observed and predicted loads were nearly the same. It should be noted that this material model cannot account for the reversing of the reduction in flow stress observed by some researchers when the size of the grains approached the size of the part or formed feature [29].

Not all microforming processes have to be simulated with the inclusion of size effects. For example, in the dieless drawing process of a superplastic tube, the material behaves more or less like it would if the process was on a conventional, macro scale. This is most likely due to the required process parameters in superplastic deformation being high temperature and small grain size. The small grain size should make the material perform more like a continuum body than a body made of only a few crystals. The high temperature will have the result of homogenizing the material further removing the size effect. Additionally, due to the absence of dies in the process there is not a work-piece die interface from which the frictional size effect can occur. This all has allowed researchers to model the superplastic dieless drawing process with conventional know how, rather than having to develop sophisticated material models to be used specifically in the micro-scale [15].

2.3 Studies on Specific Mircoforming Processes

A few examples of what roles the various size effects play on a microforming process are needed in order to clarify their importance on scaling down traditional metal forming processes.

2.3.1 Micro-Extrusion

Studies into the micro-extrusion of copper by Chan et al. show that the effect of friction increases greatly as the part size is decreased [9]. This increased friction can be observed in the form of the domination of backward extrusion in combined forward backward extrusion process. The mechanism of closed and open lubrication pockets is likely the culprit behind the increase in friction between the tool and workpiece. From the description of the size effect in previous sections one would expect that as the size of the grains increased, relative to the part size, that the flow stress and punch load would decrease. However, the researchers noted that this trend was limited to the case of the forward extrusion process. It is thought that this is because as the size of the grains increase, relative to the clearance between the punch and the die, the material begins to resist flow in the backward direction and the punch load increases. The increase in grain size was also associated with inhomogeneous material flow which resulted in an uneven cup height of the final part. It can be seen that simulations of the micro-extrusion process will need to be quite sophisticated in order to account for the size effects that are present in the process [9].

The superposition of ultrasonic waves on the extrusion of micro-parts can significantly reduce the press forces and improve the surface finish on the part. In the experiments it has been shown that the forming load could be reduced buy up to 23% when ultrasonic vibrations were added to the forming process. Micrographs of the surfaces of the extruded micro parts indicate that there was less sticking under ultrasonic conditions and that there was a roughening of the surface, indicating that there were tiny lubrication pockets that were formed by the addition of the vibrations. The friction was thought to be reduced by the high instantaneous relative velocity between the die and work-piece, which reduced the adhesion tendency of the material. The vibrations and reversal of the direction of friction also served to distribute lubricant around the die work-piece interface and ensure that the lubricant could not escape the lubrication pockets formed by the surface roughness [5]. Some of the parts that were created in this study can be seen in Figure 9.

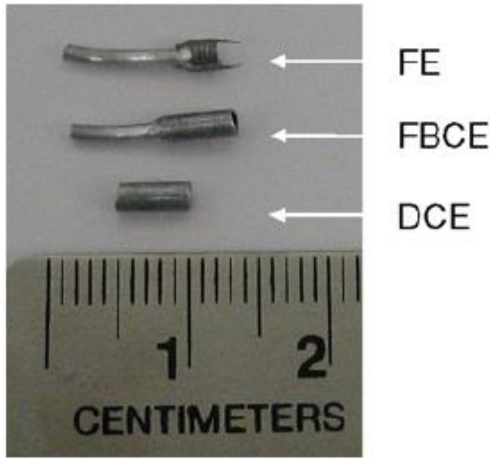

Figure 9: Parts Produced via Ultrasonic Assisted Micro-Extrusion [5]

2.3.2 Micro-Sheet Metal Forming

Fu et al. conducted research into the simultaneous blanking and deep drawing of thin copper sheets [30]. They investigate the effect of grain size relative to sheet thickness and feature size on the forming load and final part quality. They also compared their experimental results to simulations of the process created with a conventional simulation technique. The researchers found that the deformation load dropped as the grain size increased. This action was attributed to both the change in surface grain fraction and the change in grain boundary strengthening behavior, predicted by the Hall-Petch relation. In addition to the decrease in flow stress, it was observed that as the grain size increase the material began to deform in an inhomogeneous manner. This had the effect of allowing grains in favorable positions to deform, regardless of the grains around them, leading to a large localization of strain in the 'soft' grains and an overall reduction in the material strength [30].

The surface quality of the deep drawn parts decreased with increasing grain size and decreasing feature size. This effect is most likely due to the fact that when there are only a few grains in the deformation zone (around the radius of the punch and through the thickness of the material) the flow of the material becomes highly irregular. Some of the grains will deform heavily, while others will resist deformations resulting in a part which has an extremely unpredictable surface. Earing was also observed on the drawn parts, but, unlike the surface roughness, the earing was worse when a punch with a large radius was used [30]. The micro-cups created in this study can be seen in Figure 10.

Simulations of the macro scale deep drawing process were run to determine if they could be applied to deep drawing on the micro scale. It was found that the simulations predicted punch loads which were up to 15% different from the loads observed in the actual drawing process. In order for the simulations to be more accurate size effects need to be taken into account for friction and the flow stress of the material [30].

Figure 10: Deep Drawn Micro-Cups [30]

2.3.3 Micro-Tube Hydroforming

The application of the tube hydroforming process to the micro scale is currently in its infant stages, with only basic research into tube bulging without axial feed being carried out. For example, in 2008 the Advanced Metal forming and Tribology Laboratory at North Carolina State University began its research into the bulging of stainless steel 304 (SS304) micro tubes [31]. The investigation was carried out on tubes that had an outer dimension of 1.0668 mm and wall thicknesses varying from 0.0635 mm to 0.1905 mm. To accomplish the bulging the researchers developed a set of equipment which could be placed on a large press and fill with high pressure fluid from an external pressure intensifier, this tooling is pictured in Figure 11. The die features 4 cavities for the placement of micro-tubes and a conical taper on both ends of the die for high pressure fluid supply. Conical punches were presses into the conical fluid ports in such a way that a metal to metal seal was created between the two surfaces. Another seal was created between the upper and lower halves of the die by using a 1.494 MN (150 ton) press to clamp the two halves together. Finally, to seal the area around the circumference of the tubes, two Teflon sheets were placed in the die cavity such that a layered structure was created, i.e. bottom die | Teflon sheet | tube | Teflon sheet | top die. When compressed, it was shown that this created a reliable seal and prevented fluid from escaping the fluid cavity. The hydroforming process was carried out by filling the fluid cavity with the working fluid and allowing it push out any air in the tubes and fluid cavity. With this system a good seal was created which was capable of withstanding pressures of up to 140 MPa, the maximum pressure which could be supplied by the system, and the free bulging of the parts could be performed. Some of the parts created in the study are shown in Figure 12.

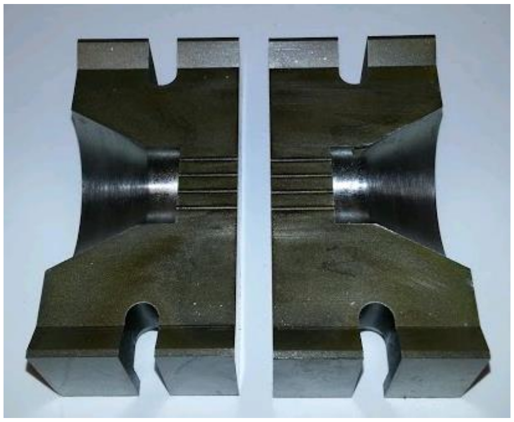

Figure 11: Dies Used in the Bulging of Mirco-Stainless Steel Tubes [31]

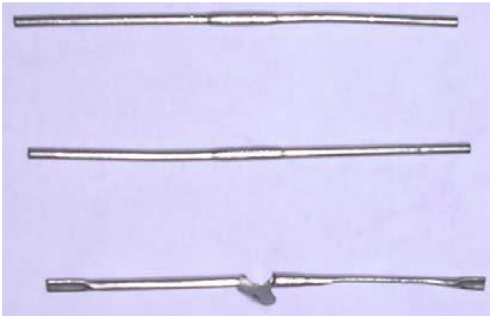

Figure 12: Bulged Tubes Formed with a Micro-Tube Hydroforming Process [31]

In another study, Zhuang et al. found that tubes would fail unpredictably in a simple bulge where the tube ends were flared to seal the tube (see Figure 13) [28]. The investigation that was then carried out utilized the finite element method to investigate the effects of various crystalline structures in the tube blank on the phenomenon of localized necking and random failure. They were able to show that, because the number of grains in a micro tubular blank is low through the thickness of the wall, the orientation and properties of each grain will play a crucial role in the deformation pattern and failure in the workpiece [28].

Figure 13: Random Failure Exhibited During the Bulging of Micro-Tubes [28]

Unlike, the previously mentioned studies, most tube hydroforming applications use a rigid die to restrain the material as it is being formed. This poses a problem, because as the tube hydroforming process is scaled down to the micro-level, there is not a significant drop in the amount of internal pressure which is necessary to fully form the tube. Hartl et al. noted that the amount of pressure needed in the micro-THF process could reach levels as high as 400 MPa [33]. He proposed that these high pressures could be enough to cause a significant level of deflection of the die cavity. Using the finite element method the authors found that the die cavity could be deflected by as much as 0.375% of the original diameter of the tube in a simple bulging case. They proposed that in order to reduce the amount of deviation from the desired shape of the tube that bending stresses be supper imposed on the die. This method would allow the processes designer to design the die so that the appropriate die cavity shape is maintained throughout the forming process. Using the finite element method on a plane strain cross section of the die cavity they showed that they could reduce the amount of defection in the die cavity to just 0.1% in one direction and completely eliminate the deflection in the other direction [33].

The PhD dissertation of Jörn Lungershausen, published in 2012, focused on the development of a micro-tube hydroforming device [34]. The research in this study was conducted with SS304 and copper tubes and was conducted as one of many projects done with funding from the EU project MASMICRO. The first part of the study covered the material testing that was completed in order to determine the formability of the various types and sizes of micro-tubes. A flaring test was chosen to represent the formability of the tubes under hydroforming conditions due to its biaxial stresses and ease of use. The researchers found that they could significantly reduce the scatter observed in the final diameters of the stainless steel samples by warming the tools and samples to 300 °C during the flaring test. The warm flaring also slightly increased the mean expansion achieved by the testing. This trend was, however not observed in the warm flaring of copper tubes. Warm forming did decrease the forming load in all cases, but the scatter in the load data was unaffected for copper tubing [34].

In order to get a better understanding of the forming limits of the tube and remove the effects of friction and compressive axial stresses present in the flaring test, the researchers decided to perform free bulging experiments. It was thought that these would be a more adequate way of evaluating sample performance under actual hydroforming conditions. The free bulging tests were conducted with no axial feeding and sealing of the tube was accomplished by plastically deforming the tube ends by wedging them between a hard conical punch and a conical mating surface. The heating of the samples during warm free bulging experiments was only done after a certain internal pressure was supplied, due to the desired temperature being well above the boiling temperature of the pressurized media at nominal pressures. The researchers noted that the bursting of the tubes did not necessarily occur in the same spot every time and could occur almost anywhere in the deformation zone. This is consistent with the findings of Zhuang et al. in the study presented at the beginning of this section [28]. It was found that equation 1, which relates the bursting pressure (P_{ib}) to the ultimate tensile strength of the material (U_{uts}) and the initial diameter (D_o)and wall thickness (t_o), could be used on both the macro and micro scales. Another finding was that the application of laser heat to the process of micro-tube hydroforming did not provide a benefit which was significant enough to warrant its application to the process. Ultimately, the free bulging tests showed that the flaring test significantly overestimated the achievable expansion ratios of the tube and that free bulging tests must be conducted to accurately determine the forming limits in a micro-tube hydroforming process [34].

$$P_{ib} = \sigma_{uts} \frac{2t_o}{D_o - t_o} \qquad \text{Equation 1}$$

In designing their micro-tube hydroforming machine the researchers were able to conclude that die design must be done in accordance to the lowest observed expansion of the micro-tubes, due to the high amount of scatter in the process. If this principle is not followed, the process will exhibit high failure rate and become uneconomical. The researchers chose to form a “camera shaft” as their desired part, see Figure 14. They conducted their hydroforming experiments without axial feeding and sealed the tube ends with a conical punch. A picture of the microforming machine developed for their micro-tube hydroforming experiments is given in Figure 15. They were able to completely form the part using annealed SS304 as seen in Figure 16. They noted that the formed tube was eccentric and attributed this to the large grain size in the material. The annealed SS304 used in the experiments had only one grain through the thickness of the wall. This may have caused inhomogeneous plastic deformation during forming and inhomogeneous spring-back behavior after forming. The researchers also stated that there were difficulties in properly aligning the tubular blanks in the exact center of the die cavity, which resulted in improper sealing in some of their tests [34].

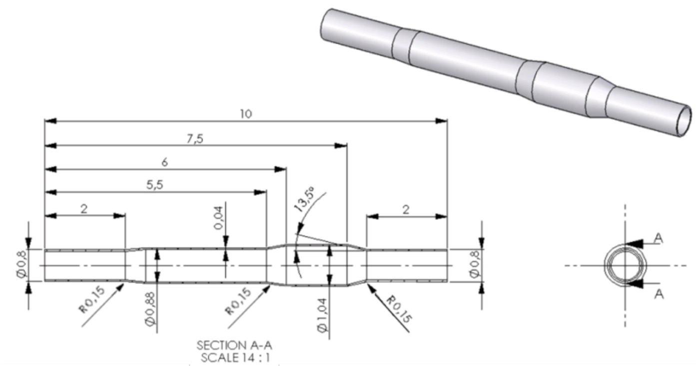

Figure 14: Camera Shaft Schematic to be created via Micro-Tube Hydroforming [34]

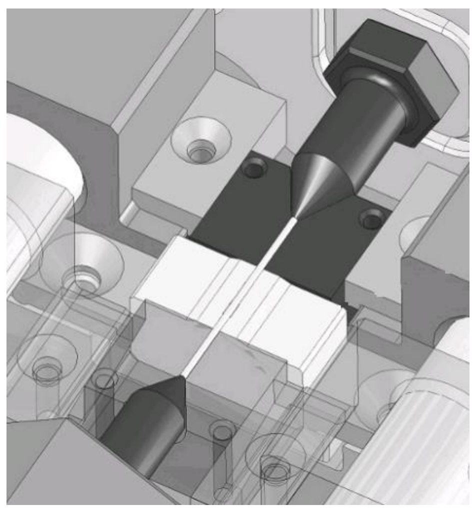

Figure 15: Die and Punch Design used for Micro-Tube Hydroforming Experiments [34]

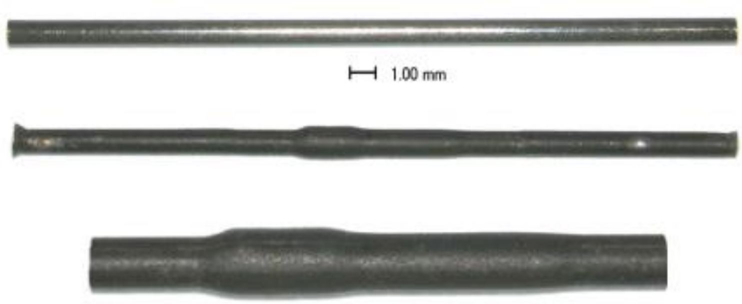

Figure 16: Successfully Hydroformed Micro-Camera Shaft [34]

In 2013, Wagner et. al were able to successfully perform free bulging experiments using a deformable gasket as a seal [35]. The system works by first fitting both ends of the tube into a small hole that goes between the outer and inner diameters of a pair of gaskets. These gaskets are then compressed into a cavity, which forces them to make tight contact with the wall of the tube. The system can then be pressurized at one end and air can be bleed off at the other. Once the air has been removed from the system the bleed valve can be shut and the pressurization of the system can take place. A picture of the tooling used in their bulging experiments is given in Figure 17.

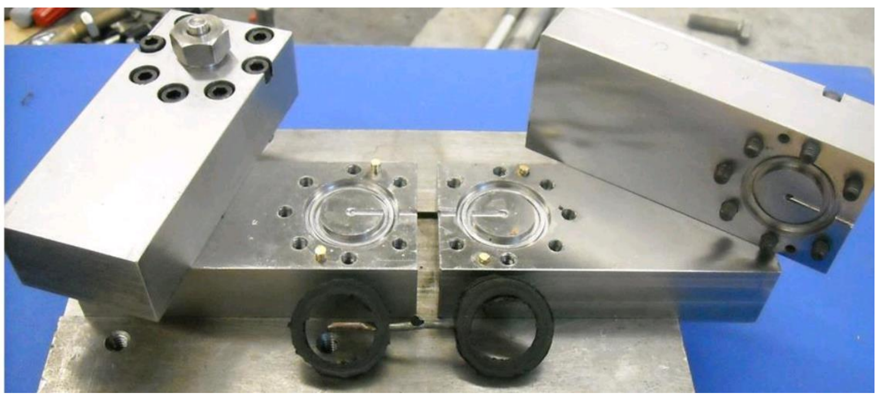

Figure 17: Micro Free Bulging System created by Wagner et. al [35]

The researchers examined rubber, annealed copper, and Teflon as possible materials for the gasket. They noted that the rubber seals could provide a high quality seal, but experience significant amounts of extrusion each time an experiment was performed. When the copper material was used for the gasket the researchers again noted that a high quality seal was created, but the copper was hard to remove from the seal cavity in the die blocks and tended to crush the ends of the tubes. The Teflon gaskets tested showed similar tendencies with the copper material. The copper material and the Teflon gaskets could not be used more than once because the hole that the tube went through was plastically deformed. The rubber material could be reused several times until it was destroyed by the extrusion created during the pressurization of the system.

Their system provided them the ability to study the effect of applying electric current to the tube as the free bulging took place. They noted that there was a decrease in bursting and yielding pressure of the tube when both continuous and discontinuous current was applied. It was however not clear, what effect the current had on the maximum expansion of the tube due to the sudden bursting of the tubes resulting in a change in the shape of the tube. It was also discovered that annealed stainless steel tubing was more effected by the current than the ‘as received’ tubing, even though there was a greater temperature rise in the ‘as received tubing. This part of their research is particularly interesting due to the reduced pressures that can be used as a result of reducing the material’s yield strength.

When comparing this method of sealing to the studies done by the AMTL and by Jörn Lungershausen’s group it can be seen that there is a clear advantage in not have to use a press and in the simplicity of the design. This makes the design a cheap way to conduct free bulging experiments, but this comes at the cost of low cycle times and an inability to provide axial feeding to the tubes. This method could prove to be an easy way to conduct material property tests, but likely would be difficult to scale up to the production rate of full scale manufacturing needs [35][36].

2.4 Concluding Remarks

Micro-forming is a widely researched topic with applications in a wide variety of fields. Extensive research on the characterization of materials on the micro-level has been conducted with a focus on a few microforming applications, like extrusion and sheet metal forming. The main challenge facing researchers who want to further develop these fields is the size effect, but there are also issues associated with handling micro-sized material, designing and creating microforming tools and machines, and simulating the work-piece behavior on the micro-scale.

The size effect creates issues in the characterization of material properties, a significant increase in friction in bulk forming operations, and a large amount of scatter in the results of any tests done on the microforming process. It is for this reason that many researchers have focused their attention not on a particular application of microforming, but rather on the study of the size effect itself. Many mechanisms have been identified which could be responsible for the observed size effects. The surface layer theory can partially explain the reduction in the material flow stress, by explaining why there is less work hardening in the grains of a micro-part. The Hall-Petch relation also is able to partially explain the reduction in forming load, by stating that the reduction in the volume fraction of grain boundaries leads to a material which is less resistant to flow. The friction increase in microforming is most readily explained by the open and closed pocket lubrication model, which is able to relate the size of a part with the ratio of open and closed lubrication pockets. Because the fraction of closed lubrication decreases as the part size decreases the friction regime switches from mixed layer lubrication to boundary layer lubrication, leading to an increase in friction. Researches also believe that the transition from a body with 'many' grains to a body with few grains causes the decreased formability of the part, as well as the increased scatter in the forming process. It is thought that the random orientations and properties of each grain begin to play an increasingly large role in deformation of a material causing inhomogeneous material flow and unpredictable results. It is hoped that, with enough understanding of the size effect, simulations of micro-scale forming operations will be made possible and the trial and error approach used in industry today can be eliminated.

Research has also been focused on scaling down the macro-sized tools and machines, in order to bring conventional metal forming processes down to the micro-scale. This process has been hampered by the fact that operations which are easy to perform on the macro-scale, like deep hole drilling and maintaining appropriate clearances, become much more difficult or impossible when scaled down. This is best exemplified in the process of tube hydroforming, which has currently only been partially realized on the micro-level. In the case of micro-tube hydroforming, researches have been able to accomplish bulging and have even created machines designed for this purpose, but have been unable to produce axial feeding in the tube in combination with bulging. This has significantly reduced the complexity of the parts which can be created with the process and has hindered the development of fields which would require the use of metallic micro-tubular structures.

Further advancement in the field of microforming should allow industries that produce micro-components to mass produce a large variety of components at a very low cost. This could bring about a new age of small consumer machines and devices as well as advancements in medical technology that reduce patient pain and recovery time.

Thus, the main focus of this study has been to develop a micro-tube hydroforming system that can facilitate both material feeding and expansion. It is with these capabilities that complex micro-tubular geometries can be realized.

CHAPTER 3: CONCEPTUALIZING MICRO-TUBE HYDROFORMING EQUIPMENT

3.1 Introduction

Due to the current inability to create adequately complex micro-tubular components there are a very limited number of assemblies that include metallic micro-tubular components. However, that is not to say that there are no applications for these very small tubular parts. For example, micro-tube hydroformed parts could be implanted into the human body as part of a circulatory implant, or small shunt. They could also be useful in micro fluidic devices or micro heat exchangers, due to their thin walls and potential for very complex shapes. Additionally, due to the work hardening involved in tube hydroforming there is also the potential that they could be used as micro-shafts in micro-electro-mechanical systems (MEMS). It should also be noted that there may be numerous applications to research in any number of scientific fields that are not currently being realized (or imagined) simply due to the inability to mass produce these complex micro-tubular components.

In order to bring the field of micro tube hydroforming to the level where the potential parts mentioned above could be mass manufactured, it is imperative that axial feeding of the material be carried out simultaneously with the hydraulic expansion of the tube. As researchers have, as of yet, been unable to produce a system which is capable of material feed, it is suffice to say that the tools and dies which were developed for conventional (macro) tube hydroforming will need to be reexamined at a fundamental level. After the conventional system is analyzed, it is necessary to identify the potential problems that arise as a result of scaling down the macro tooling and propose a system which can overcome these difficulties.

3.2 Conventional Tube Hydroforming Systems

The process of tube hydroforming usually consists of five steps. 1.) the tube may be bent into the desired shape so that it fits into the die cavity. 2.) the tubular blank is lubricated and placed into the die cavity. 3.) the dies are clamped around the tube, the sealing punches are brought into contact with the tube ends, and the tubes are filled the working fluid. 4.) the forming takes place as the working fluid is pressurized and (optional) the tube ends are pushed (fed) towards the die cavity. 5.) the system is opened and the hydroformed part is removed. This is illustrated in Figure 18.

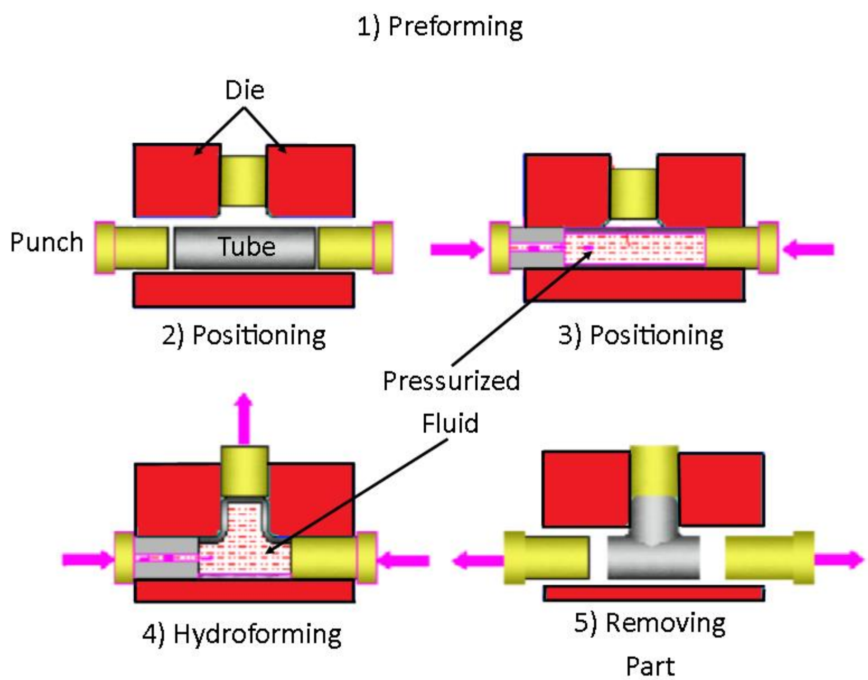

Figure 18: Five Steps in a Tube Hydroforming Process

A conventional tube hydroforming system consists of three main parts, the tubular blank, the dies, and the punches. The tubular blank may be a straight tube or it may be bent or preformed in some way. The dies are generally segmented into two halves, so that the part can be ejected after the process is finished. There are two main features of the dies, the die cavity and the guiding zone. The die cavity contains the geometry that the final part will take and the guiding zone is the cylindrical cavity in the die which keeps the outer dimensions of the tube constant during the feeding of the tube so that a seal can be maintained. The punches used in tube hydroforming take many shapes, but are essentially hard metal cylinders with a hole in the middle that allows for fluid transfer.

There are also two main interfaces in the conventional system and each performs a few specific tasks. The first is the interface between the tube and the die. Its function is to restrain the workpiece material and provide lubrication so that the material flows into the die cavity the proper final shape is obtained. The second interface is between the punch and the tube. This interface serves to provide fluid to the inside of the tube, seal the system so that high pressure can be maintained, and provide axial feed to the system. A basic sketch of these concepts is presented in Figure 19.

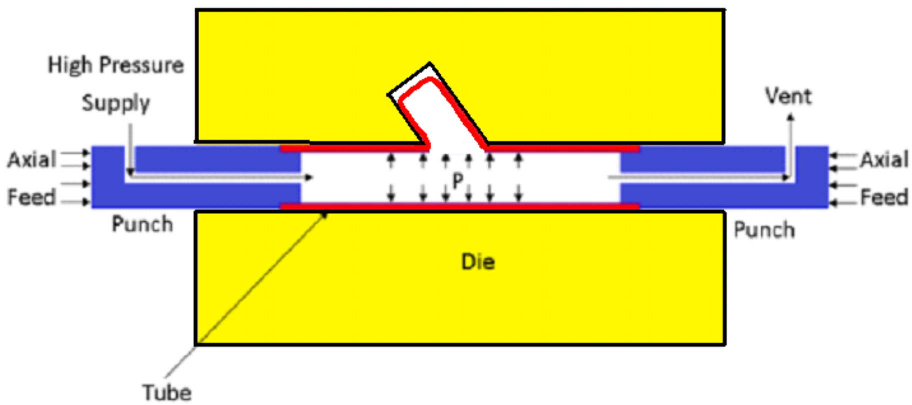

Figure 19: Conceptual Drawing of Conventional Tube Hyrdroforming Tooling

The interface between the tube and die is important because it will directly influence the final shape of the part. In order to ensure that the desired part is achieved the designer must consider the material flow during the process as well as the forming forces that appear during the process. The forming forces must be properly compensated for to ensure that the top and bottom dies do not separate during the forming and that the die cavity is not misshapen due to elastic deformation caused by excessive clamping force. The proper clamping force is usually attained by multiplying the projected area of the finished part by the maximum internal pressure used in the operation. Careful attention must also be placed in the lubrication of the system to ensure that there is no excessive resistance to material feeding and to ensure that the material can flow around the corners in the die cavity. If the designer pays close attention to proper design protocols and uses the finite element method they can easily arrive at a solution that gets them close to the desired final shape.

The punch-tube interface is arguably the most important interface in the system because it is responsible for supplying and maintaining the high pressure in the working fluid as well as feeding the workpiece into the die cavity. In order for this interface to function at all, a reliable seal must be created that moves with the material of the tube so that both expansion and feeding can take place simultaneously. As shown in Figure 20, there are numerous methods of producing a seal. For simple hydroforming applications that do not require material feeding the wedge sealing system provides and adequate seal by plastically deforming the tube ends between a conical punch and a conical mating surface on the die. This prevents the material from moving and creates a strong reliable seal. Both the conical and stepped sealing systems also create a seal by plastically deforming the tube ends, but have an advantage in that they are able to provide axial feed to the tube. This is because the ends of the tube are not pressed against a mating surface. The down side to this type of seal is that the positioning in the system needs to be very precise or there will be an uneven pressure distribution on the tube ends, which could lead to leakage. Elastomeric and O-Ring type seals compress a soft rubber material between the punch and the tube ends to prevent high pressure fluid from escaping. This gives a distinct advantage by eliminating the need to scrap the tube ends after the hydroforming process, saving time and reducing waste. The down side is that these seals cannot be used in high temperature applications and will break down sooner than metal to metal contacting seals. Note that, all of the methods of sealing shown in require the use of either metal to metal contact or an elastomeric seal and that they all require that the punch make contact with the part.

A proper understanding of material flow is also important in the punch-tube interface due to a phenomenon called material self-feeding. This happens when the internal pressure in the tube is great enough to cause the material to be pulled into the die cavity without the assistance of the sealing punches. If unprepared, a designer can lose the seal on the tube end without knowing the cause. This can be avoided by caring out finite element simulations of the process to determine the proper forming loads and displacements.

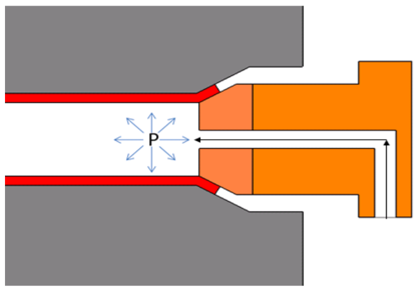

a.)Wedge Sealing System

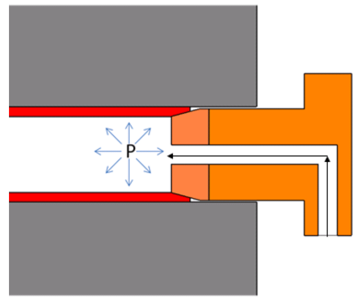

b.) Conical Sealing System

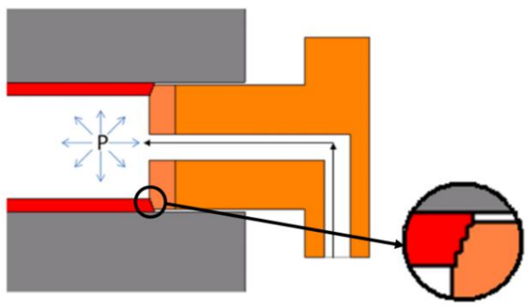

c.)Stepped Sealing System

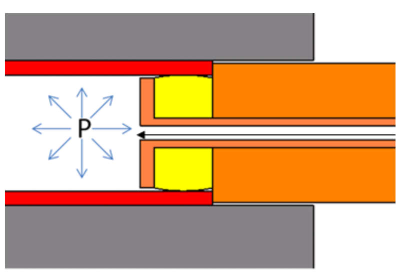

d.) Compressed Elastomer Sealing System

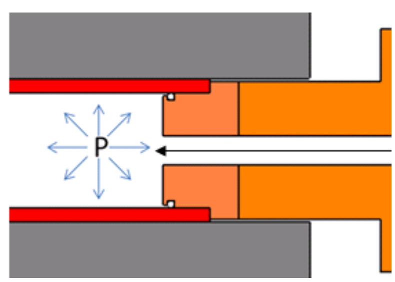

e.) O-Ring Sealing System

Figure 20: Variations on the Conventional Tube Hydroforming Sealing Systems [37]

3.3 Scaling Conventional Tube Hydroforming Tooling

As with all other microforming applications the designer runs into several challenges when attempting to scale down a conventional process. The first is that due to the small size of the tooling, the system must have very tight tolerances and precise positioning. This can be exacerbated by tool deflections caused by forming forces as well as vibrations of the tools during the forming process. The second is that it can be hard to predict the forming forces and workpiece material behavior due to an inability to quantify the size effect present in the process. Finally there are process specific problems which are unique to the metal forming process that is being miniaturized.

In the case of micro-tube hydroforming it would appear that the major reason that a system has not been created which is capable of mass producing complex tubular geometries, those which require material feeding, is that sealing the system is difficult. This occurs for several reasons. First, due to the small nature of the tubular blank, the positioning of the punch must be extremely accurate to achieve an even distribution of pressure on the tube ends. As stated in section 3.2, this is imperative to prevent leaks at the punch interface.

Second, the structural integrity and resistance to elastic deflection of the punch will be less then desired due to an increased ratio in the fluid hole diameter to the outer diameter of the punch. The increased ratio is the result of an inability to create 'deep' holes which are very small in diameter. To get a better understanding of this phenomenon one must consider the process forces involved in the hydroforming of a tube (illustrated in Figure 21). The loads consist of normal and frictional loads (F_p and F_f, respectively) at the punch-tube junction and normal and frictional forces (F_w and F_{wf}, respectively) at the die-tube interface. Additionally, the pressure of the working fluid (P_i) exerts forces on the punch and the tube. The external feeding force (F_{feed}) applied to feed the punch into the tube should be a function of: (i) the axial force which deforms the tube onto the punch taper, (ii) the frictional force (F_f), and (iii) the force due to the pressurized fluid acting on the surface of the punch.

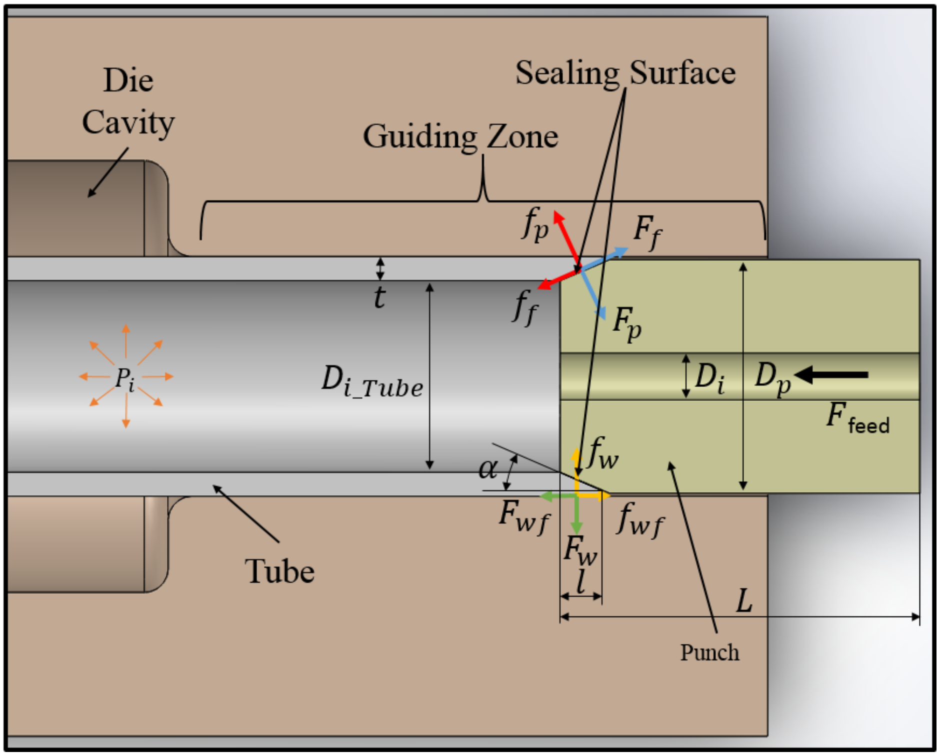

Figure 21: Process Forces on in the Conventional Tube Hydroforming Equipment

The process forces on the punch can be further broken down into their component forms, as shown in Figure 22. It can be assumed that the shear forces on the punch are small in comparison to the normal force that results from the tube being pressed into the tube and can be ignored for the purposes of this examination. The normal force (F_p) can be broken into two components, axial (F_a) and radial (F_r), using the principle of superposition. The axial force is the force required to feed the tube and the radial force is then given by Equation 2, Where α is the angle between the horizontal and the surface of the punch as shown in Figure 21.

$$F_r = F_a \tan(\frac{\pi}{2} - \alpha) \qquad \text{Equation 2}$$

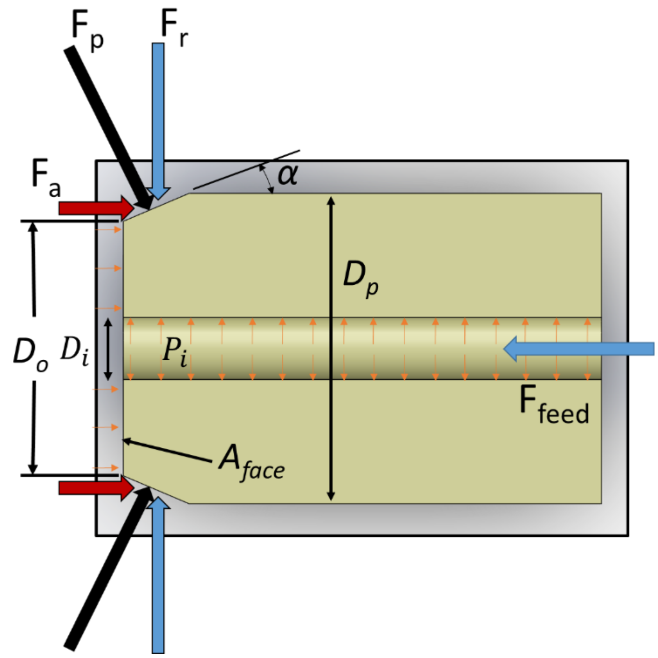

Figure 22: Stresses Produced on the Surface of the Punch as a Result of the Process Forces

These forces can be translated into stresses by dividing them by the area which they are projected over (note: one must remember to use the current thickness of the tube rather than the initial thickness). To further simplify the analysis of the stresses in the punch, the radial and hoop stresses were determined with the assumption that the punch could be considered a thick walled pressure vessel. Furthermore, it is assumed that maximum stress in the punch occurs at the tip of the punch and because of this the outer radius of the pressure vessel was considered to be the outer radius at the punch tip. The size of the stress in the hoop direction (σ_h) at an arbitrary radius inside the punch can then be determined by using the equation for the hoop stress in a thick walled pressure vessel, given in Equation 3. Similarly the radial stress inside the punch (σ_r) is given by Equation 4. Where P_o is the radial stress from the contact with the tube, P_i is the internal pressure from the working fluid, r_o is the outer radius at the tip of the punch, and r_i is the internal radius of the punch (as shown in Figure 23). The thick walled pressure vessel assumption requires that there is an evenly distributed stress on the flat inner and outer surfaces of the vessel and that the area being examined is far from the edges of the punch. Strictly speaking, these assumptions are violated in the area of the punch being examined, but it is assumed that the error will be insignificant.

$$\sigma_h = \frac{p_i r_i^2 - p_o r_o^2 - \frac{r_i^2 r_o^2 (p_o - p_i)}{r^2}}{r_o^2 - r_i^2} \qquad \text{Equation 3}$$

$$\sigma_r = \frac{p_i r_i^2 - p_o r_o^2 + \frac{r_i^2 r_o^2 (p_o - p_i)}{r^2}}{r_o^2 - r_i^2} \qquad \text{Equation 4}$$

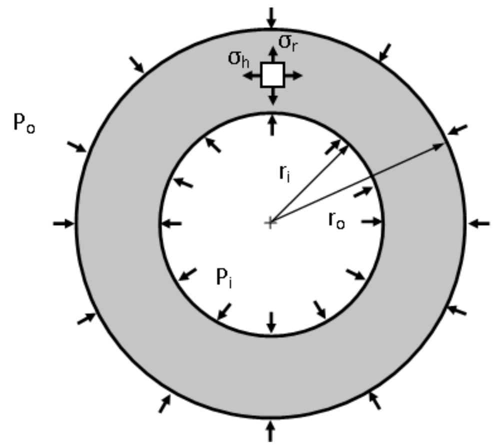

Figure 23: Diagram of the Punch Nose Acting as a Thick Walled Pressure Vessel

It is assumed that the force used to feed the tube has little influence on the axial stresses at the tip of the punch. Essentially, because feeding force is distributed over the taper of the punch, the total amount of axial force applied to the punch tip is small. The axial stress (σ_a) is thus the same as the pressure of the working fluid (P_i).

These hoop, radial, and axial stresses are assumed to be the principal stresses and can be used to find the effective (von-Mises) stress using Equation 5. The von-Mises stress can be used to find the maximum stress in the punch material for a given inner and outer diameter, wedge angle (α), feeding force, and applied internal pressure.

$$2\sigma'^2 = (\sigma_r - \sigma_a)^2 + (\sigma_a - \sigma_h)^2 + (\sigma_h - \sigma_r)^2 \qquad \text{Equation 5}$$

Consider a 1mm punch with a wedge angle (α) of 20° which is used to hydroform a tube with a wall thickness of 0.181mm when the maximum axial force is applied. The maximum internal pressure was 180MPa and the force required to feed the tube has been shown to be 685N (this is explained later in chapter 4). Using equations 2 through 5 one can plot the maximum von-Mises stress as a function of the diameter of the hole in the middle of the punch. These results were compared with those which were gained through simulations of the tapered punch using the ANSYS Workbench static structural module. The tube was simulated as a 2D axisymmetric body with a Young's modulus of 200Gpa and a poisons ratio of 0.3. The simulations show that the assumption that the stresses will occur at the tip of the punch is correct. The results of the model are plotted side by side with the results of the simulations in Figure 24. The yield stress of hardened tool steel is typically considered to be 2000MPa which is below the stress vs punch internal diameter curve presented in Figure 24. This suggests that there is not an internal diameter at which the hollow tapered punch can be used for this particular hydroforming operation. It can be seen that the model matches the simulation very well, suggesting that it can be used to quickly determine the internal diameter required for hollow tapered punch to withstand the forming forces so long as the feeding force and the tube thickness are known.

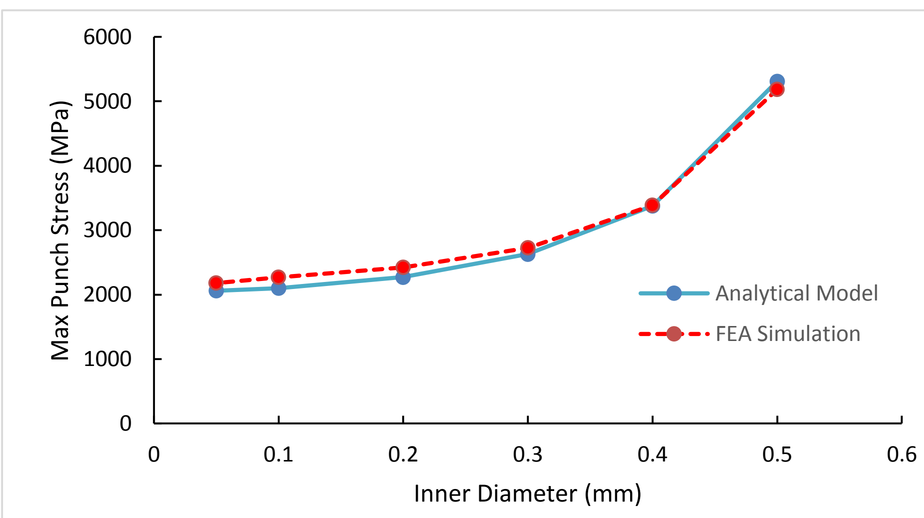

Figure 24: Maximum von-Mises Stress in the Punch vs Hole Diameter for the 1mm Diameter Case Study

Now consider another hydroforming operation which is carried out using 2mm diameter punch with a taper angle of 20°. The force required to feed the workpiece is 1487N and the thickness of the tube when the maximum force is applied is 0.229mm. The pressure used to form the tube as 180MPa. Applying the thick pressure vessel model to this problem, one can again plot the punch stress against the internal diameter of the punch. Figure 25 shows that the analytical model is in good agreement with the finite element simulations. In this case, the stresses are lower than the theoretical yield stress of the tool steel for some internal diameters as opposed to the 1mm diameter punch shown in Figure 24. The critical hole diameter in this case is 0.6mm, meaning that the stress in the punch will exceed the yield stress of the punch if the internal diameter of the tube is above 0.6mm. Again, it can be seen that the model follows the FE data closely, lending validity to the thick walled pressure vessel model.

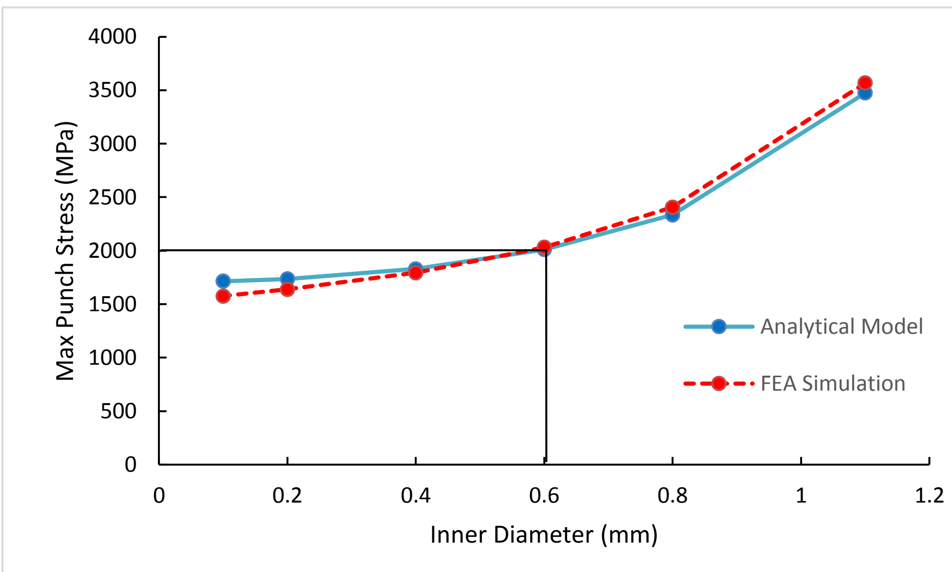

Figure 25: Maximum von-Mises Stress in the Punch vs Hole Diameter for the 2mm Diameter Case Study

The thick walled pressure vessel model can be used to generate these curves rapidly so long as the modeler knows the feeding force required, the thickness of the tube, and overall geometry of the punch. This makes it a very powerful tool for determining the maximum allowable diameter in the punch. However, just because the model says that there is an acceptable inner punch diameter does not mean that it can be fabricated. The designer must use the information about the maximum allowable inner diameter to determine if it will be cost effective or even possible to create a hole with the required diameter in the punch. This is especially true when the process is scaled down to the micro level because as the punch shrinks the hole size becomes extremely small.

Another reason that sealing is difficult is that the creation of an elastomeric sealing system on the order of hundreds of micrometers is difficult due to the large pressure gradient over the rubber material. This pressure gradient will cause the seal to be extruded and destroyed allowing the high pressure fluid to be released. Furthermore, it is likely that the wear rate in such a system would be extremely high because of the low amount of material present in the elastic seal. In short, due to the small diameter of the part it is likely that any of the sealing systems shown in Figure 20 would be impractical, or even impossible to implement.

Another problem with simply scaling the conventional tooling to the micro-scale is the issue with the speed at which the parts can be created, or cycle time per part. It is evident that the scatter in the process will cause an unusually high number of failed parts, especially when the process calls for the tube to be pushed to the upper end of its forming limits. Additionally, a small system is vulnerable to requiring a large amount of time for the handling the blank and the final part. Essentially, the accuracy and fine motion control that is required of the handling system is only achievable with motors which have very fine resolution, which are typically slow. Thus, the low cycle times and low batch numbers (typically only one tube is produced at a time) will result in a process which consumes an excessive amount of time and process cycles to produce a large number of parts, driving up the cost of the parts.

The research presented in the remainder of this thesis was conducted on the notion that the major limitation of the micro-tube hydroforming system was the use of strictly conventional tooling designs. It is proposed that the best way to achieve the goal of micro-tube hydroforming is to reexamine the hydroforming system on a fundamental level.

3.4 Novel System for the Micro-THF Process

3.4.1 Overview

The realization of a micro-tube hydroforming system, which is capable of mass producing complex geometries requiring axial feeding of the workpiece, is best done through a reexamining of the tube hydroforming system as a whole. This will be done by first identifying the relevant process variables present and the needs of the system using a fundamental knowledge of the tube hydroforming process.

One of the reasons that the conventional tube hydroforming process is so expensive is that the high clamping forces needed to keep the dies closed requires the use of massive presses. As stated previously, the pressure required to complete the forming process is roughly the same for both micro and macro tubes and depends mainly on the ratio of diameter to wall thickness. This means that the clamping force required to close the dies, is significantly smaller in a micro scale operation. This lower clamping force means that a significantly less expensive presses may be used to complete the forming of the part, because it is likely that there exists, general purpose presses which are capable performing adequately. Additionally, it should be mentioned that because the cost per ton of clamping force is smaller for smaller presses, it is possible to hydroform multiple parts on the same press without adding a significant amount of cost to the process.

The most important part of any hydroforming application is the difference in pressure between the inside of the tube and the die cavity. It is this pressure difference which causes the material to flow into the die and take on its desired shape. According to Lungershausen [34], the internal pressure required to fully form the part can be as high as 400 MPa. It is extremely important to remember that the forming is caused by a large pressure gradient, rather than simply a large internal pressure. This leads to the conclusion that so long as the high pressure medium does not reach the die cavity it is not important where else it goes in the system.

The feeding of the tubes into the die cavity is another extremely important part of the hydroforming process. In order for this to happen, the tube ends must be pushed towards the die cavity without blocking the flow of fluid into the tube. In other words, the punch must make contact with the tube ends without affecting the internal pressure of the tube. If the flow of fluid is blocked during the process it will become impossible to control the internal pressure in the system and the tube will likely burst or buckle as a result.

It should be noted that the tribology of the system is another important process variable. However, it is far more dependent on the lubricant used and the surface finish of the dies than the design of the tooling in the system. Thus it is out of the scope of this study and will be left as possible future research.

In order for a complex tube hydroforming operation to take place, all of the areas mentioned in this section must be accounted for. However, it is not necessary for them to be accomplished in the same way that conventional tooling accomplishes them. The specific function of each tool-workpiece interface may therefore be modified to suit the needs of the designer. Using the information presented in this section a novel tube hydroforming system can be developed to overcome the barriers that are present when scaling down the traditional tooling.

3.4.2 Concept

The major feature of the new hydroforming system to be designed is that the function of the two tool-workpiece interfaces has been modified to better suit the needs of a micro-scale process. Specifically, the function of sealing will be decoupled from the punch-tube interface and added to the die-tube interface. This will allow for significantly more freedom in the punch design and avoid many of the issues involved with creating a reliable seal with the punch.

The sealing will instead be accomplished by the die-tube interface using Teflon sheets as a sealing media. The Teflon sheet will be placed between the tube and the die cavity, where it will be compressed as the two die halves are pressed together in the closing phase of the process. This concept is illustrated in Figure 26. The proposed system should create a strong seal which is capable of preventing the high pressure medium from entering the die cavity. Once the tubes and seals are clamped between the dies, it is possible to carry out a simple tube hydroforming process by simply supplying a high pressure fluid to the outside of the die and allowing it to flow into the inside of the tube.

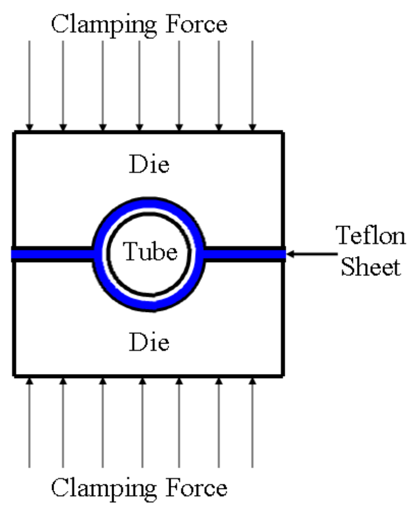

Figure 26: Proposed Die Sealing System

The traditional method of supplying the fluid to the inside of the tube can also be changed in this redesign of the hydroforming tools. Instead of being supplied by a hole in the punches, the fluid can completely surround the die and tube assembly. In other words the die and tubes are completely submerged in the high pressure media. In this way the fluid is allowed to completely penetrate the inside of the tubes, but is prevented from entering the die cavity by the Teflon seals in the guiding zone, as shown in Figure 27. It can be seen that this system can accomplish the creation of a large pressure gradient across the thickness of the tube between the inside of the tube and the die cavity. The pressure of the surrounding fluid is precisely controlled from the outside and is contained in a pressure vessel (discussed later in this section).

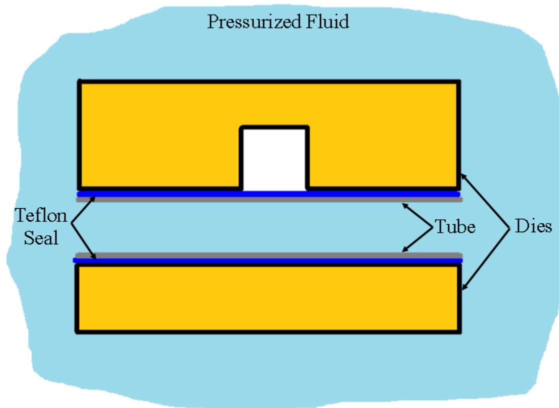

Figure 27: Concept of the Teflon Sheet Sealing System

Now that two of the functions of the punch have been decoupled from the punch-tube interface, the feeding of the tube into the die cavity can be discussed. Recalling that the fluid is no longer supplied by the punch, it is possible to eliminate the hole in the center of the punch because it has no bearing on the material feed. However, the tube must be feed without preventing the fluid from transferring in and out of the tube. So, in order to avoid trapping or starving the inside of the tube from fluid, the punch can be notched to allow for the passage of fluid between the inside of the tube and the outside fluid supply. Figure 28 shows the concept of the punches discussed above. Any method of providing the feeding force to the punches should capable of producing material feeding of the workpiece.

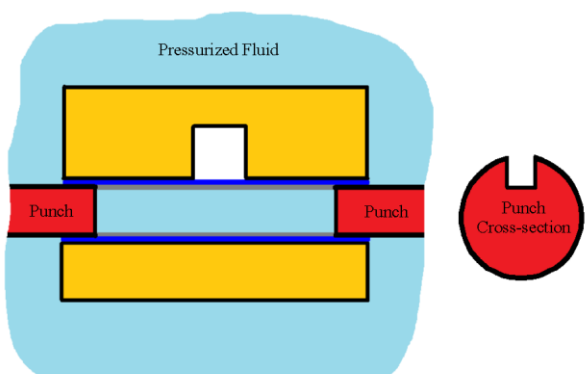

Figure 28: Punch Concept

The only remaining piece of the tooling to clarify is the pressure vessel, which will house the tooling and maintain the high pressure working fluid that the dies and punches are submerged in. The pressure vessel needs to consist of at least two parts, a die housing and a sealing plate. The die housing consists of a deep cavity that contains features that are used to locate the dies, punches, etc. The depth of the cavity must be sufficient to fully submerge the equipment placed in the die cavity. The die holder must also contain two high pressure fluid ports, one that allow for the supply of high pressure fluid and the other to bleed the air out of the system. The mechanism or electronics which are used to supply the feeding force to the punches must also be allowed to pass through the die housing into the die cavity. The sealing plate consists of a flat plate with a male seal that mates with a female seal in the die housing and a backer plate to ensure that the die halves are clamped shut. The seal between the two parts is achieved when the system is clamped together by the press. The complete concept of the tooling is shown in Figure 29.

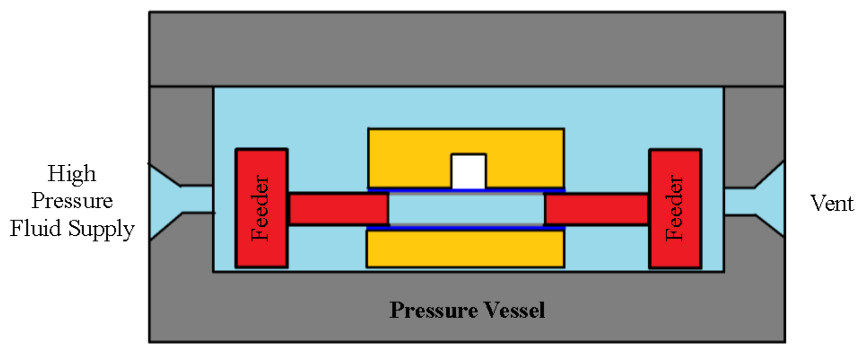

Figure 29: Conceptual Micro-Tube Hydroforming Equipment

The micro-tube hydroforming tooling proposed in this section belongs to a totally new class of tooling, and has been dubbed ‘floating die’ tooling because the dies are submerged in the working fluid.

3.4.3 Advantages and Disadvantages

The proposed floating die micro-tube hydroforming system is very different from the conventional hydroforming tooling and as such presents many advantages. The floating die system, for example, sidesteps the issues associated with creating a seal at the punch-tube interface and instead relies on a much more reliable seal at the die-tube interface. Removing the responsibility of supplying the fluid from the punches has the advantage of eliminating the need for expensive micro hole drilling processes from the fabrication of the punches. It also should be able to significantly increase the rigidity of the punches by allowing them to be solid over a large portion of their length rather than hollow. The flexibility of the system is excellent, as the system used modular dies, punches, and feeding systems. The designer also has the freedom to move the system from press to press and from fluid supply to fluid supply at a moment's notice.

The production rate of the floating die system also lends itself to being scaled up to the high production rates which are necessary for the mass production of micro-tubular parts. Large batch sizes can be utilized as the added projected area for each tube is small and the cost per unit force of small presses is small, when compared to macro-scaled tube hydroforming presses. Furthermore, the modular nature of the tools means that after the forming process takes place it can be rapidly set up again via a complete exchange of the forming tools and workpieces. This could work in a three step cycle using three sets of tooling that rotate through the various stages to increase the amount of time the pressure vessel is being used in the forming process. First, the tubes and seals are placed in the die set and the punches are positioned. Second the assembly is moved to the pressure vessel and the hydroforming process takes place. Third, the assembly is removed from the pressure vessel and the formed parts are removed from the cycle. This has a distinct advantage over the traditional method requiring the press to be idle while the workpieces are being exchanged.

It is necessary to also mention the advantages of the system come at a cost. Namely, that the designer now has to create a pressure vessel which is capable of meeting the requirements outline in section 3.4.2. Furthermore, the capacity of the press must be increased because the projected area of the fluid is now the entire area of the cavity in the pressure vessel instead of just the projected area of the formed part. Finally, it can be difficult to diagnose problems in the floating die system due to the many layers between the operators and the tubes.

CHAPTER 4: FINITE ELEMENT ANALYSIS

4.1 Introduction

Developing the tooling described in chapter 3 will require detailed knowledge about micro-tube hydroforming process parameters. The proper design of the tooling is dependent on knowing the forces and pressures which are required to successfully form a part. Once this information is known, it can be used to evaluate potential design alternatives for the floating die based micro-tube hydroforming system. This chapter will therefore focus on establishing the relevant process parameters in the micro-tube hydroforming process via the finite element method. The information gained about the forces and pressures required, will then be used as the inputs for a set of finite element simulations to determine the size and shape of tools to be used in the forming process. In this way, a reliable and adaptable system can be developed for the hydroforming of complex micro-tubular parts.

It should be noted that no attempt to simulate the size effects will be made in this analysis. This is due to the lack of knowledge about the strength of micro-scale tubes and the lack of a robust method of simulating the effects of a complicated grain structure. Though many researchers have turned to the crystal plasticity finite element modeling to simulate the size effect, the method is very time consuming, heavily dependent on the initial grain structure, and generally only able to provide qualitative information [28]. Therefore the standard finite element analysis based on continuum mechanics will be used to perform the simulations of the micro-tube hydroforming process. It is assumed that this type of simulation will be able to provide results which are close enough to reality to be useful in designing the hydroforming tooling.

4.2 Tube Hydroforming Simulations

The creation of equipment which is capable of properly hydroforming micro-tubular blanks is dependent on understanding the process parameters which were involved in the process. Specifically, the designer needs to know the forming pressure, and the amount of axial feed necessary to make a particular part. To accomplish this, the finite element method is applied due to its ability to rapidly check a large number of possible forming parameters without the use of costly and time consuming experiments.

In order to gain a complete picture of the forming pressures and forces that could arise in the hydroforming of small tubes, three families of tube geometries were studied, the bulge shape, the T-shape, and the Y-shape. These geometries represent parts of varying complexity and are representative of a large number of other hydroforming applications. In each set of simulations the tube length was varied from 12 to 20 mm, the diameter was varied from 1 to 2mm, and the coefficient of friction was varied from 0.05 to 0.1. The wall thickness was set to 0.1mm for the 1mm diameter tubes and 0.15mm for the 2mm diameter tubes. These values represent the dimensions of the tubing which was available to the investigators at the time of the study. The pressure profile used in the simulations was based on a formula given in a paper written by Ghosh et al. and modified based on the results of the simulations until an acceptable pressure profile was produced [38]. In general the pressures arrived at were higher than could be created by the current equipment available for the experiments. Therefore, some of the simulations were run with the pressures which could be achieved by the current equipment (130MPa) so that they could be compared to the results of the hydroforming experiments. The amount of material feeding was iterated upon in each simulation to arrive at the appropriate amount of axial feed in each case and the force required to produce this axial feed was determined. The results of the simulations were then collected and used as inputs in structural simulations of the hydroforming tooling.

This set of simulations was carried out using the ANSYS Workbench module Explicit Dynamics. Final time of the simulation was set to 0.01s and the mass scaling parameters used in the simulation were a requested time step of 1e-6s and an allowable mass scaling of 1000. The tube was considered a rigid plastic body which followed the power law ($\bar{\sigma} = K\bar{\epsilon}^n$) and was given the material properties of stainless steel (K= 1275 MPa and n= 0.45). The tube was meshed with 1700 to 3000 quadrilateral shell elements, depending on the length of the tube. The dies were considered fixed, rigid bodies and their geometry was approximated by a mesh of tetrahedral elements. The axial feed was supplied with displacement boundary conditions, rather than punches, to simplify the simulation. The friction between the die and the tube was simulated with the Coulomb friction model.

4.2.1 Bulge Shape

The first set of micro-tube hydroforming experiments run was the bulge shape due to its simplicity. Strictly speaking, it is possible to create a bulge shape without material feeding, but symmetric material feeding was added to the simulation to increase the size of the attainable bulge. The diameter of the die cavity, and thus the maximum bulge, was set to 1.5 times the outer diameter of the blank and the length of the cavity was set to 4mm. All of the pressure loading paths in this set of simulations followed the load path in Figure 30, however, feeding loading paths were not all the same. The feeding load paths all followed the form of loading path on the right of Figure 31, but the magnitude of the maximum force was lowered to 1mm in the case of the simulations of the 2mm diameter 12mm long tubes to prevent over feeding of the workpiece. An example of the mesh used in the simulations can be seen in Figure 32.

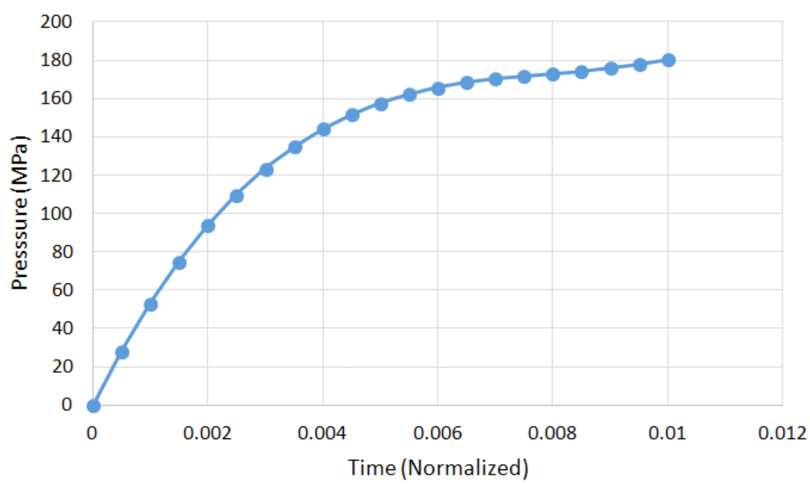

Figure 30: Pressure Loading Path used for the Simulations of the Bulge Shaped Parts

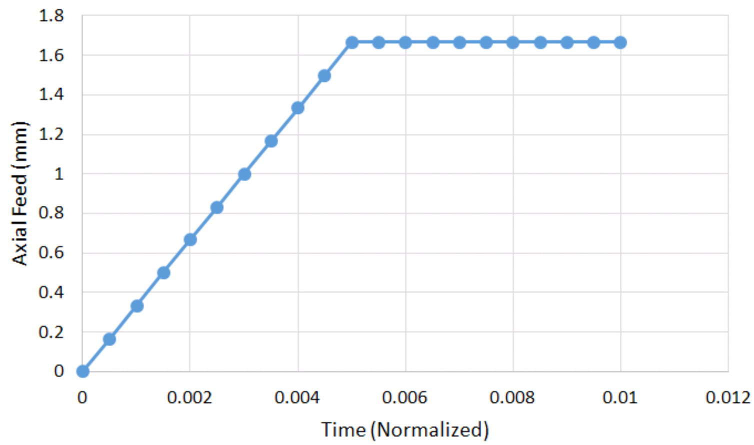

Figure 31: Loading Paths Axial Feed Path Load Path used for the Simulation of the Bulge Shaped Parts

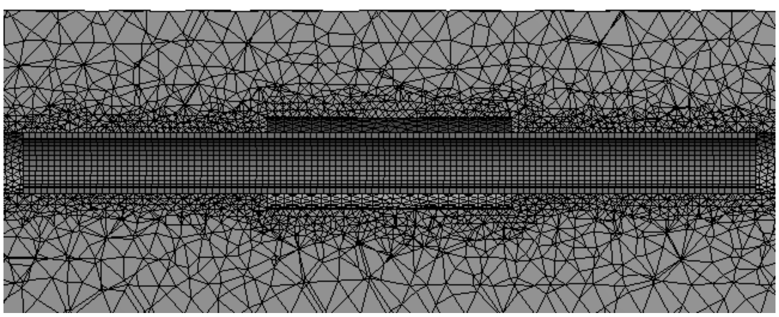

Figure 32: Example of the Mesh used in the Bulging Simulations

The results of the simulations of the 1mm diameter parts are shown in Figure 33. It can be seen that the thickness and shape of the part vary as the length of the blank and the frictional parameters change. The low friction and short tubes result in parts with a more sudden transition from the original diameter to the bulge diameter, which can be observed as smaller radii at the corner of the bulge in Figure 33. These factors also resulted in an increased wall thicknesses in the bulging zone. Specifically, the thinning rate changed from 19% in the short tube low friction case to 29% in the long tube high friction case. In this set of simulations, the length of the tubes appears to play a much more important role in the final shape and thickness distribution of the tube than the friction at the tube die interface.

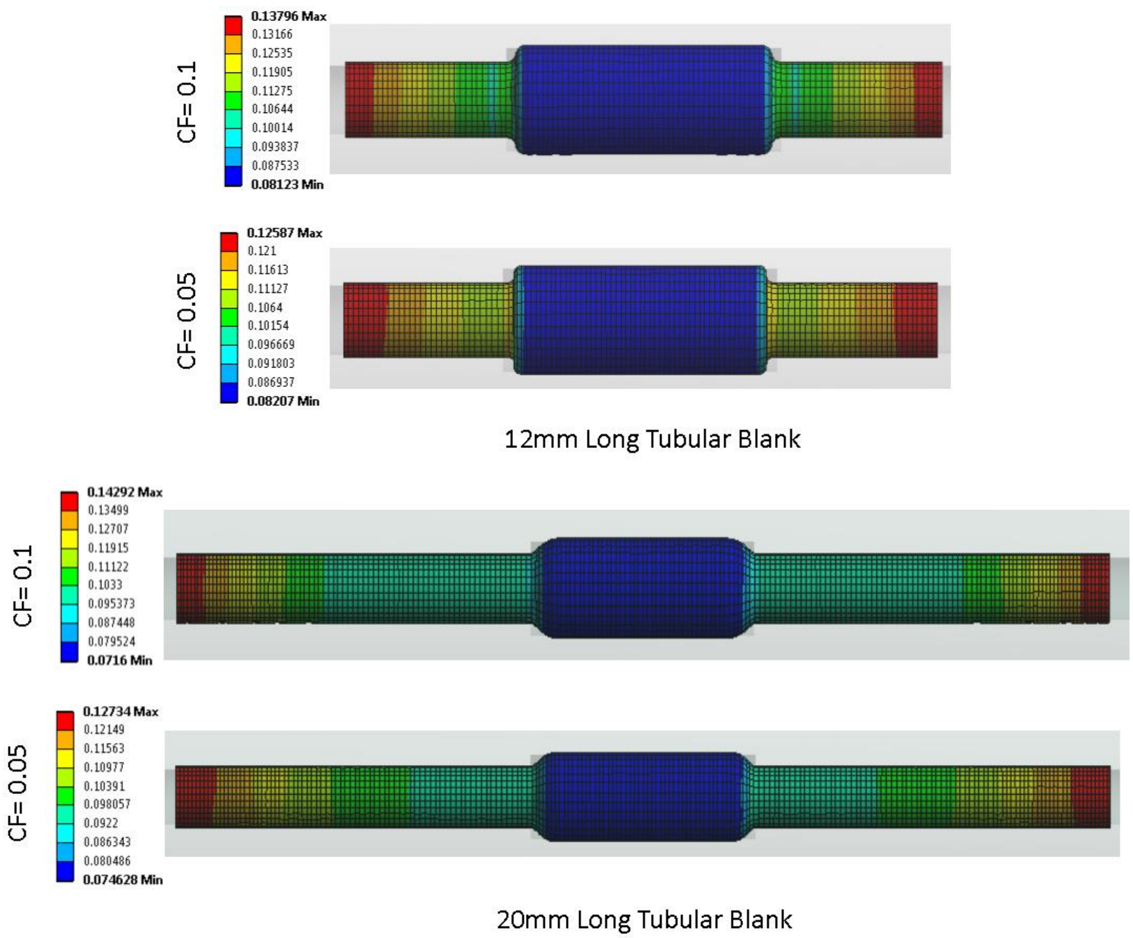

Figure 33: Thickness Distribution [mm] for the Simulations of the Bulge Shape on 1mm Diameter Tubes

The 2mm diameter simulations showed the same trends, except for the 12mm tube length simulations showed that the material would buckle at the transition to the bulge diameter if the feed was kept the same as it was in the other simulations. The feed in these simulations was therefore reduced to 1mm to ensure the creation of a good part. The reduced thickness of the 2mm diameter tubular blanks is likely the cause behind the buckling in the transition zone. This is because the material will yield earlier creating large diameters and a more sudden transition in diameters, leading to a reduced resistance to the buckling of the tube. The reduced feeding in the tubes also significantly reduced the thickness in the bulge zone. The thinning rate in the bulge zone of the 12mm long 2mm diameters tubes was around 30% compared to 19% in the case of the short smaller diameter tubes. It is clear that this amount of expansion will be difficult to achieve due to the reduced material stability.

Simulations of the 12mm long tubes at lower pressures, i.e. those pressures which are currently achievable using available equipment, showed that the reduced pressure will make the tubes much more likely to wrinkle. In the case of the 1mm diameter tube, the tube began to wrinkle early in the simulation and the internal pressure in the tube was not able to remove the defect form the part. However, in the case of the 2mm diameter tube, the wrinkles that were created early in the simulation were much smaller and were removed by the end of the process. The difference between the two simulations is likely due to the fact that the 2mm tubes are relatively thinner and therefore more likely to expand enough to remove the wrinkles at low pressure. A side by side comparison of the 1mm and 2mm low pressure simulations can be seen in Figure 34.

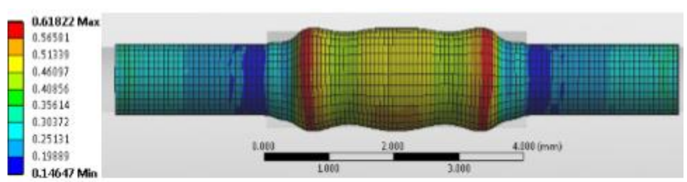

Low Pressure Simulations of the 1mm Bulge Shape

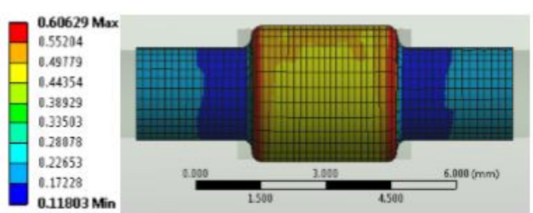

Low Pressure Simulations of the 2mm Bulge Shape

Figure 34: Low Pressure Simulations of the Bulge Shape

4.2.2 T-Shape

The second set of hydroforming simulations were run on the T-shaped geometry. The successful creation of this geometry requires the addition of axial feed to the hydroforming process. The symmetric nature of the tube means that the amount of axial feed is the same on both ends of the tube. The pressure and axial feed loading paths are shown in Figure 35 and Figure 36, respectively. An example of the mesh used in this set of simulations is given in Figure 37.

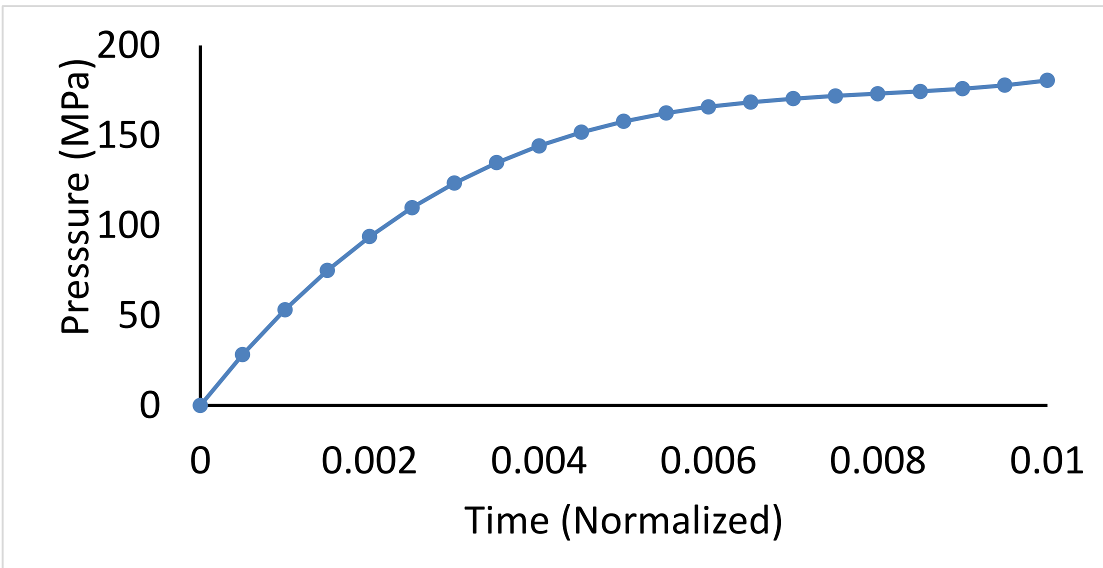

Figure 35: Pressure Loading Path used in the Simulations of the T-Shaped Geometries

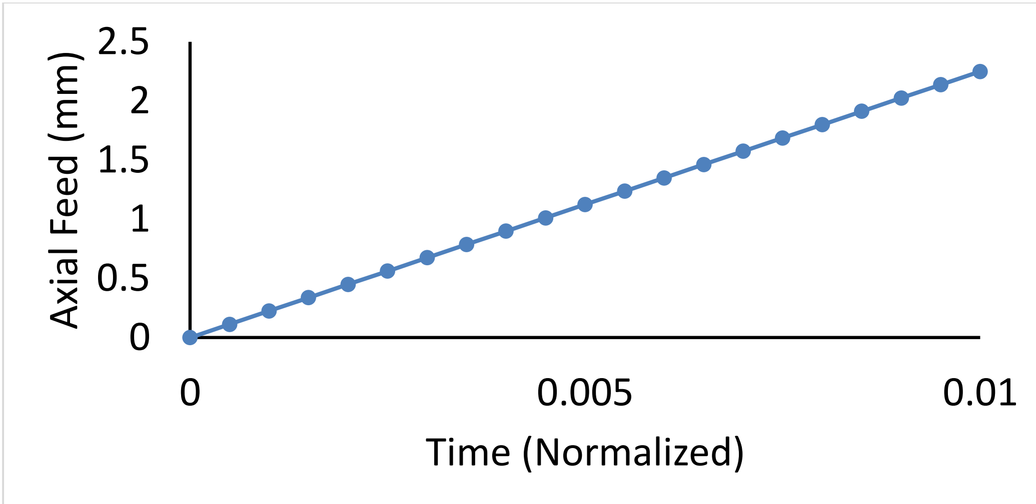

Figure 36: Axial Feed Loading Path used in the Simulation of the T-Shaped Geometry

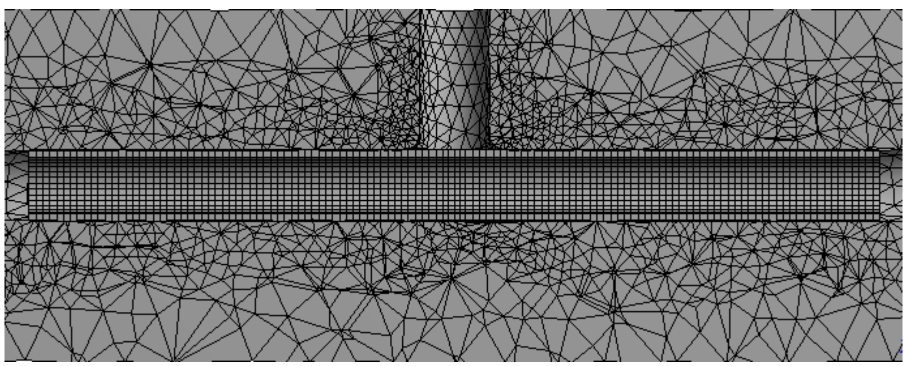

Figure 37: Example of the Mesh Used in the Simulations of the T-Shaped Geometry

The simulations show that the T-shaped geometry can be fully formed with these conditions. The maximum bulge height attained in the simulations was 0.84mm for the 1mm tubes and 2.01mm for the 2mm tubes. Figure 38 shows the results of the hydroforming simulations done with 1mm tubes. As is expected, increased friction on the tube reduced the height of the bulge. The height of the bulge was also effected by the length of the tube, with longer tubes having significantly smaller bulges than their shorter counterparts. The reduction of the bulge height in the case of longer tubes and higher friction is the result of resistance to the material's flow in the guiding zone. It was observed that this added resistance to the formation of the bulge resulted in increased thinning in the bulge area and caused excessive thickening of the tube ends. This effect can be seen by comparing the low friction low length case, which had a maximum thinning rate of 11%, with the high friction, high length case, which had a maximum thinning rate of 22%. It can also be seen that the complete formation of a T-shaped bulge is not possible with a 20 mm long 1mm tube with a thickness of 0.1mm.

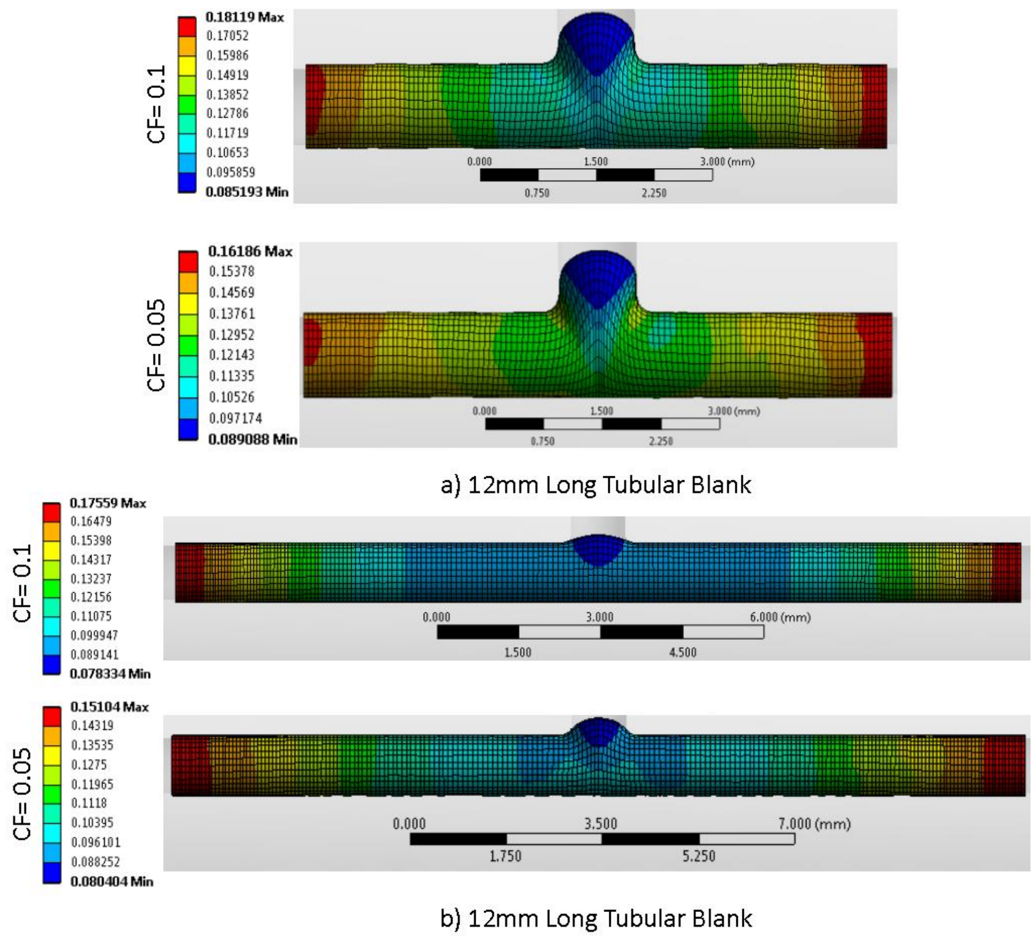

Figure 38: Thickness Distribution [mm] for Simulations of the T-Shaped Geometry on 1mm Diameter Tubes

Similar trends were seen with the simulations of the 2mm diameter tubes, however, due to the reduced ratio of the thickness to diameter ratio in the 2mm diameter tubes, taller bulges were obtained relative to the original diameter of the tube. It should also be noted that the thinning rate in the tubes was also much greater than the 1mm tubes. In the case of the 20mm long blanks the thinning rate rose to as much as 42.6%, well above the 30% limit which is traditionally imposed as the maximum for a good part. In the case of 12mm tubes, the thinning rate was as high as 23%, which was considered acceptable. For the purposes of comparison, Figure 39 shows a side by side comparison of the thickness distribution on the 1mm and 2mm diameter T-shaped geometries simulated with the same friction, initial length, and loading paths.

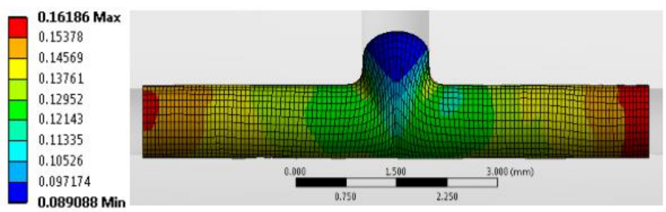

a) 1mm Diameter 12mm Long Tube Simulated with a Coefficient of Friction of 0.05

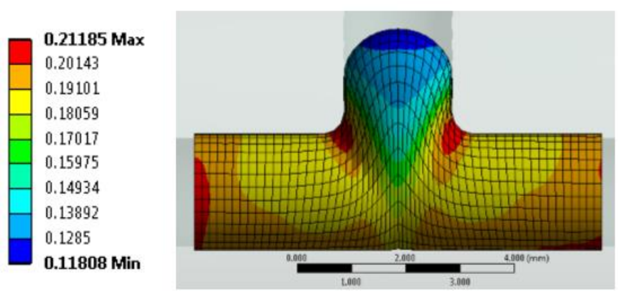

b) 2mm Diameter 12mm Long Tube Simulated with a Coefficient of Friction of 0.05

Figure 39: Comparison of the Thickness Distribution [mm] between the 1mm and 2mm T-shaped Simulations

In general the force required to produce the axial feeding in the tubes followed the path shown in Figure 40. It was found that the creation of a good 1mm part could require forces of 685 N and 2mm T-shaped parts could require forces of 1487 N. These forces represent the feeding force obtained from simulations of 12mm long parts because the 20mm long parts were not well formed. In order to get an accurate representation of the normal pressure which is transferred to the punch as a result of these forces one needs to know the area over which the force can act. It is therefore, necessary to know the thickness of the tubes ends. The thickness of the tube ends corresponding to the previously mentioned forces are 0.1811mm and 0.22921mm respectively.

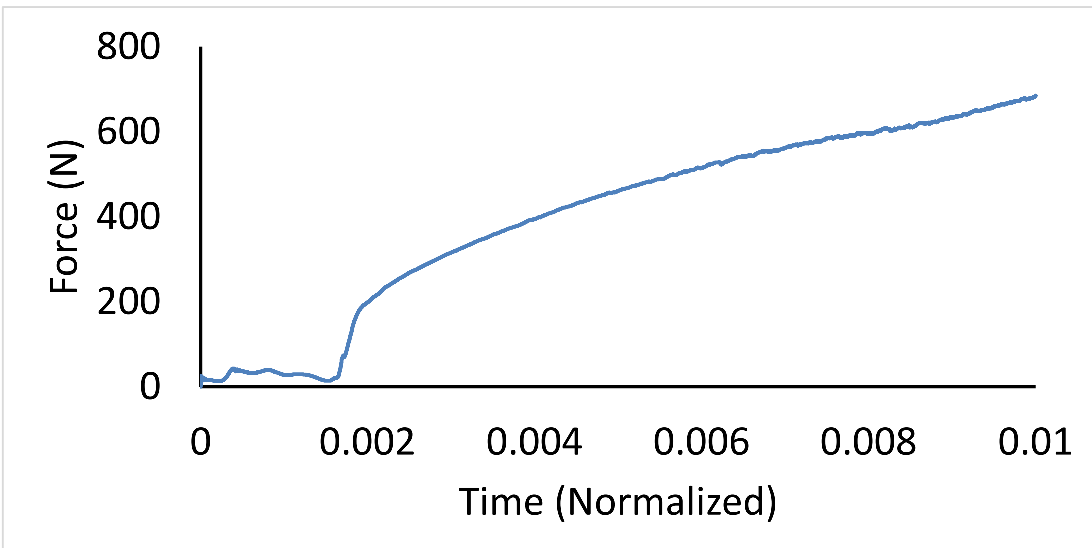

Figure 40: Force Required to Produce Axial Feed in the Simulation of the T-Shaped Geometry for a 12mm Long 1mm Tube with a Coefficient of Friction of 0.1

One simulation for each tube diameter was run with a reduced maximum forming pressure of 130 MPa because this was the maximum pressure which could be produced by the system available for the experiments. The simulations were carried out with 12mm long tubes and a coefficient of friction of 0.05. They showed that pressures which could be generated by the available equipment were adequate to form an acceptable T-shaped part. Figure 41 shows the thickness distribution which was simulated with a reduced maximum pressure. Note the small bit of wrinkling which is present opposite to the bulge on the part, this indicates a reduced resistance to bucking as a result of having less pressure to stabilize the tube. The simulations predict that the maximum attainable height with a system which is only capable of achieving pressures of 130 MPa is 0.75mm for a 1mm tube and 1.67mm for a 2mm tube.

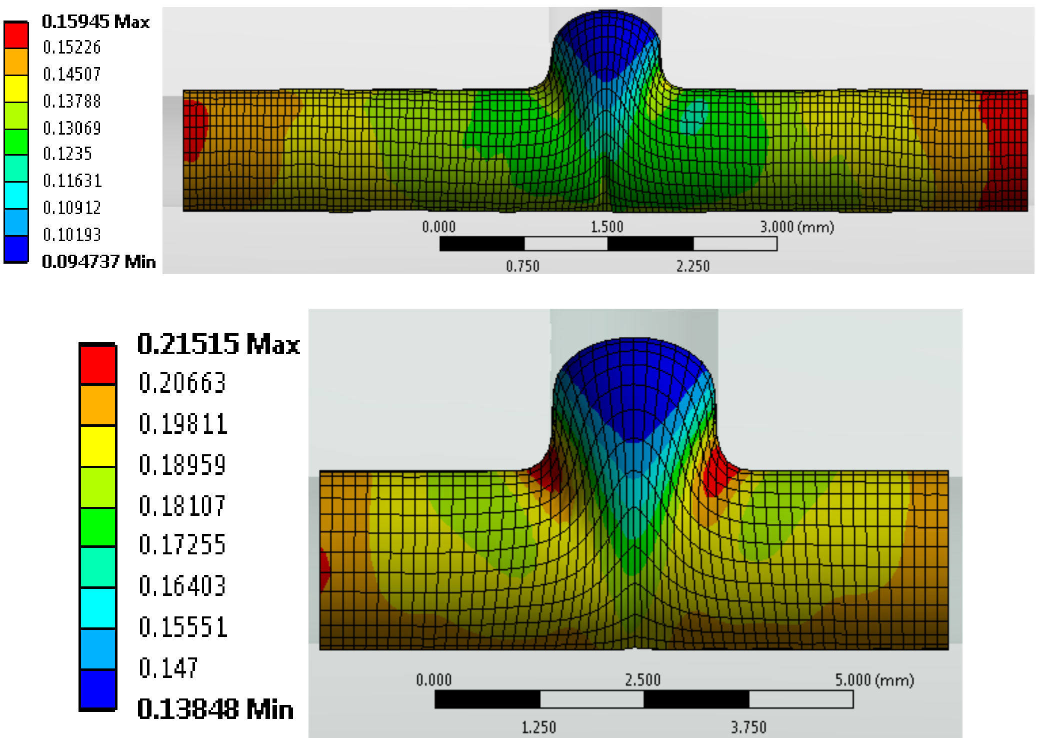

Figure 41: Thickness Distribution from a 1mm diameter (top) and 2mm Diameter (bottom) T-Shaped Part with a Maximum Internal Pressure of 130 MPa

4.2.3 Y-Shape

The hydroforming of Y-shaped part is a bit more complex than the T-shaped part. Due to the lack of symmetry in the part, different axial feeds are required for each end of the punch. In other words there are three independent variables that must be accounted for when creating a y-shaped part instead of the two needed for the T-shaped simulations. The pressure loading path used in this set of simulations is shown in Figure 42. After many iteration a good pair of axial feeding loading paths was arrived at, these are shown in Figure 43. The same load path was used in all simulations in this set so that the results will be more comparable. An example of the mesh used in the Y-shape simulations is given in Figure 44.

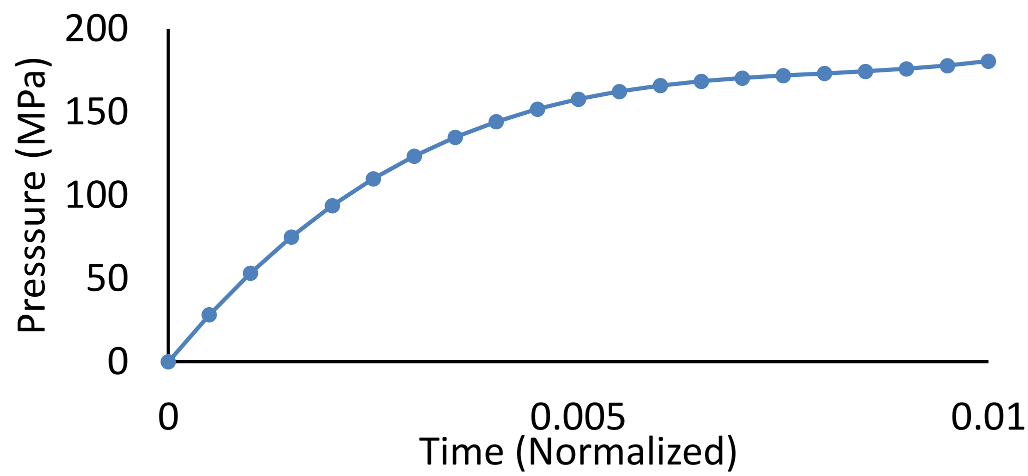

Figure 42: Pressure Loading Path used for the Simulations of the Y-Shaped Part

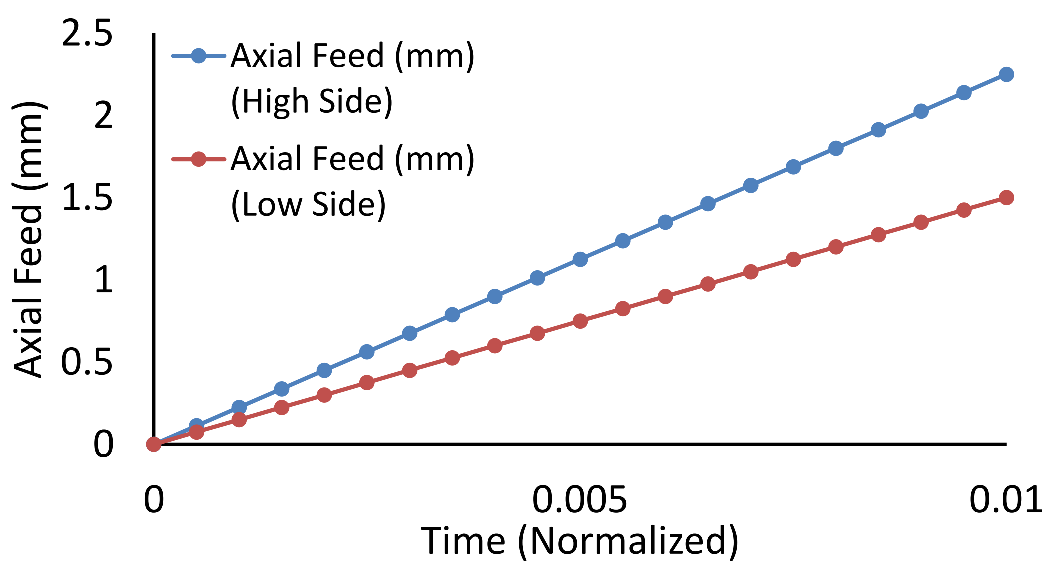

Figure 43: Axial Feed Loading Path used in the Simulation of the Y-Shaped Part

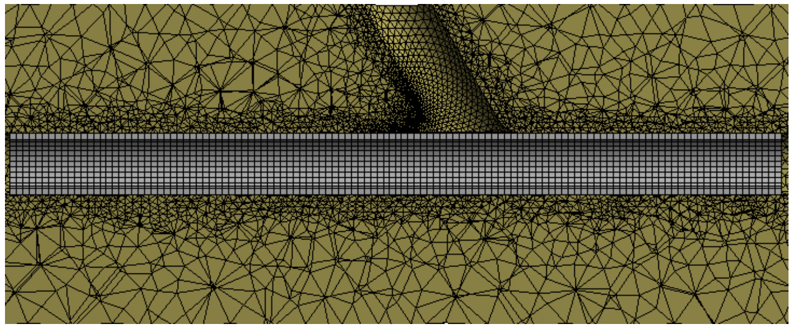

Figure 44: Example Mesh for the Y-Shaped Simulations

Simulations of the 1mm diameter parts show trends which are very similar to the T-shaped geometry. Namely, that the size of the bulge and the thickness distribution is heavily influenced by the increase in the length of the tubular blank and the amount of friction in the system. The height of the bulge produced can vary from 1.01 mm to just 0.35mm if the coefficient of friction is changed from 0.05 to 0.1 and the length of the tube is increased from 12mm to 20mm. By viewing the contour plots in Figure 45 one can also see that the material thickness over the formed part can vary significantly depending on the frictional conditions and the length of the tubes. Specifically, the thinning rate can vary from 14.5% to 26.5% if the length of the tube and the friction in the system is increased.

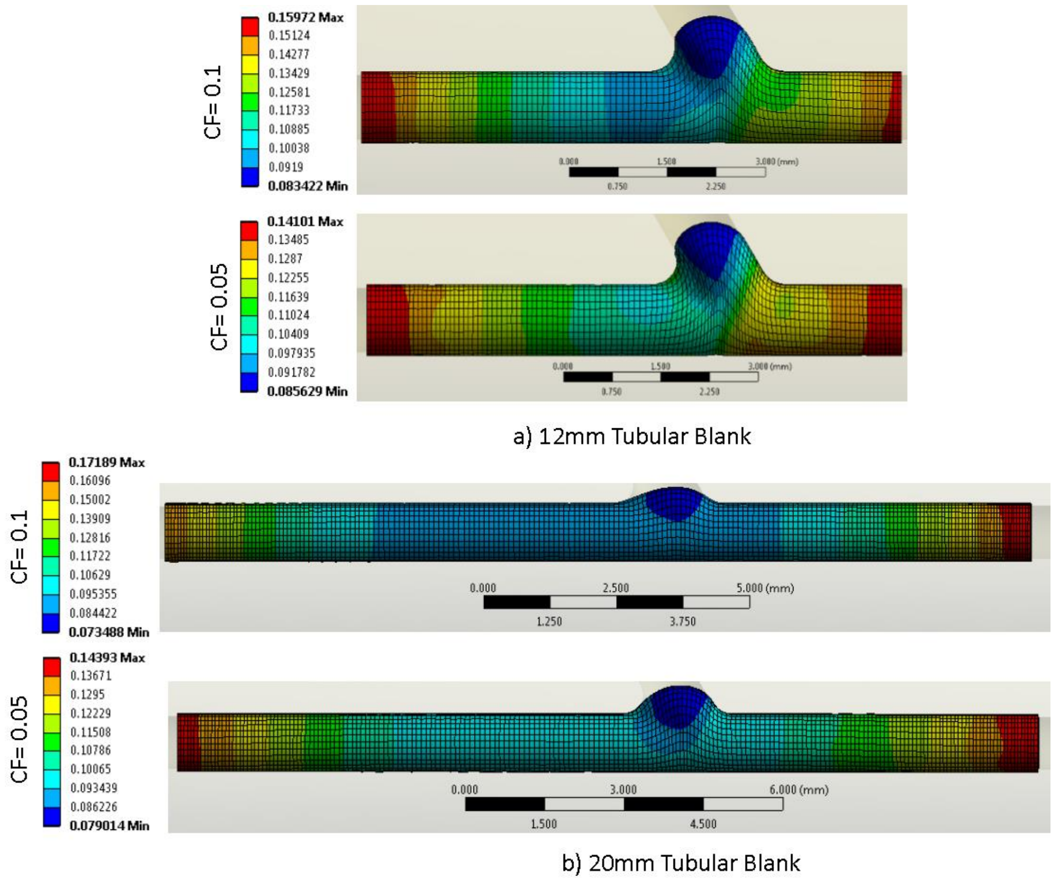

Figure 45: Thickness Distribution [mm] for Simulations of Y-shaped parts with 1mm Diameter

Again, the 2mm diameter tubes show results which are similar to those of the 1mm diameter tubes. The decreased thickness to outer diameter ration has resulted in taller bulges relative to the OD of the tube and in an increased thinning distribution. The height of the best produced protrusion was 2.00mm and the maximum thinning rate of the part was 28.3%. Simulations of the process with high friction and longer blanks results in a thinning rate which is above the 30% that is generally considered the maximum acceptable thinning rate. This suggest that the pressure used in these simulations is bordering on the bursting pressure for the high friction, high length case.

The discussion of the forming forces will be confined to simulations of the 12mm long tubes, as the simulations of blanks that were 20mm long did not show that good parts could be formed. The force required to produce the feeding of the tubes generally followed the path shown in Figure 46. 587N was the maximum applied force required to feed the 1mm diameter tubes and 1373N was the maximum force needed to feed the 2mm diameter tubes. These values are just below those which are required to form the T-shaped tubes. It should also be noted that, even though there is a different amount of feeding for the left and right punches, the loads which must be produced by the punches are nearly identical. This occurs as a result of the forces needing to be balanced to prevent the tube from sliding one direction or the other during the forming process. For the simulations with the maximum feeding forces the thickness of the ends of the tubes at the end of the forming process (when the force is maximum) is 0.160mm for the 1mm diameter parts and 0.215mm for the 2mm diameter parts.

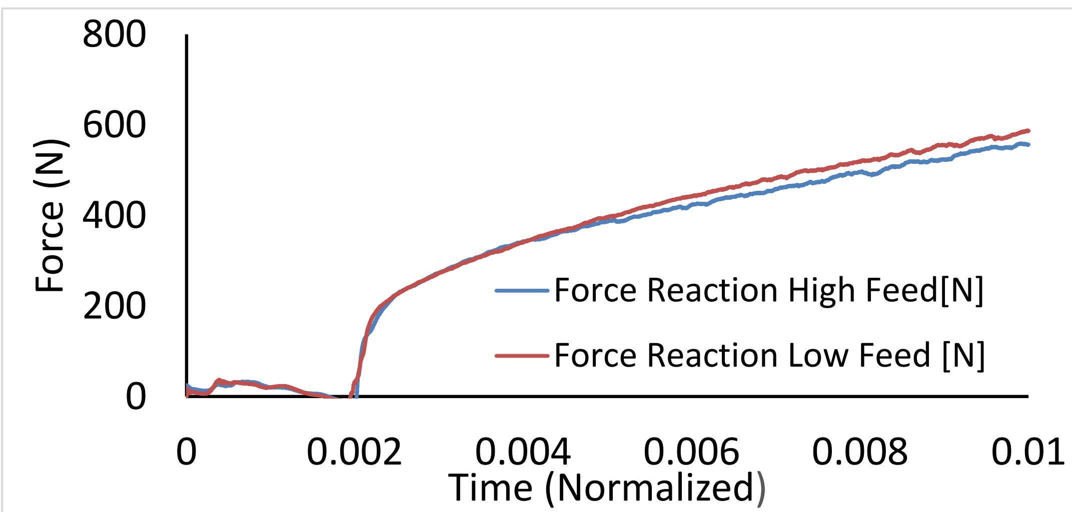

Figure 46: Force Required to Produce Axial Feed in the Simulation of the Y-Shaped Geometry for a 12mm Long 1mm Tube with a Coefficient of Friction of 0.1

Simulations of the y-shaped geometry were run to determine if Y-shaped parts could be formed using the available pressure supply of 130MPa. Simulations of the Y-shaped tubes with a maximum forming pressure of 130MPa showed that a bulge for reduced height could be produced. Figure 47 shows the thickness distribution on the 1mm diameter part which was produced with the lower maximum pressure, note that the bulge is much thicker than it is in any of the simulations with higher maximum pressures. The attainable height of the bulge for the 1mm part was 0.872mm and for the 2mm part the bulge was able to grow to a height of 1.649mm.

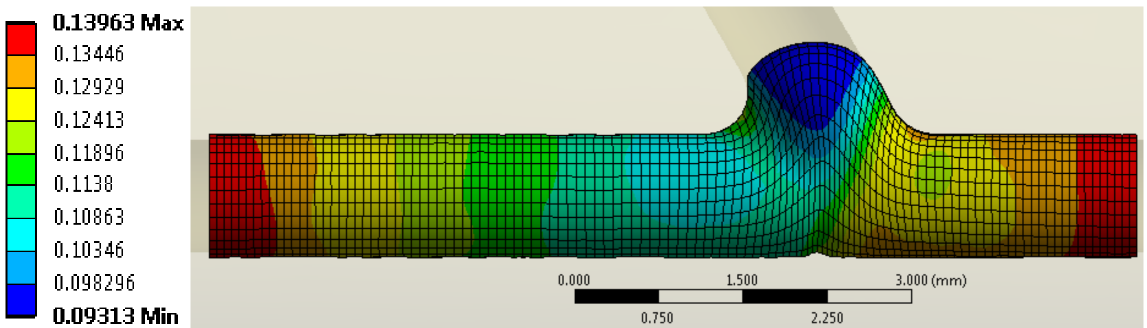

Figure 47: Thickness Distribution from the Simulation of a 1mm Y-Shaped Part with a Maximum Internal Pressure of 130 MPa

4.2.4 Discussion of Tube Hydroforming Simulations

It was seen in all of the sets of simulations that changes in final part dimensions are heavily dependent on the length of the tube and the amount of friction at the tool tube interface. Clearly the friction at the interface can cause the material to resist moving towards the die cavity, but the reason the tube length is also a factor in the flow of the metal is less obvious. The best way to understand the role of the length of the tube in the final dimensions of the part is to consider the state of stress in the tube. In the simple case of upsetting, the stress increases rapidly as the change in length approaches the total length of the part. Thus, because the overall length of the part is different, identical amounts of feed will cause different stress states near the bulging zone. Specifically, a longer tube will result in a lower stress state for identical amounts of axial feed. Recalling that the material's ability to deform depends on the maximum shear stress in the deformation zone, it is clear that high compressive axial stresses caused by material feeding coupled with the high hoop stresses caused by the internal pressure will lead to a decreased resistance to material flow. The Mohr's Circle diagram in Figure 48 gives a pictorial representation of this idea.

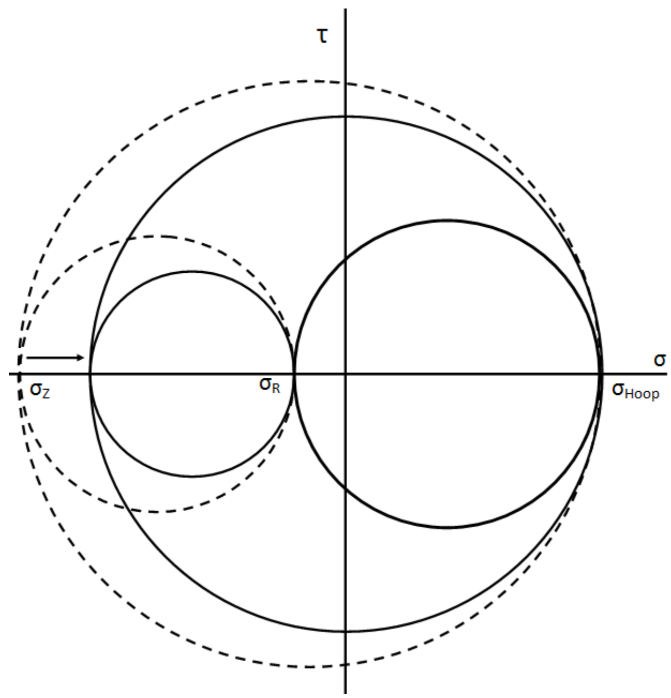

Figure 48: Mohr's Circle Demonstrating How the Decreased Axial Stresses Resulting from Longer Tubes can Result in Decreased Maximum Shear Stresses an Increased Resistance to Material Flow

It is also important to remember when the tube is pushed towards the die cavity, shear stresses develop on the surface of the tube to counteract this motion. This friction shear stress is a function of the pressure between the surface of the tube and the guiding zone, which is itself a function of the internal pressure in the tube and is roughly independent of tube length. This information can be used to explain the difference between the thickness distribution of the short and long tubes by considering a stress element which is made up of an incremental length of the tube in the guiding zone (see Figure 49). It can be seen that for very thin tubes the amount of stress transferred to the next element in the tube ($\sigma_a + d\sigma_a$) is equal to the difference between the axial stress transferred into the tube (σ_a) and the frictional stresses (σ_f). Also, for the case of thin tubes, the frictional stress is equal to the internal pressure multiplied by the friction factor. This means that the axial stress decreases linearly as one moves away from the edge of the tube. For longer tubes, the amount of axial stress needed to alter the state of stress at the edge of the guiding zone can be higher than the yield stress of the material, leading to thickening of the tube ends caused by upsetting.

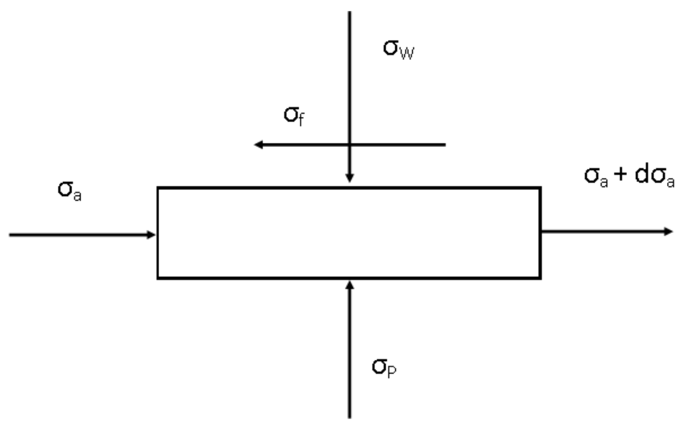

Figure 49: Stress Element Made up of a Differential Length of Tubing

The design of the feeding system will be based off the assumption that the initial length of the blank is 12mm because this tube length produced much better parts than their 20mm long counterparts in the simulations. In terms of the design of the feeding system, the important takeaways from the tube hydroforming simulations is the feeding force required to produce the required axial feed and the area to which these forces should be applied. The forces required by the system are summarized is Figure 50, which shows that the highest forces occur in the T-shaped parts. The worst case feeding force was 685N for the 1mm diameter parts and 1487N for the 2mm diameter parts. The area over which these forces are applied is taken as the cross sectional area of the tube ends, which can be calculated using the outer diameter of the die and the thickness of the tube at the end of the forming process. The thicknesses of the tube ends in the worst case scenarios for the 1mm and 2mm diameter parts are 0.181mm and 0.229mm, respectively. These values represent a thickening of the tube by 81% and 52%, respectively.

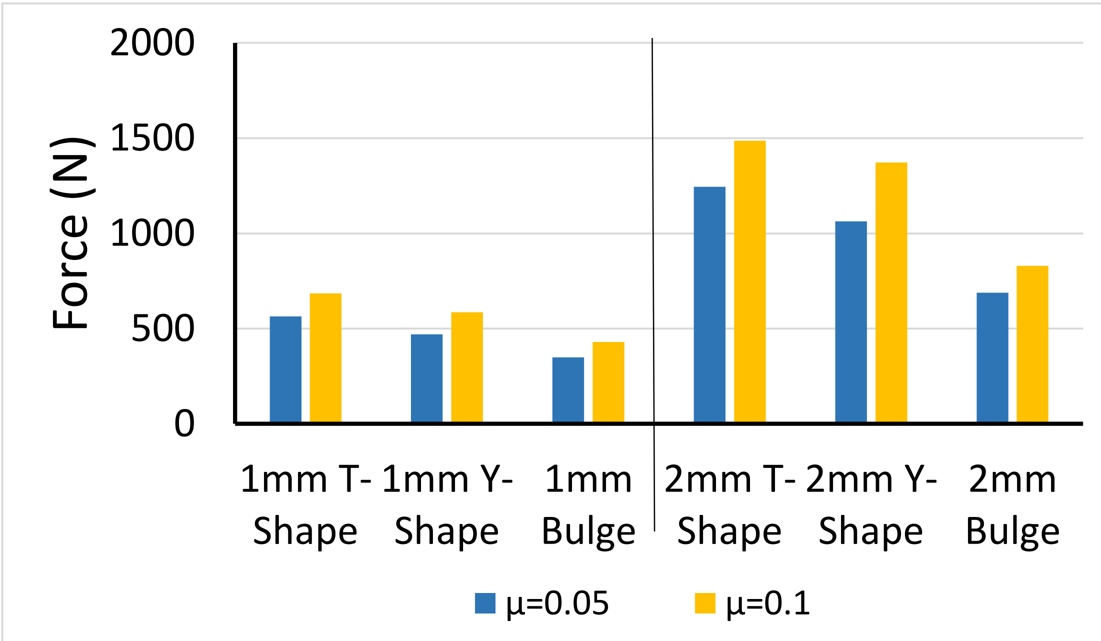

Figure 50: Maximum Feeding Force for 12mm Long Tube Simulations

4.3 Punch Simulations

The added flexibility in the punch design afforded by the proposed hydroforming tooling allows for the use of a wholly new type of punch. Specifically, the designer can move away from the constraint that punches must be hollow tubes. They can instead function by simply allowing fluid to enter the tube through a notch in the punch because the high pressure fluid totally surrounds the punch. Using information about the feeding forces provided by the simulations of the tube hydroforming process, it is possible to examine several different punch designs to determine their usefulness to a micro-tube hydroforming system. The stresses that occur in each variety of punch will be evaluated using the static structural module of ANSYS Workbench. In order to ensure that accurate results were obtained, a convergence test was imposed on the stress results. This automatically refined the mesh in areas with high stress gradients until the change in the maximum stress was less than 5%.

Several variation of punches will be evaluated, including the conventional style punch with both as high and low inner diameter and several varieties of notched punches. The types of punches which will be investigated in this section of the thesis are shown in Figure 51. Each type of punch will be tested in the 1mm diameter case and the 2mm diameter case using loading data obtained from tube hydroforming simulations. Specifically, the 1mm diameter punches will have a 685N load applied to the area between the outer diameter of the punch and a diameter of 0.638mm and the 2mm diameter punches will have a 1487N load applied to the area between the outer diameter of the punch and a diameter of 1.542mm. The punches will also be loaded with the maximum pressures that they will see during the forming process.

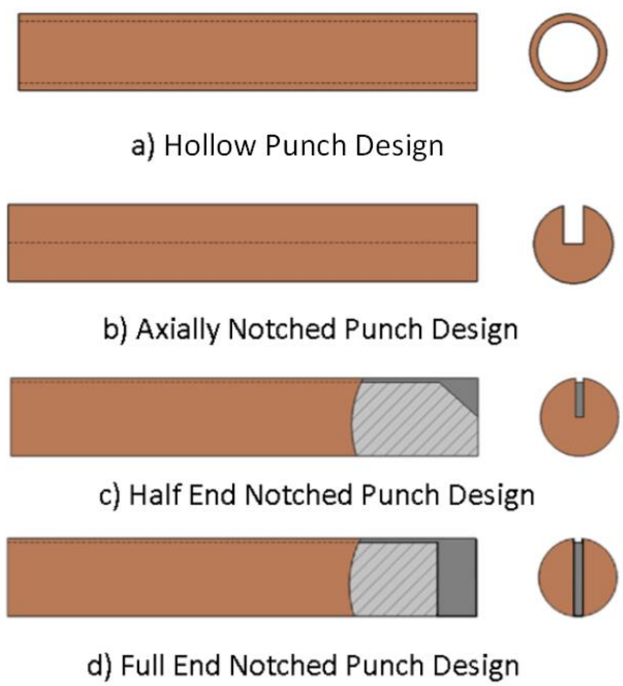

Figure 51: Punch Variants to be evaluated with Static Structural Simulations

4.3.1 Hollow Punch Design

The hollow punch design relies on a small hole to allow the pressurized fluid to get to the inside of the workpiece. Ideally, these holes are small when compared to the diameter of the punch, but due to the difficulties that arise when drilling very small holes, say on the order of 0.35mm, it is likely that the holes sizes would begin approaching the outer diameter of the punch as the punch is scaled to the micro-level. This design has the advantage of applying an even distribution of pressure to the tube ends, but it is likely that hole size which can be achieved in the punch will be too large if the diameter of the punch is small. This could lead to high stresses which could yield or otherwise destroy the punch.

Simulations of the hollow punch type show how the size of the hole effects the stresses in the punch for both sizes of punch (see Figure 52). It can be seen that the stresses in the 1mm and 2mm punches with 0.35 mm holes stay within the elastic limit of many tool steels, many of which have yield points as high as 2000MPa. This suggests that if a 0.35mm hole could be created thorough out the length of the punch that the feeding could be provided without incident. However, a hole of 0.35mm would be extremely hard to fabricate at the lengths which are required of the punch. If the diameter of the inner hole is increased to a more attainable 0.8mm, the stresses increase to over 2200MPa for the 1mm diameter punch. This amount of stress is high enough to permanently deform the punch, even if it is made out of hardened tool steel. Unlike the in 1mm diameter punch, the stresses do not increase significantly between the small and large hole case for the 2mm diameter punch. The reason that the stress increases in the 1mm diameter case and not the 2mm diameter case is because the increase in the size of the hole reduces the wall thickness of the 1mm diameter punch significantly. In fact, the 1mm diameter punch with a 0.8mm hole has a wall thickness which is less than that of the tube end after forming, reducing the amount of area that the forming forces could be distributed over. The 2mm diameter punch with a 0.8mm hole does not face the same increased stresses because wall thickness of the punch remained greater than the tube thickness.

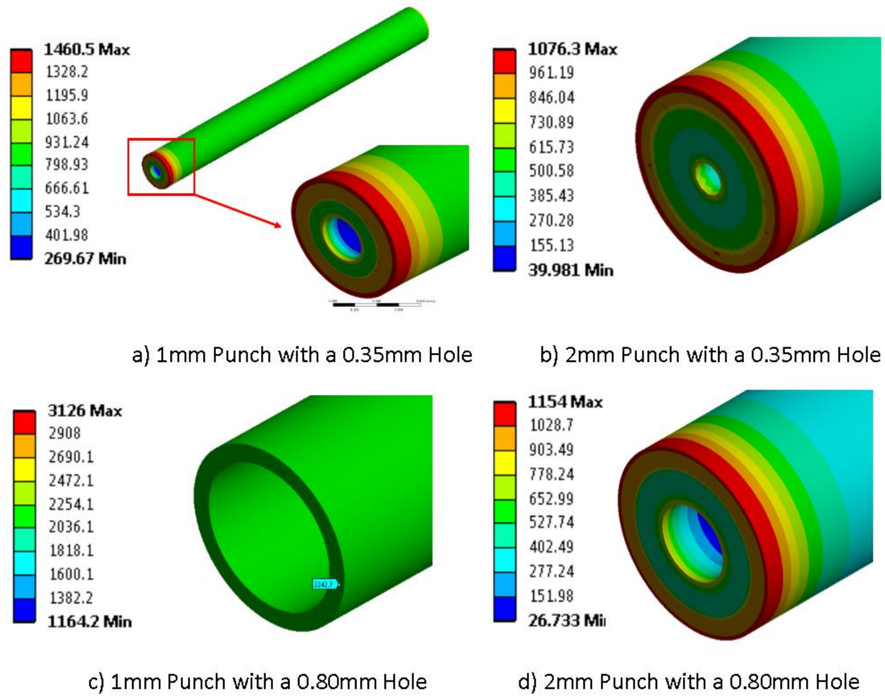

Figure 52: Equivalent Stress Contour Plots of the Hollow Punch Simulations

4.3.2 Axially Notched Punch Design

In order to avoid the problems with a hollow punch and ease the fabrication of the punch, a notched punch design is proposed. The notch can be created easily via a single wire EDM process where the punch is cut out of a solid block of hardened tool steel. This notch will run the entire length of the punch and will allow high pressure fluid to move freely into the blank. The width of the notch was chosen to be 0.4mm, the minimum width that could be created by the machines available to the researchers. The simulations of the 1mm diameter variant of this design show that stresses can go as high as 1965MPa, but these stresses are highly concentrated to the corner radii of the notch (see Figure 53). The average stress in the region of contact between the punch and tube is closer to 1600MPa, which is more than acceptable, for most tool steels. The stress in the 2mm diameter punch was much lower, with a maximum of 1577MPa in the corner radii and 1050MPa in the region of contact between the tool and workpiece. The stress is much higher in the 1mm diameter punch than the 2mm diameter punch due to the increased ratio of the notched width to the diameter of the punch. It is important to note that the size of the notch could be reduced to as low as 20μm if the correct equipment is available, which would likely reduce the stress observed in the 1mm diameter punch. It is likely that the reduction of the notch in the punch would not incur a significant cost increase, as the only difference in the EDM operation would be the size of the wire used.

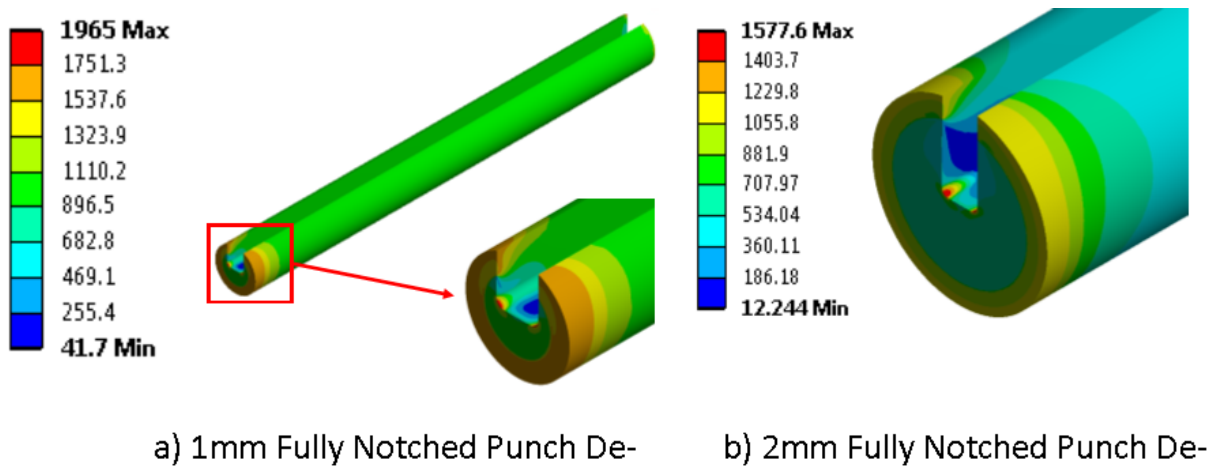

Figure 53: Stress Contour Plot for the Axially Notched Punch Design

4.3.3 Full End Notch

Another option to avoid the use of a hollow punch is the put a notch only on the end of the tube. This variant of the notched punch would allow fluid to pass between the punch and guiding zone and enter the tube via a notch that spans the diameter of the tube. This design would have increased rigidity when compared to the axially notched punch at the cost of decreased contact area and an increased resistance to fluid flow. Additionally, this design would require the use of an additional wire EDM step to produce the end notch after the overall punch shape is produced. Simulations of these punches show that the stresses (see Figure 54) for the 1mm diameter variant of the punch are extremely high (2464MPa), this is likely due to the severely reduced contact area caused by the large size of the notch relative to the diameter of the punch. Simulations of the 2mm diameter punch show that maximum stress is lower than in the axial punch design, but that the stress in the contact area has increased due to reduced contact area. Still the stress in the 2mm diameter punch is well within acceptable levels, for most tool steels. It is clear that, in order for a 1mm diameter punch to utilize this design, a much smaller notch would need to be fabricated on the end of the punch.

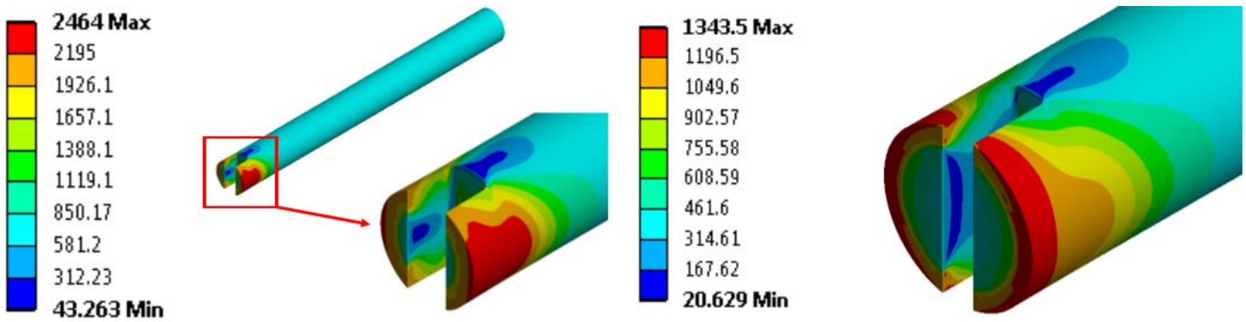

a) 1mm Full End Notch Punch Design   b) 2mm Full End Notch Punch Design

Figure 54: Stress Contour Plot for the Full End Notch Punch Design

4.3.4 Half End Notch

In an effort to increase the contact area of the end notched punch designs, the shape of the notch was changed to a triangular wedge whose height was equal to half the punch diameter. This design hopes to combine the rigidity of the fully end notched punch with the improved stress distribution of the axially notched punch, without sacrificing the ease of fabrication of the design. Stress contour plots (Figure 55) of the simulations show that the stress in the 1mm diameter punch has indeed been reduced from the full end notch case. The maximum stress (1792MPa) is within the elastic range of currently available tool steels, but it is still rather high. Again, it is worth noting that the stresses in the punch could be further reduced if the size of the notch were decreased. The 2mm diameter punch on the other hand has maximum stresses in the range of 1217MPa which is about 100MPa lower than in the full end notch design.

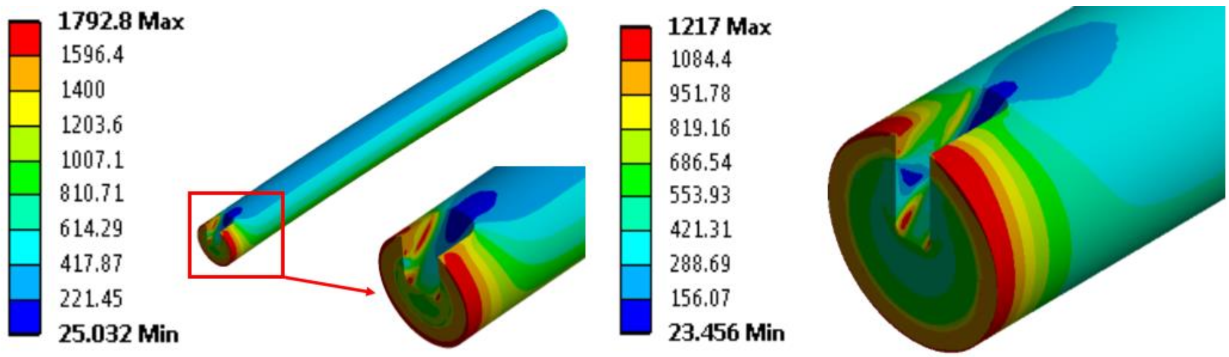

a) 1mm Half End Notch Punch b) 2mm Half End Notch Punch

Figure 55: Stress Contour Plot for the Half End Notch Punch Design

4.3.5 Influence of a Notched Punch on the Deformed Part

Unlike the hollow punch which produces an even pressure distribution on the tube ends, the notched punches, will produce an uneven distribution of force on the ends of the tube during the forming process. This may have an effect on the quality of the part which can be produced by the notched punch. A simulation was run applying the T-shaped geometry to a 1mm diameter part to ensure that the part could be fully formed using the notched punch. The blank used in the simulation was a 12mm long tube and the coefficient of friction between the tube and the die was 0.05, while the contact between the punch and tube was considered to be frictionless for simplicity's sake. The loading paths for the simulation were kept the same as all the other T-shaped simulations (Figure 36).

Figure 56 shows the results of the forming simulation. It appears that the presence of the notch does not prohibit the creation of the bulge in the part, but clearly there is a tab formed on the ends of the tube. The deformation of the tube ends will require the addition of a trimming step to the process to get back to a clean edge. However, the deformation of the tube ends is not uncommon, even in conventional tube hydroforming, and it is likely that this step would be needed even if a conventional punch design was used.

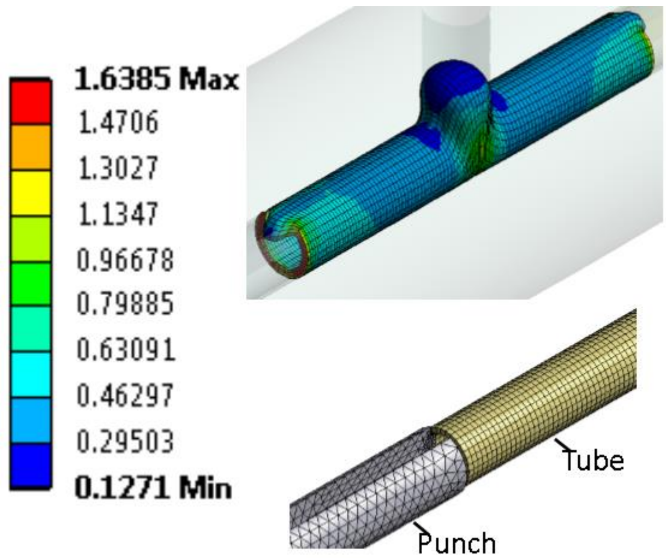

Figure 56: Effect of the Notched Punch on the Deformation of the Tube (Equivalent Plastic Strain Contour Plot)

4.3.6 Discussion of Punch Simulations

Simulations of the various punch designs clearly show that there are many different designs which could be applied to the floating die micro-tube hydroforming system. Clearly the ideal design, not considering cost, would be to use a punch which has a very small hole in its center. This type of punch exhibited the lowest stresses of all the punch designs and would apply pressure more evenly to the tube ends, but it is also difficult or, in some cases, even impossible to fabricate. The major restriction is that in order for the process to be flexible and have material feeding take place, the punches need to be rather long. This means that the holes drilled into the insides of the punch would need to be relatively deep, making the production of the holes troublesome. Another troublesome aspect to the drilling of micro holes in the punches is that, due to the stresses observed in the punch simulations, the material would need to be hardened to resist yielding during the forming process. The hardening process typically results in the dimensional change of the part, which is dangerous in the micro world due to the close tolerances which must be kept. In order to maintain the accuracy in the system the punches should be fabricated after they are heat treated, which will make it even harder to produce the micro hole at the center of the conventional punch design.

The notched punch design is a good alternative to the conventional design because it is easy to fabricate with wire EDM. As stated earlier in section 4.3.2, the punch can be fabricated easily from a block of hardened tool steel because there are no internal features. While some of the notched punch designs require two EDM steps, neither is so complicated that the expense of the system is greatly driven up. Another advantage of the notched punch design is the possibility of increasing the rigidity of the punch by maintaining a larger portion of the material in the punch. Furthermore, simulations have shown that the notched punches are capable of withstanding the forming forces present in the system. It should also be noted that a notched punch can be much longer than a hollow punch, making their application more flexible. For example, the notched punch can be fabricated longer than it needs to be to accomplish the feeding needed in the system, allowing the excess material to be secured to a device which provides the feeding force to the punch. This allows for the punches to be rapidly switched, reducing time lost to change over of the tools. Their low cost, ease of fabrication, increased rigidity, and increased flexibility in their application make notched punches an attractive alternative to the conventional punch design.

4.4 Summary of Finite Element Analysis

Simulations of the tube hydroforming process have revealed that the currently available system is capable of creating acceptable parts, but that greater pressures would need to be achieved to reach the full potential of the system. Additionally, they have revealed the types of forces which will be present in the system during the tube hydroforming process. This information be used to help design the equipment used to perform the hydroforming operation. In the case of the punches, simulations showed that notched punches could be used as a viable alternative to the hard to manufacture conventional punches. It should now be possible to design and fabricate a working micro-tube hydroforming system capable of both expanding and feeding the workpiece.

CHAPTER 5: MICRO-TUBE HYDROFORMING DEVELOPMENT AND EXPERIMENTS

5.1 Introduction

Testing the concepts laid out in chapters 3 and 4 requires that physical attempts at micro-tube hydroforming are carried out. This will require the design and creation of all the equipment which is to be used in the process, including the pressure vessel, feeding equipment, and dies. The pressure vessel must be capable of reaching pressures of up to 200MPa as well as housing the floating die and feeding equipment. It must also be able to be opened easily to facilitate the placement and removal of the parts before and after the hydroforming process. A last requirement is that it guide the motion of the feeders and ensure the proper placement of the dies and the punches to prevent any misalignment. The feeding equipment will consist of a power source, intermediary between the punch and source, and the punches themselves, all of which must be contained within the pressure vessel. For this stage of the development, the motion of the feeders does not need to be automated. If the system can be shown to work, an automation system can be designed later to improve the accuracy of the system. The dies used in the process will contain multiple areas for tube placement, each with a different die cavity design so that experiments can be run on multiple geometries simultaneously to facilitate rapid testing of the new floating die concept. The die should also be made in such a way that its placement is simple and exact so that it can easily be placed with little room for human error in aligning the tools.

5.2 Micro-Tube Hydroforming Tooling

5.2.1 Design

The system will be designed from the center out because each system's form and function will depend heavily on the way that the previous system has been designed. Thus, the design will start with the dies to be used in the micro-tube hydroforming process, then move to the feeding system and, finally, conclude with the design of the pressure vessel.

The main goals behind the design of dies are to create a die assembly which is easy to place and remove, facilitate the simultaneous hydroforming of multiple tubes, and rigid enough to resist deflection due to the process forces in the system. Starting with easy placement of the assembly, the two die halves must be designed in such a way that they consistently are placed in the same position relative to each other every time. This is especially important when one considers the alignment of the guiding zones of the two halves because if they are not coaxial the tube can be crushed between the two halves during assembly. Proper alignment can be accomplished by creating two sets of mating sloped surfaces on the dies, as shown in Figure 57. These sloped surfaces will guide the two die halves together as they are placed and as they are clamped together to ensure that the misalignment between the axis of the guiding zones in the two die halves is never more than a few thousandths of a millimeter off. Alignment is also important in the direction along the axis of the tubes, because this determines whether or not the die cavities of the top and bottom halves will line up properly. Because misalignment in this direction does not disrupt the shape of the guiding zone, more error is allowable and the positioning of this part can be accomplished by keeping a very small clearance between the die block and the walls of the pressure vessel. Modern manufacturing practices should be able to reduce the error in this direction to under two thousands of an inch.

In order to increase the production rate of the system, multiple die geometries are to be included into one die block. The die cavity should be spaced sufficiently far apart so that the bursting of one tube will not cause the high-pressure fluid to spill from one die cavity to another. Though this does not produce a specific spacing amount, the designer can use their intuition to make an educated guess and if their guess does not work the spacing can be changed. Because the dies should be rigid and resistant to wear and plastic deformation, they should be made out of a hardened tool steel. This makes the process of iterating the spacing expensive, as a new die set will need to be fabricated for each experiment, so the designer should try to be conservative in choosing this dimension. In order to increase the variety of shapes that could be produced by the die set, the designers chose to use four different die cavity shapes: the bulge shape, the flat bulge shape, the T-shape, and the Y-shape. However, in a production scale micro-tube hydroforming operation, it is likely that all of the shapes in the die would be identical so that only one load path would need to be used for each pressurization of the system.

Finally, some consideration must be made into how to keep the two halves of the die set closed during operation and setup. The initial closing of the die may be accomplished by clamping the bottom half of the die between the top half and the bottom of the pressure vessel using bolts. This will ensure that the system is properly aligned before the pressure vessel is closed, but may not prevent the two halves from separating during pressurization of the system. Luckily for the designer, the floating die concept has the advantage of being surrounded by the same high pressure working fluid which is inside the tubes. If the sealing system between the two die halves works properly, there will be areas between the two die halves that are not subjected to the high pressure (e.g. the die cavity), which will ensure that the net tendency of the pressure in the system will be to clamp down on the die halves causing them to stay shut during pressurization of the system. For added safety against opening the designer may include a backer plate on the top piece of the pressure vessel to ensure that the die cannot open once the pressure vessel is closed. Figure 58 shows how a die block with the proposed geometry would look.

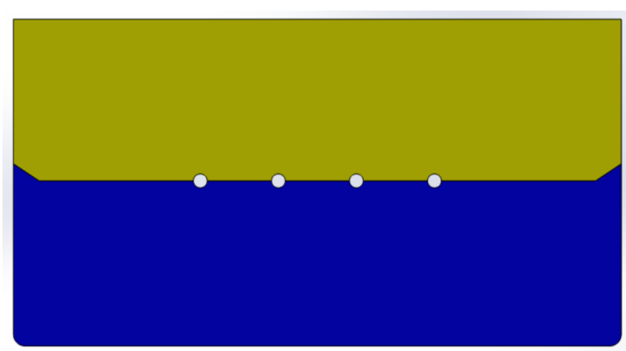

Figure 57: Proposed Aligning Geometry for the Die Block

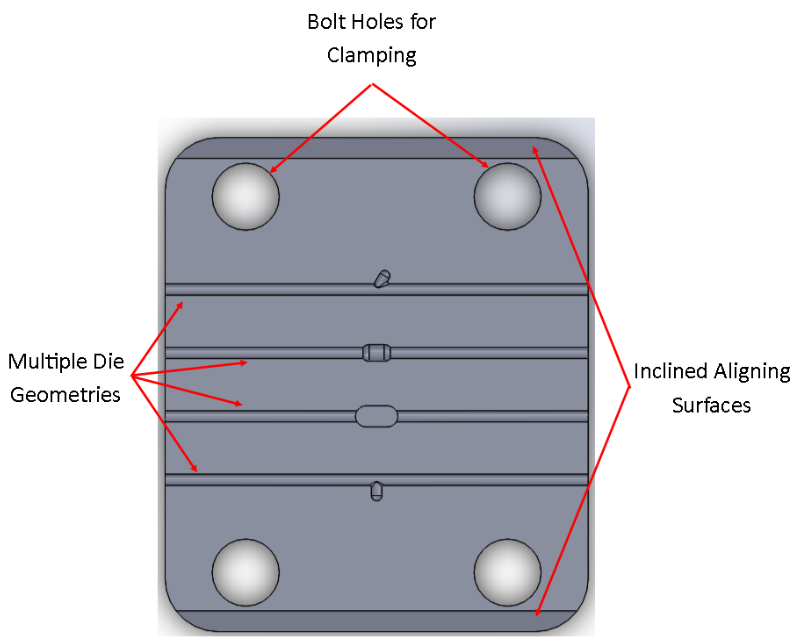

Figure 58: Proposed Multiple Geometry Die Block

The feeding system must have the ability to provide enough force to move the punches as much as 3mm into the die cavity. This means that it must provide a sufficient amount of force to produce the feeding, as well as predictably position the punches. In order to increase the flexibility of the system, the punches can be made as long cylinders with a constant OD so that they can be interchangeable. This will allow multiple punch designs to be tested, using the same feeding equipment. Additionally, the system is more flexible, as tubes of various lengths can be hydroformed by simply exchanging punches of one length for punches of another. The notched punch design makes this prospect even more attractive, because the notched punches can be rapidly produced at very little cost. However, there is a down side to using interchangeable punches, which is that they must be accurately positioned and manipulated without the use of a solid connection.

To fix the problem of having to feed multiple interchangeable punches at the same time, it is necessary to include an intermediary component between the power provider and the punches themselves. This intermediary will serve to align the punches and ensure that they are moved into the die correctly. The guiding of the punch holder can be accomplished by making the clearances between it and the pressure vessel very close and allowing the punch holder to slide in the pressure vessel. The matter of coupling the punches and the punch holder can be accomplished by drilling holes in the punch holder that match the diameters of the punches. The proposed punch holder would appear as shown in Figure 59. Punches can then be placed into the punch holder in such a way that part of the punch is in the die, part in the punch holder, and a small part (the maximum amount which the tube should be fed) is exposed between the punch holder and die set, as shown in Figure 60.

Providing the motion to the feeding system can be done through a cam, which can be manipulated from outside the pressure vessel. The system needs to be very rigid so that the motion of the system is predictable and repeatable regardless of changes in the process forces in the system. This cam should also be able to be easily changed to produce various feeding paths or be periodically replaced when it is worn. This can be accomplished by making the cam and the driving shaft two separate pieces, whose rotation is accurately coupled through the use of matching male and female key profiles on the two pieces. To increase the rigidity of the system the shaft should have a bearing surface on either end of the cam. A mockup of this system is shown in Figure 61.

Manipulating the cam from the outside of the pressure vessel poses a few risks, namely being able to maintain the pressure in the working fluid if the driving shaft penetrates the wall of the vessel. For now, it will be assumed that creating a reliable seal is possible so that the design of the feeding system can be completed and the problem of designing a reliable seal will be dealt with later. To rotate the shafts that are attached to the cams the designer needs to create a system which can provide enough torque to overcome the friction in the system and the force required to feed the tubes. This is best done by machining a profile in the exposed ends of the driving shafts so that a wrench like arm can provide a mechanical advantage to the system. This arm should be firmly secured to the end of the shaft on one end and coupled with a means of rotating the system on the other end. In order to provide an additional mechanical advantage to the system a large screw is used to push down on the lever arm and produce the force required to rotate the cam system. This screw is held in place by a threaded collar, which ensures that the rotation of the screw forces the motion of the arm and thus the entire cam feeding system.

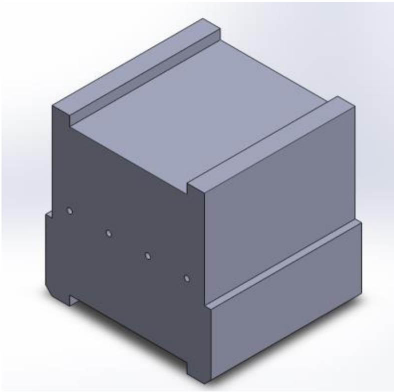

Figure 59: Proposed Punch Holder

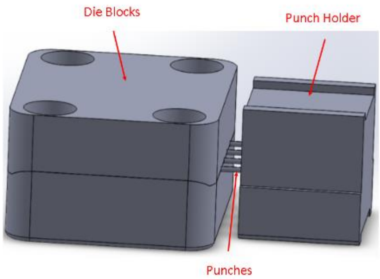

Figure 60: Proposed Punch and Punch Holder System

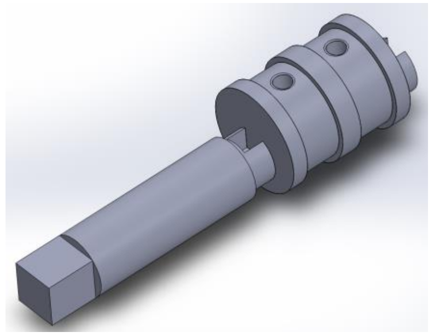

Figure 61: Cam Feeding System

The pressure vessel must include allowances for the feeding system and the die set, as well as, ensuring that the working fluid can be brought up to the desired pressure. The cavity of the pressure vessel must be shaped so as to provide contact surfaces which align the die set and the punches. The dimensions of this cavity depend on the dimensions of the feeding system and the die set and, therefore, is a fixed requirement of the design and must take the shape shown in Figure 62. The fabrication of this cavity must be very precise to ensure that unnecessary errors are not introduced into the system. The designer must work around the defined dimensions of the vessel in order to ensure that the pressure vessel is structurally sound and can maintain the required pressures.

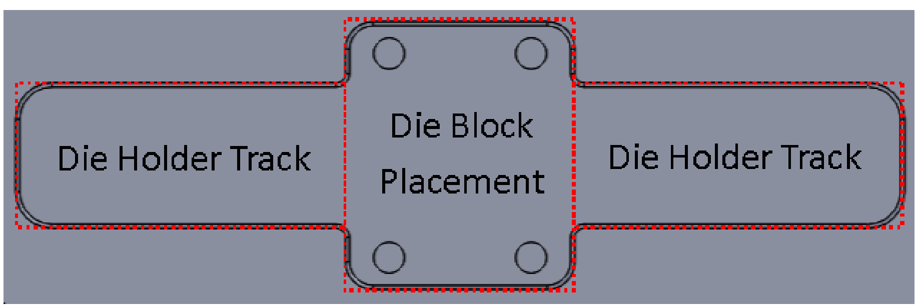

Figure 62: Required Shape of the inside of the Pressure Vessel

The sealing system is easier to design if the seals for all the openings in the pressure vessel are made independent of each other. The sealing systems can therefore be broken into three pieces, the sealing of the fluid inlet port and bleed off valve, the sealing of the area between the top and bottom halves of the vessel, and the sealing of the area around the shafts which penetrate the wall of the pressure vessel. Due to the high pressure of the working fluid the sealing of the fluid ports is accomplished by threading a special fitting onto a tapered hole in the die. This creates a small ring of metal to metal contact where the pressure can be quite high, preventing the fluid from being able to escape around the fitting. The sealing of the two die halves can be done by creating a mating pare of male and female seals. In bottom of the female seal a strip of Teflon, which is cut in the shape of the female seal, is placed. The Teflon has a thickness which is greater than the clearance between the bottom of the female die and the top of the male die so that when the two halves of the die are brought together, they crush the seal into any gaps between the male and female seals.

The most complicated seals in the system are the seals which prevent the working fluid from escaping around the shafts. The basic principle of these seals is to compress a soft plastic ring axially, causing the seal to expand in the radial direction and clamp down tightly on the shafts. In practice this can be accomplished by machining a seal cavity in the side of the die wall which will provide the confined space needed to from a seal with the deforming plastic. If the ends of the ring are flat the pressure will be distributed across the sealing surface of the shaft equally, which reduces the normal stress at the contact surfaces and decreases the pressure which can be sealed. Increasing the normal stresses between the seal and the contact surfaces will result in increasing the sealing capacity of the system. This can be accomplished by either increasing the axial stress applied to the seal or changing the shape of the seal to redistribute the pressure. The latter approach gives the designer the opportunity to maintain pressures well above what is capable for a flat faced seal. The shape of the seal is created by first machining a plastic ring with flat faces and then using a sharp thin tool to machine a triangular profile into the ring, which would then look like the seal shown in Figure 63. A strong reliable seal can now be created by pushing a seal expander with a matching male profile into the seal. This forces the seal to expand heavily in the area at the edge of the V-shaped grove. However, because the seal is confined by the walls of the seal cavity and the shaft going through its center the material cannot expand easily and high normal stresses are generated between the seal and the contact surfaces. These increased normal stresses can significantly increase the sealing power of the shaft seals.

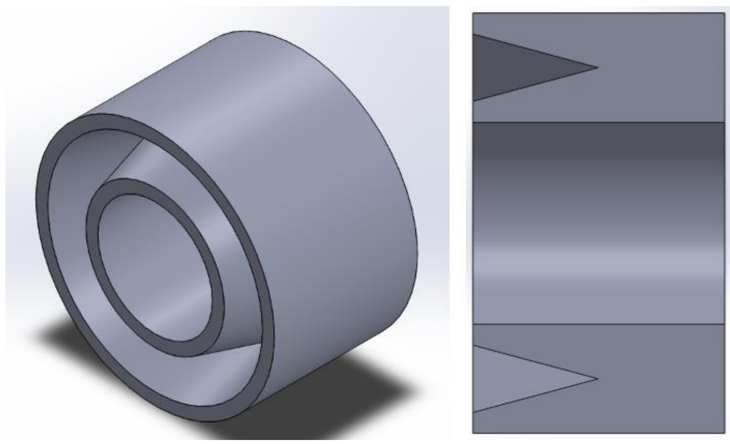

Figure 63: Seals with a V-Shaped Grove for Enhanced Sealing Effectiveness

The finite element method should be utilized to ensure that the dimensions of the pressure vessel are sufficient to avoid a catastrophic failure when the system is pressurized. In this design the finite element method was carried out using the Static Structural module of ANSYS Workbench. The simulation was done with a half model of the pressure vessel and the boundary conditions are shown in Figure 64. To summarize, a fixed displacement condition was applied to the bottom surface of the vessel, while the top surface of the pressure vessel had an 890 KN clamping force applied to it. Furthermore, a symmetry boundary condition was placed on the cut surfaces of the half model and a pressure of 130MPa was applied to all the surfaces which constitute the inside of the pressure vessel. The contact between the top and the bottom halves of the pressure vessel was simulated as a frictional contact with a coefficient of friction of 0.5. The simulations results shown in Figure 65 indicate that there are very high stresses present in the pressure vessel, but that they are also highly localized. This may simply cause small scale yielding in the area of high stresses, but due to the shape of the feeders and dies it will have little effect on the overall system. In general the stresses in the pressure vessel are blow 1000 MPa, but in the radius between the wall and floor of the vessel the stresses levels in the range of 1400 MPa (baring the localized area of high stress. It can be seen that a tool steel such as A2, which can have a yield stress as high as 2000MPa, can easily withstand the stresses applied to the pressure vessel.

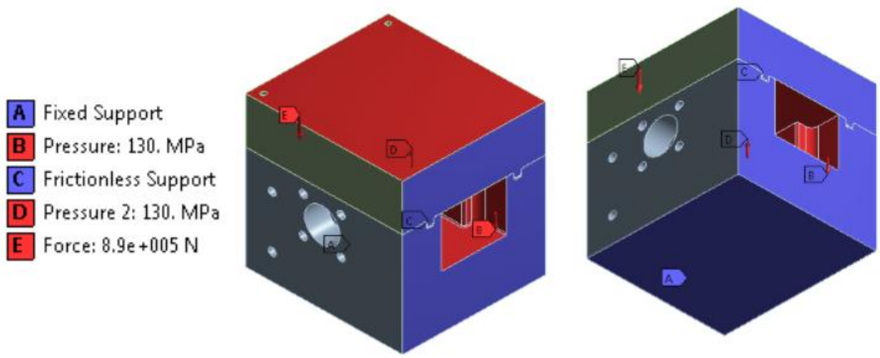

Figure 64: Boundary Condition used in the Static Structural Simulation of the Pressure Vessel

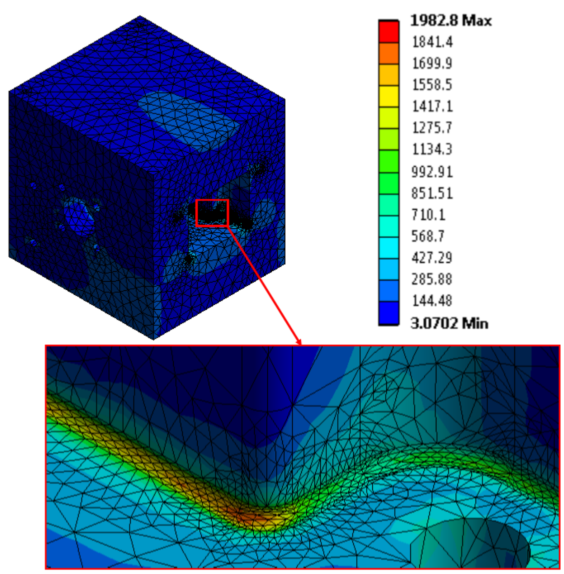

Figure 65: Stress (MPa) Contour Plot of the Static Structural Pressure Vessel Simulation

When all the individual pieces of the Micro-Tube Hydroforming are put together, they would look something like what is shown in Figure 66.

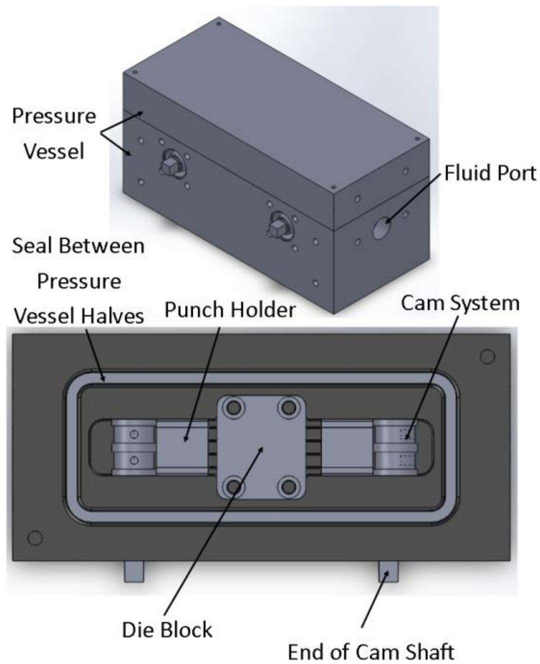

Figure 66: Annotated View of the Assembly of the Components in the Micro-Tube Hydroforming System

5.2.2 Fabrication

The die blocks used in the hydroforming experiments are created from A2 tool steel blocks. The creation of the die blocks requires the use of wire EDM to get the guiding zones to line up properly. Wire EDM is also used to size the die block so that it fits snugly into the pressure vessel. After the basic profile is cut out, a CNC mill is used to create the geometry of the die cavity. Next, a chamfer is ground into the bottom facing side of the bottom die block to ensure that any radius that is at the bottom of the pressure vessel pocket does not interfere with the alignment of the dies. Finally, the block are heat treated to obtain a hardness of 60 HRC. The completed die blocks are shown in Figure 67.

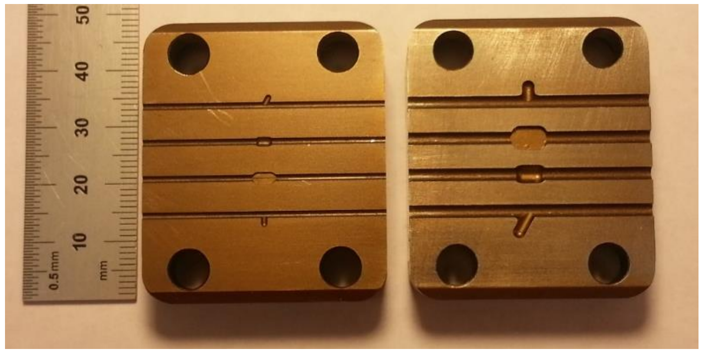

Figure 67: 1mm and 2mm Die Blocks

The punches were fabricated from a block of hardened tool steel using a wire EDM process. The axially notched punches were created with a single operation because they have a constant cross section. The end notched punches required two operations to create, one to create the cylindrical slug and another to put a notch in the end of the punch. No further heat treatment was carried out as the punches maintain the hardness of the base material. An axially notched punch and an end notched punch are shown in Figure 68.

Figure 68: Notched Punches (Left) Full End Notch (Right) Axial Notch

The shafts and cams used in the feeding system were fabricated from A2 tool steel using several machines. The shafts were fabricated using a mill and lathe, while the cams were fabricated using a lathe and wire EDM machine. The wire EDM process was required to make the key profile in the cam which is used to lock the cam to the shaft so that the two pieces could be rotate together. After the parts were machined, they were heat treated to a hardness of 50 HRC.

The two halves of the die holder were created on a CNC milling machine from two large blocks of A2 tool steel. Basic low grade tools were used to perform a rough cut of the pocket and seal geometries. High quality carbide tools were used to make the finishing cut in order to ensure that as close a tolerance as could be achieved was held. The two halves of the pressure vessel were then heat treated to a hardness of 50 HRC. The completed pressure vessel is shown in Figure 69 and Figure 70. After all the parts were heat treated, they were ground and lapped as needed to obtain the close fit desired for the system.

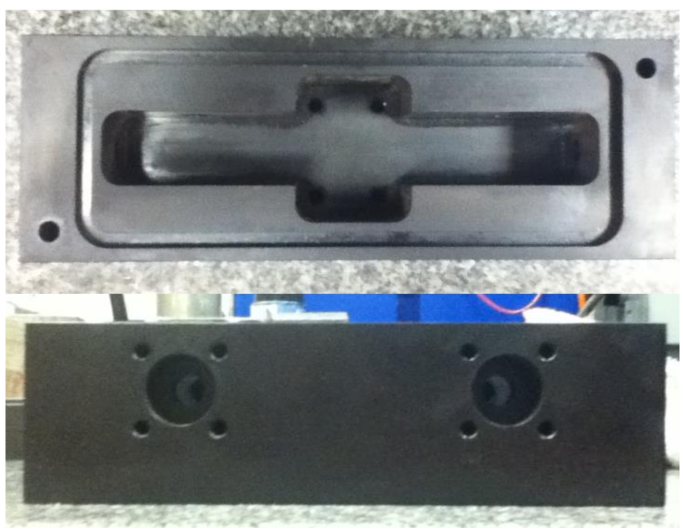

Figure 69: Bottom Half of the Pressure Vessel

Figure 70: Top Half of the Pressure Vessel

5.2.3 Operation and Experimental Setup

The basic pieces of equipment used in the micro-tube hydroforming experiments are a 150 ton hydraulic press, a 140 MPa pressure intensifier, and the tooling described in 5.2.1. The hydraulic press is used in combination with the lever clamp assembly to keep the die closed as the system is pressurized. The pressure intensifier is used to provide the working fluid (ISO 32 Light Hydraulic Oil) to the inside of the pressure vessel. During the experiment the pressure is varied linearly from 0 to the maximum pressure used in the experiment (105 or 130 depending on the test) in 100 seconds. The feeding applied to the tubes takes place when the pressure is between 35 and 80 MPa and is done manually. The 1 and 2mm diameter tubes used in the hydroforming experiments are made out of annealed SS 304 and have lengths of either 12 or 20mm. The wall thickness of the 1mm tubes was 0.1mm and the wall thickness for the 2mm tubes was about 0.15mm. The Teflon sheet which serves as a seal on the outside of the tubes also serves as the lubricant in the system. After the hydroforming operation, the tube length was measured with calipers and in some cases the tubes were mounted in epoxy and cut in half to reveal the thickness distribution of the tubes.

During the initial setup of the micro-tube hydroforming, the cams and shafts must be fit into the system. This requires that they be pressed into the shaft seals meaning that they cannot be removed from the pressure vessel until one is ready to also remove the shaft seals, as doing so would ruin the shaft seals. Therefore, the pressure vessel already has the cams placed before the setup of the experiments and the first task to be accomplished at the start of a test is to prepare the die block and feeding system. To do this, the bottom half of the die block is first placed into the pressure vessel. Then a thin sheet of Teflon is laid over the die cavity and the punch holders with punches attached are placed into the die cavity so that the punches are positioned on top of the Teflon layer. Any die cavities which are not going to be used in testing are filled with brass plugs to keep the working fluid out of the die cavity. Figure 71 shows what the system looks like just before the tubes are placed into the die cavity, note the layer of plastic underneath the punches and brass plugs. Now the tubes can be placed into the system, a second Teflon sheet can be placed on top of the tube and punches, and the top half of the die block can be bolted onto the bottom half. The arms that are used to actuate the cams and the fluid ports are next attached to the pressure vessel, as shown in Figure 72. Once the pressure vessel is closed, it can be moved to the 150 ton press, shown in Figure 73, so that it can be clamped shut. Additionally, the high pressure line must now be attached to the fluid port.

Figure 71: Setup just before the Tubes are placed into the Die

Figure 72: Assembled Tooling before Pressure Vessel is Closed

Figure 73: 150 Ton Press used to Clamp the Pressure Vessel Shut

Now that the system is properly positioned in the press, the hydraulic press can be used to seal the two halves of the pressure vessel. Once the pressure vessel is clamped shut, the air bleed is performed by filling the vessel with the working fluid from the supply port and allowing the air to escape through the bleed off valve. The microforming system is now pressurized slowly and the arms which actuate the cams are turned manually, providing axial feed to the system. The feeding continues until the user determines that an appropriate amount of feed is reached, at which point the feeding is stopped and the system is allowed to pressurize to the maximum pressure without feed. Once the maximum pressure is reached the system is unloaded and switched off. To remove the hydroformed tubes, the pressure vessel is opened and die block is unbolted. A pair of channel locks is then used to remove the top half of the die block from the bottom, exposing the tubes. The tubes, punches, and brass plugs are then removed from the system and the cams are reset to their original position. The system can now reset to make it ready to be used for the next set of experiments

5.3 Results and Discussion

Experiments using the developed floating die equipment were run to determine the viability of the system. Specifically, a) can the system simultaneously axially feed and expand the tube? b) can the sealing systems keep the pressurized fluid out of the die cavity? c) how will the notched punches effect the deformation of the tube? d) is the system reliable enough for repeated use?

Figure 74 shows the first parts which were hydroformed using the floating die equipment presented in this thesis. It can be seen that the pressure at which the tubes were formed was not great enough to fully form the desired geometry. It should be noted that, the pressures reached were significantly lower than those simulated in section 4, so a less formed part than in the simulations is expected. When compared to samples shown in Figure 75, which were hydroformed at the same pressure, but with additional feed, there is a distinct difference in the size of the shape of the bulge part. The parts with additional feed have wrinkled at the transition between the bulge and nominal diameter, while the bulge part with low feeding has a smooth transition. This wrinkling phenomenon is clear evidence that the tubes have been successfully feed into the die cavity while simultaneously being expanded by high pressure. Figure 76 shown the thickness distribution in one of the wrinkled 1mm bulge parts. It can be seen that the bulge zone is about 25% thinner than the guiding zone and that the transition between the two thicknesses occurs at the location of the wrinkle. This suggests that the tube had already undergone some expansion by the time the feed reached the critical value and the part buckled under the axial load. Figure 77 shows the deformation of the tubes under much higher pressures.

Figure 74: 1mm OD, 12mm Long, P=100MPa, feed 0.5

Figure 75: Wrinkled Bulge Shaped Parts with an Undeformed Tube, 1mm OD, 20mm Long, P=100 MPa, Feed=1mm

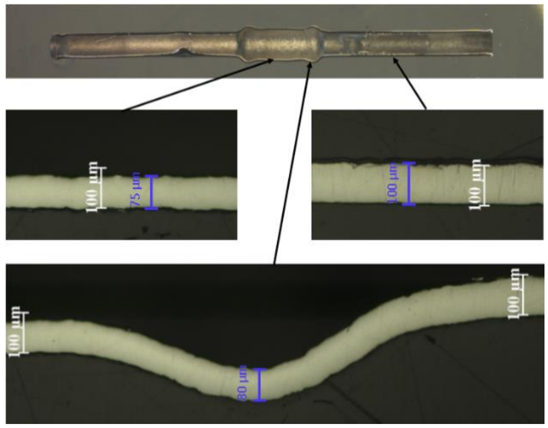

Figure 76: Thickness Distribution of a 1mm OD 20mm Long Bulge Shaped Part with 1mm of Feeding

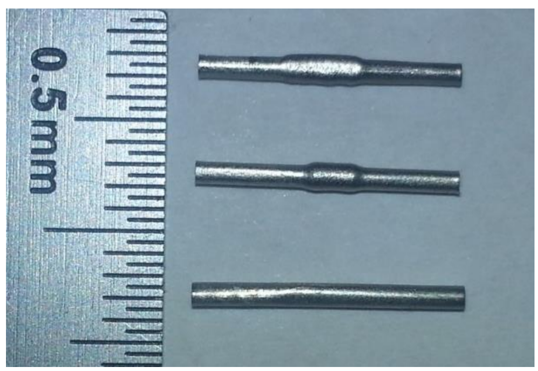

Figure 77: 1mm OD 12mm Long Round and Flat Bulge P=132.3MPa, Feed=0.37mm

Figure 78 shows the 2mm bulge shapes which were formed without the use of axial feed. The bulges on the 2mm parts appear to be much better formed than their 1mm counterparts. The thickness distribution across the 2mm round bulged part is depicted in Figure 79, which shows that the thickness of the part transitions from a value of around 155μm to a value of 110μm, a reduction of 29%. Also note the ratio of the original thickness (in the guiding zone) to the outer diameter of the tube is much smaller for the 2mm tubes than for the 1mm tubes. This results in a tube which is much more formable at low pressures than the thick 1mm tubes. A large amount of feeding was added to the hydroforming of the round and flat bulge shapes to produce the results shown in Figure 80. The large amount of feeding produced large wrinkles on the round bulge and caused the flat bulge shape to collapse before it was able to form two full lobes. The thickness distribution for the two parts is shown in Figure 81. When compared to the thickness distribution of the free bulged part it can be seen that adding material feed to the hydroforming process reduced the thinning which takes place in the bulge zone of the part.

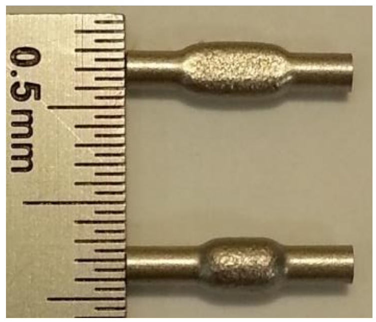

Figure 78: 2mm OD, L=12, P=100 MPa No Feed

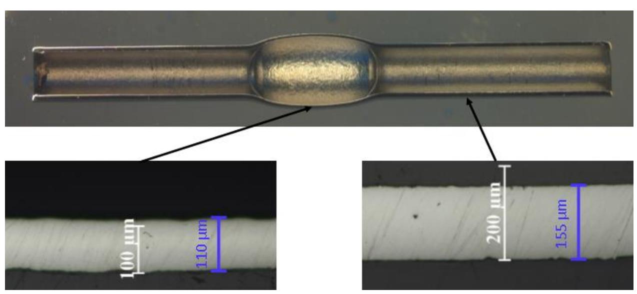

Figure 79: Thickness Distribution of the 2mm OD 12mm Long Bulged Part with no Feeding

Figure 80: Round and Flat Bulge Parts with Wrinkling, 2mm OD, 12mm Long, P=100 MPa, Feed=2mm

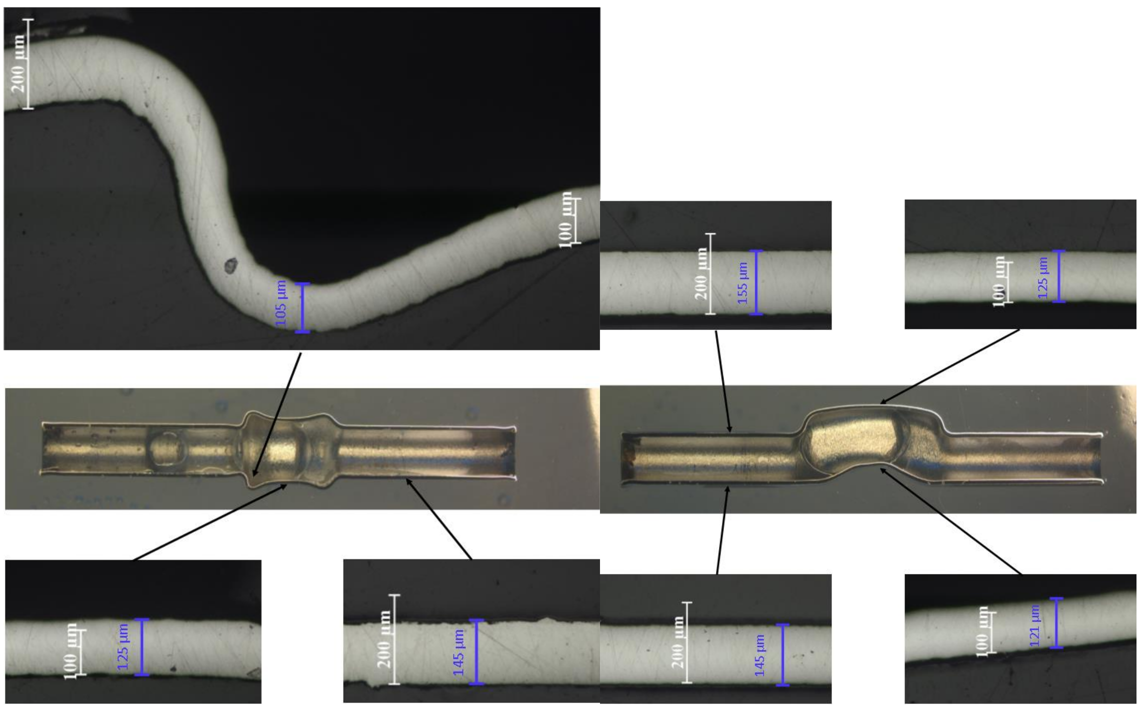

Figure 81: Thickness Distribution for the 2mm OD 12mm Long Bulge Part (left) and the Round Bulge Part (right) with 2mm Feed

The hydroforming of more complex Y and T-Shape parts was also attempted with the 2mm tubes. Figure 82 shows a Y-shaped part which was partially formed using about 1mm of feed and a maximum pressure of 100MPa and the thickness distribution on the part. The maximum height of the bulge is about 0.7mm. The reason that the part did not fully form is likely the relatively low maximum pressure supplied to the tube during the deformation process. Higher, better defined protrusions could be obtained if higher pressures were supplied to the tube, as shown in Figure 83. The maximum bulge height obtained in the hydroforming of 2mm tubes was 1mm and it is thought that if higher pressures can be obtained bulges with heights closer to those seen in the simulations could be obtained. Attempts to increase the amount of axial feeding supplied to the resulted in the buckling of the tube at the deformation zone as shown in Figure 84.

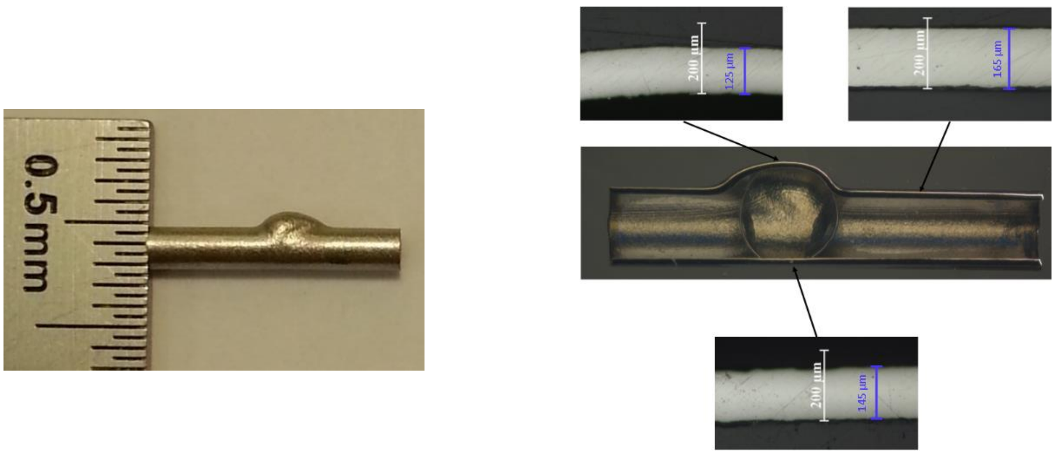

Figure 82: (left) Y- Shaped Part 2mm OD, L=12MM, P=100 MPa, Feed=1mm (right) Thickness Distribution of the Y-Shaped Part

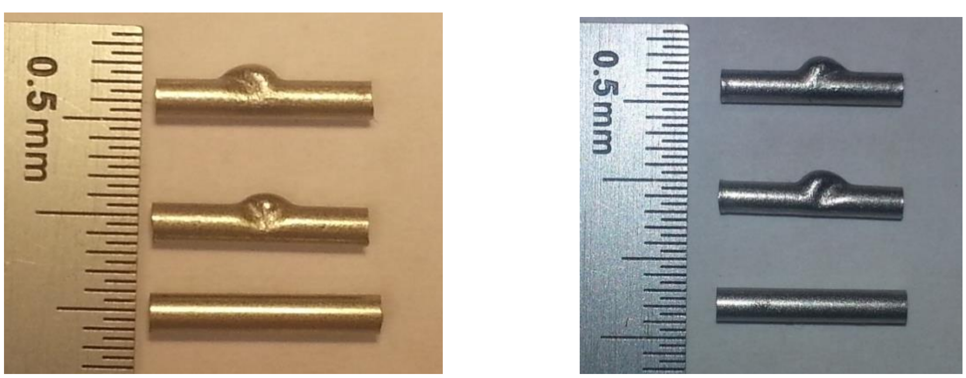

Figure 83: Y and T Shapes 2mmOD, 12mm long, P=132.3MPa, (left) Feed=0.7mm (right) Feed =0.5mm

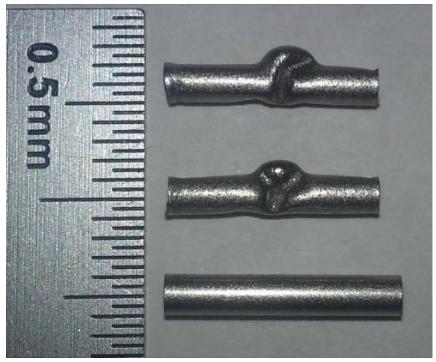

Figure 84: Y and T Shapes 2mm OD, 12mm Long, P=132.3MPa, Feed=1.1mm

During the testing of the hydroforming system it was noted that turning the cams which controlled the feeding of the punches became increasingly difficult at higher pressures. This phenomenon is not quantitatively shown because there is not currently a way to measure the torque on the shafts in the system. Tests of the system with no tubes also showed an increased resistance to rotating the cams, leading the researchers to conclude that this is a result of the increased pressure on the back of the seal. Essentially, as the pressure on the back of the seal increases the seal is pushed into the V-shaped expander, which pushes the seal material radially away from the expander. This raises the normal pressure on the shafts and die cavity and increases the frictional load as the shafts rotate against the seal. This action is essential to ensuring that the system maintain a strong, reliable seal as pressure increase, but results in increased power requirements for the feeding of the system.

The information gained in these experiments serves as a proof of concept. The next step for the equipment is to try and make fully formed parts. This will require the system to be more repeatable than it was for the proof of concept experiments. Clearly, the manual feeding of the tubes is the cause of much of the randomness in the system, as the loading path of the process is subject to human error and changes every time the process is performed. Increasing the repeatability of the system will clearly involve automating the feeding of the tubes with a computer controlled system. Additionally, the system needs to be fitted with a way to measure the feeding force separately from the force required to overcome friction in the feeding system. After this is accomplished, an accurate measure of the repeatability of the system can be established through accurate load stroke curves and measurements of the tube geometry for identical loading paths.

CHAPTER 6: AUTOMATION

6.1 Introduction

In order to move the floating die micro-tube hydroforming system beyond the proof of concept stage, an automated feeding system must be developed. This system will be used in combination with the existing automated pressure system to produce accurate and reproducible loading paths.

6.2 Overview

The automations system will consist of a combination of hardware and software that works in combination to precisely control the feeding of the tubes. The hardware is comprised of the motors, encoders, and data acquisition devices used to operate the feeding system. The software is used to take in information from the encoders, translate that information into the amount of feed produced, and send out an appropriate control voltage to drive the motors. The basic requirements of the automation system are: a) the two shafts should move independently b) the system should be able to produce a 180 degree rotation of the shafts in 30 seconds c) the computer should be able to produce and accurate and repeatable load path d) the computer should compensate for any nonlinearities in the system.

In order to produce the feeding in the system the motor must be able to overcome the forces created when feeding the tubes, as well as the frictional forces which are inherent to the system even under no load conditions. Testing of the system under no load conditions has shown that the amount of torque needed to produce a rotation of the cam shafts is about 27 N-m. The amount of torque which is required to carry out the feeding of the tubes, ignoring the friction on the shafts, can be calculated by multiplying the total feeding force by the moment arm of the cam. The total force needed to feed four tubes simultaneously is about 6000N and the maximum moment arm of the cam which is currently being used is 3mm, resulting in a feeding torque of 18N-m. The total torque that must be produced to feed the tubes is then found by adding the torque required to feed the tubes and the torque required to overcome friction, or 45N-m.

6.3 System Design

The low speed of the shafts and the high torque required to feed the motors suggests that the electric motors which power the system will need to be geared down. If the shafts are to rotate at 1-2 RPM and the amount of torque which needs to be produced is 45Nm, the power needed to turn the shaft is 9.42 W. Assuming that the gear drive in a gear motor system is about 50% efficient, the power rating of the motor would need to be around 20W. Coupling the output of the gear motor to the cam shaft can be done with another gear system, which will also allow the designer to further increase the torque transmitted to the motor, and also make assembly and disassembly of the system easy.

From here the designer need only mount the motors so that their placement is consistent and correct. This can be done by creating a mounting structure consisting of a plate which can be tied to the press frame and a piece of angle that the motors can be mounted onto. The mount can then be bolted into the plate to establish a rigid repeatable connection. The final system may look something like Figure 85.

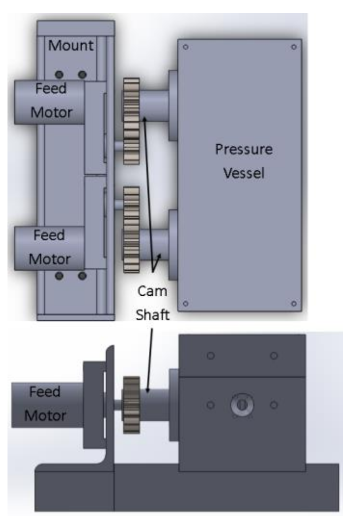

Figure 85: Depiction of the Automated Feeding Hardware

To transfer position data to the computer the system needs to be fitted with encoders. These would need to be attached to a data acquisition device capable of interpreting the pulses from the encoder as counts. The counts can then be processed with a computer to determine the current position of the cam shaft and, by using appropriate relationships, the punch holder. As can be seen in Figure 86 the total feed (f) that occurs when a circular cam is rotated from the minimum (dotted) position by an arbitrary amount (θ) is the same as the amount horizontal change in the position of the center of the circle which makes up the cam. Trigonometry can relate this feed to the offset between the center of rotation and the center of the cam (O) and the angle of rotation (Equation 6).

$$f_{0-1} = O(1 - \cos(\theta)) \qquad \text{Equation 6}$$

The feed from an arbitrary starting point can be found by subtracting the total feed from the stopping point by the total feed from the starting point (relative to the minimum point), as shown in Equation 7. This is further simplified in Equation 8 and Equation 9.

$$f_{1-2} = f_2 - f_1 = O(1 - \cos(\theta_2)) - O(1 - \cos(\theta_1)) \qquad \text{Equation 7}$$

$$f_{1-2} = O(\cos(\theta_1) - \cos(\theta_2)) \qquad \text{Equation 8}$$

$$f_{1-2} = -2 * O\left[\sin\left(\frac{1}{2}(2\theta + \Delta\theta)\right)\sin\left(\frac{1}{2}(-\Delta\theta)\right)\right] \qquad \text{Equation 9}$$

Equation 4 is especially useful for the use of encoders because each pulse from the encoder will represent some change in the rotated angle and a computer can be used to keep track of the current position.

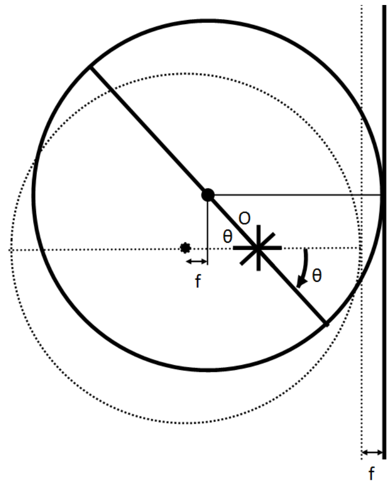

Figure 86: Geometry of the Circular Cam System (Black: Current Position) (Dotted: Initial Position)

After the position of the cam is determined by the computer, it can be used as the feedback signal in a control loop. The control loop would measure the error in the system's motion and then send an appropriate control voltage to the feed motors. It is likely that the computer will not be able to send enough power to the motors to run the circuit, so an amplifier would have to be used to provide sufficient power to the system. If the correct control algorithm is chosen, this system can provide a much more accurate and repeatable feed path than could ever be attained by manual operation. Ultimately, the automated control system will allow manufactures to rapidly and accurately create a large number of micro-tube using the floating die micro-tube hydroforming system.

CHAPTER 7: CONCLUSIONS AND FUTURE WORK

7.1 Conclusions

A new system for the creation of complex metallic micro-tubular components has been presented. The floating die system is able to combine the expansion of the tube with axial feeding of the tube ends. This was accomplished by determining the requirements of the system on a fundamental level and then designing the system to meet the particular needs of the micro-tube hydroforming process. Finite element simulations of the process were carried out to help in the design of the tooling and to better understand the variables involved in the hydroforming process. Micro-tube hydroforming equipment was designed, fabricated, and tests were run one 1mm and 2mm SS304 tubes. Finally, a system for automating the feeding of the tubes was developed to increase the repeatability and accuracy of the feeding of the tube ends. The following conclusions were drawn from this research.

- Scaling down the traditional macro-scale tooling to the micro scale is a difficult, if not impossible, and expensive proposition.
- Many of the roadblocks that are present when scaling down conventional tube hydroforming tooling can be avoided by changing the responsibilities of the punch and the die. Specifically, the interdependence between the material feeding and the sealing of the tube is eliminated.
- A Teflon seal can create a strong a reliable seal on the die cavity so that hydroforming can occur by submerging the sealed die block into the high pressure working fluid.
- Removing the sealing and fluid supply responsibilities from the punch gives designers great freedom when it comes to the shape of the punch. Specifically, the punch no longer needs to have a hole through its center and can instead be fabricated as a notched punch. This serves to increase the rigidity of the punch as well as reducing its cost by easing its fabrication.
- Finite element simulations and experimental results proved that the floating die system could perform a micro-tube hydroforming operation that successfully applied

both axial feed and expansion to the workpiece. In order to fully form parts, the system will, however, need to be tested under higher pressures.

- Both experimental results and finite element simulations showed that the notched punch could be used as a viable alternative to the hollow punches used in conventional tube hydroforming tooling. The only drawback of using the notched punch was the formation of a 'tab' on the ends of the tube due to an uneven distribution of pressure on the tube face. This will require the ends of the component to be trimmed, however, it does not affect the overall integrity of the part.

7.2 Future Work

The future work in this research should be focused in creating fully formed and useful parts. To this end, the system should be tested under higher pressures and for different geometries. The repeatability of the system should be improved by applying precise controls to the feeding system, so that precise feed paths can be established for desired parts. The floating die system should also be tested on verity of different geometries, smaller as well as bigger, to determine its applicability and usefulness in the broader sense of tube hydroforming equipment. It is likely that this new class of hydroforming will be useful on the meso scale in addition to the micro-scale. Further study into micro-tube hydroforming should also seek to establish design guidelines that allow engineers to quickly determine what type of tube hydroforming equipment best suits their needs.

REFERENCES

[1] Saotome, Y., and H. Iwazaki. "Superplastic Extrusion of Microgear Shaft of 10 m in Module." *Microsystem Technologies* 6.4 (2000): 126-9. Web.

[2] Vollertsen, F., et al. "State-of-the-Art in Micro Forming and Investigations into Micro Deep Drawing." *Journal of Materials Processing Technology* 151.1-3 (2004): 70-9. Web.

[3] Engel, U., and R. Eckstein. "Microforming - from Basic Research to its Realization".Web.

[4] Messner, A., et al. "Size Effect in the FE-Simulation of Micro-Forming Processes." *Journal of Materials Processing Technology* 45.1–4 (1994): 371-6. Web.

[5] Bunget, Cristina, and Gracious Ngaile. "Influence of Ultrasonic Vibration on Micro-Extrusion." *Ultrasonics* 51.5 (2011): 606-16. Web.

[6] GUO, Bin, et al. "Flow Stress and Tribology Size Effects in Scaled Down Cylinder Compression." *Transactions of Nonferrous Metals Society of China* 19, Supplement 2.0 (2009): s516-20. Web.

[7] Tiesler, Nicolas A. "Microforming - Size Effects in Friction and their Influence on Extrusion Processes." *Wire* 52.1 (2002): 34-8. Web.

[8] Engel, U. "Tribology in Microforming." *Wear* 260.3 (2006): 265-73. Web.

[9] Chan, W. L., M. W. Fu, and B. Yang. "Study of Size Effect in Micro-Extrusion Process of Pure Copper." *Materials & Design* 32.7 (2011): 3772-82. Web.

[10] LIN, Jun-feng, Feng LI, and Jin-feng ZHANG. "A New Approach to Investigate Real Flow Stress in Micro-Extrusion." *Transactions of Nonferrous Metals Society of China* 22, Supplement 2.0 (2012): s232-8. Web.

[11] Fu, M. W., and W. L. Chan. "Geometry and Grain Size Effects on the Fracture Behavior of Sheet Metal in Micro-Scale Plastic Deformation." *Materials & Design* 32.10 (2011): 4738-46. Web.

[12] Kals, T. A., and Ralf Eckstein. "Miniaturization in Sheet Metal Working." *Journal of Materials Processing Technology* 103.1 (2000): 95-101. Web.

[13] Chan, W. L., and M. W. Fu. "Experimental Studies of Plastic Deformation Behaviors in Microheading Process." *Journal of Materials Processing Technology* 212.7 (2012): 1501-12. Web.

[14] Mirzai, Mohammad Ali, Ken-ichi Manabe, and Taihei Mabuchi. "Deformation Characteristics of Microtubes in Flaring Test." *Journal of Materials Processing Technology* 201.1–3 (2008): 214-9. Web.

[15] Furushima, T., and K. Manabe. "Experimental and Numerical Study on Deformation Behavior in Dieless Drawing Process of Superplastic Microtubes." *Journal of Materials Processing Technology* 191.1–3 (2007): 59-63. Web.

[16] Eichenhueller, B., E. Egerer, and U. Engel. "Microforming at Elevated Temperature - Forming and Material Behaviour." *International Journal of Advanced Manufacturing Technology* 33.1-2 (2007): 119-24. Web.

[17] Egerer, Emil, and Ulf Engel. "Process Characterization and Material Flow in Microforming at Elevated Temperatures." *Journal of Manufacturing Processes* 6.1 (2004): 1-6. Web.

[18] Eichenhuller, B., U. Engel, and S. Geidorfer. "Process Parameter Interaction in Microforming." *International Journal of Material Forming* 1 (2008): 451-4. Web.

[19] Mahabunphachai, Sasawat, and Muammer Koç. "Investigation of Size Effects on Material Behavior of Thin Sheet Metals using Hydraulic Bulge Testing at micro/meso-Scales." *International Journal of Machine Tools and Manufacture* 48.9 (2008): 1014-29. Web.

[20] Geissdorfer, S., U. Engel, and M. Geiger. "FE-Simulation of Microforming Processes Applying a Mesoscopic Model." *International Journal of Machine Tools & Manufacture* 46.11 (2006): 1222-6. Web.

[21] Fulop, T., W. A. M. Brekelmans, and M. G. D. Geers. "Size Effects from Grain Statistics in Ultra-Thin Metal Sheets." *Journal of Materials Processing Technology* 174.1-3 (2006): 233-8. Web.

[22] Sanchez-Salmeron, A., et al. "Recent Development in Micro-Handling Systems for Micro-Manufacturing." *Journal of Materials Processing Technology* 167.2-3 (2005): 499-507. Web.

[23] Eike Foremny, Arne Bloem, Philipp Wilhelmi, Christian Schenck, Bernd Kuhfuss. "Vision Based Feeding System for Linked Parts", *International conference on micro manufacturing (ICOMM2014), March 2014, Singapore.*

[24] XU, Jie, et al. "Surface Finish of Micro Punch with Ion Beam Irradiation." *Transactions of Nonferrous Metals Society of China* 19, Supplement 2.0 (2009): s526-30. Web.

[25] Razali, Akhtar Razul, and Yi Qin. "A Review on Micro-Manufacturing, Micro-Forming and their Key Issues." *Procedia Engineering* 53.0 (2013): 665-72. Web.

[26] Saotome, Yasunori, and Takeshi Okamoto. "An in-Situ Incremental Microforming System for Three-Dimensional Shell Structures of Foil Materials". *5th Asia Pacific Conference on Materials Processing, June 25, 2001 - June 25.* 2001, Web.

[27] Ku, T. W., B. S. Kang, and S. M. Hwang. "Finite Grain-Element Analysis and its Experimental Confirmation of Micro-Yoke Forming." *Journal of Materials Processing Technology* 153-154 (2004): 558-64. Web.

[28] Zhuang, W., et al. "Experimental and Numerical Investigation of Localized Thinning in Hydroforming of Micro-Tubes." *European Journal of Mechanics - A/Solids* 31.1 (2012): 67-76. Web.

[29] Liu, J. G., M. W. Fu, and W. L. Chan. "A Constitutive Model for Modeling of the Deformation Behavior in Microforming with a Consideration of Grain Boundary Strengthening." *Computational Materials Science* 55.0 (2012): 85-94. Web.

[30] Fu, M. W., B. Yang, and W. L. Chan. "Experimental and Simulation Studies of Micro Blanking and Deep Drawing Compound Process using Copper Sheet." *Journal of Materials Processing Technology*213.1 (2013): 101-10. Web.

[31] G. Ngaile and C. Yang, Bulge hydroforming of micro tubes for fiber optic sensor enclosures, NCSU, EM Photonic Inc., report, 2008

[32] Ngaile, G., Lowrie, J. "Punch Design for Floating Based Micro-Tube Hydroforming Die Assembly", *International conference on micro manufacturing (ICOMM2014), March 2014, Singapore.*

[33] Hartl, C., et al. "Investigation into Reduction of Die-Cavity Deflection in Micro-Hydroforming Processes using FEA." *The International Journal of Advanced Manufacturing Technology* 47.9-17 (2010): 853-8. Web

[34] Lungershausen, Jörn. "Fundamental Studies On Tube Hydroforming And Laser Assistance In The Manufacture Of Micro-Parts." Doctorial Dissertation, The University of Strathclyde, Glasgow. (2012)

[35] Wagner, Scott W.; Ng, Kenny; Emblom, William J.; Camelio, Jaime A. "Novel High Pressure Sealing System for Tube Hydroforming Operations", *International Manufacturing Science and Engineering Conference (MSEC), June 2013, Madison, Wisconsin.*

[36] Wagner, Scott W. "Analysis of a Non-Traditional Micro Tube Hydroforming Process." Doctorial Dissertation, Michigan Technological University. (2013)

[37] M. Krie, State of the art of sealing techniques for hydroforming tools, Hydroforming of tubes, extrusions and sheet metals, (Edited by K. Siegert) International conference on Hydroforming pp. 4411-461, Felbach Germany, 1999.

[38] Ghosh, Angshuman, Karan Deshmukh, and Gracious Ngaile. "Database for Real-Time Loading Path Prediction for Tube Hydroforming using Multidimensional Cubic Spline Interpolation." *Journal of Materials Processing Technology* 211.1 (2011): 150-66. Web.